NOTICE

The quality of this microform is heavily dependent upon the quality of the original thesis submitted for microfilming. Every effort has been made to ensure the highest quality of reproduction possible.

If pages are missing, contact the university which granted the degree.

Some pages may have indistinct print especially if the original pages were typed with a poor typewriter ribbon or if the university sent us an inferior photocopy.

Reproduction in full or in part of this microform is governed by the Canadian Copyright Act, R.S.C. 1970, c. C-30, and subsequent amendments.

AVIS

La qualité de cette microforme dépend grandement de la qualité de la thèse soumise au microfilmage. Nous avons tout fait pour assurer une qualité supérieure de reproduction.

S'il manque des pages, veuillez communiquer avec l'université qui a conféré le grade.

La qualité d'impression de certaines pages peut laisser à désirer, surtout si les pages originales ont été dactylographiées à l'aide d'un ruban usé ou si l'université nous a fait parvenir une photocopie de qualité inférieure.

La reproduction, même partielle, de cette microforme est soumise à la Loi canadienne sur le droit d'auteur, SRC 1970, c. C-30, et ses amendements subséquents.

Kinetic Study of the Speciation of Nickel(II) Bound to a Fulvic Acid.

John Allen Lavigne

A Thesis

in

The Department

of

Chemistry

Presented in Partial Fulfillment of the Requirements
for the Degree of Doctor of Philosophy at
Concordia University
Montréal, Québec, Canada

November, 1987

ISBN 0-315-64690-X

TABLE OF CONTENTS

ABSTRACT

Kinetic Study of the Speciation of Nickel(II) Bound to a Fulvic Acid

John Allen Lavigne, Ph.D.
Concordia University, 1988

The distinguishable species present in solutions of Ni(II) equilibrated with a soil fulvic acid (FA) are identified by a kinetic method of analysis based on reaction with 4-(2-pyridylazo)resorcinol (PAR). An approximate Laplace transform is used to assign the number of species and a non-linear regression routine is used to obtain final parameter values. Numerical methods are carefully evaluated using simulated data including synthetic noise.

Four rate constants , 0.67, 0.15, 0.021, and 0.0026 s^{-1} consistently represent components of samples initially equilibrated at pH 4, 5, and 6.4. The first is associated with $Ni(OH_2)_6^{2+}$. Species' concentrations vary in a reasonable way with pH and with FA/Ni(II) ratio, and seem to provide a realistic model. One important feature is found at pH = 6.4, where the weakest acid carboxylic groups of the fulvic acid have been deprotonated; 40% of Ni(II) is then bound in a species which requires ten days for complete reaction with PAR.

A comparison of multi-component kinetic analysis results to a fluorescence monitored titration procedure is presented. The kinetic analyses were performed at three points along the titration curve for the pH 6.4 set, at points equivalent to 0.67, 1.0, and 2.33 mmoles of Ni(II) per gram FA for an FA concentration of 5.0×10^{-6} M. These speciation results, when compared to fluorescence quenching results, gave an "effecti " binding capacity for the Armadale FA of approximately 3.1 mmoles bidentate complexing sites per gram of FA.

In memory of Dora Pallot.

ACKNOWLEDGEMENTS

I am deeply indepted to Professor Cooper H. Langford III for his gentle guidance, sociable disposition, and being a formidable teacher. I am grateful to Mark K. S. Mak for his contribution in constructing the non-linear regression program. I would also like to show my awareness of the fine peoples which compose our department.

LIST OF TABLES:

TABLE: Page

LIST OF FIGURES

CHAPTER 1: INTRODUCTION

A: General considerations:

This study was an attempt to determine the chemical speciation (1,2,3,4) of aqueous Ni(II) in the presence of a soil fulvic acid. The approach used was a multi-component colorimetric method of kinetic analysis in which the metal-humic equilibria are perturbed by the addition of a large excess of a colorimetric ligand and by a pH change.

For an understanding of such issues as chemical reactivity, bioavailability, toxicity and fate of metals in natural water systems, it is imperative to know the species that a metal forms. These include the following: free metal aquo ions, inorganic complexes, organic complexes, colloidal and large polymer associations, surface bound and solid bulk phases and lattice associated complexes (5). It has been extremely difficult to identify all species at prevailing concentrations. In particular the distinction between soluble and adsorbed species has been a troublesome task.

Nickel is of significant interest to environmental chemistry only when problems of contamination are concerned (i.e. where concentrations are high as compared to average levels) (6). A general order of decreasing toxicity towards organisms is $Hg^{2+} > Ag^{+} > Cu^{2+} > Cd^{2+} > Zn^{2+} > Pb^{2+}$

> Cr^{3+}, Ni^{2+} > Co^{2+} (7). In addition, the metals Al, Cd, Cu, Hg, Mn, Pb, and Zn have proven to be of great importance relative to changes in pH (8), however there exists only scant knowledge as to the potential risk of nickel in environments of different pH.

We have chosen Ni^{2+} for this study, not for its relative toxic importance, but for its kinetic convenience. The lability of simple Ni^{2+} complexes is less than that of the other ions mentioned on page 1. This means that the study can be initiated with the assurance taht all Ni^{2+} species including the free metal ion will be observable. Even when using stopped flow methods, an ion such as Cu^{2+} might react too fast to measure. Ni^{2+} is situated midway on a scale of water-exchange rates (9) from extremely fast to extremely slow as depicted in Figure 1.

Marine geochemical data on nickel has been well documented (10), but information on nickel's speciation in fresh waters is lacking. Seawater contains from 0.2 to 0.7 ug/L dissolved nickel (11). An uncontaminated fresh water level between 0.5 to 0.8 ug/L was found in the Adirondacks (12). Commonly, levels for nickel in natural waters are usually low, however anthropogenic sources of nickel include metallurgical industries involving smelting, plating, and manufacturing, or from fossil fuel refining and combustion (13). Nickel finds its way to water by leaching of the abundantly soluble salts or by atmospheric deposition, or by direct addition (13). Nickel present in

Figure 1: Rate constants for water-exchange (inner sphere) of some characteristic metals (9).

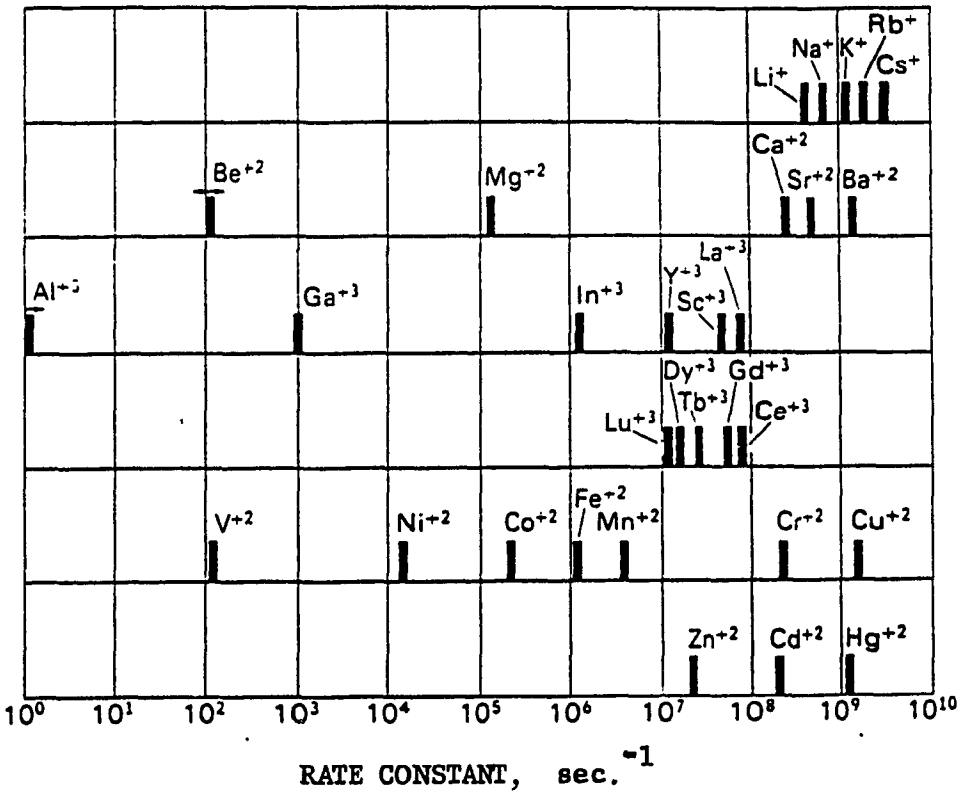

highly contaminated surface waters was found to range from between 5.9 to 6.4 mg/l in Alice Lake near Sudbury Ontario.

Toxicity testing on marine phytoplankton gave LC50 values (the concentration of toxicant at which 50 % of the test population has died after a set period of time) of 2.0 mg Ni^{2+}/L for a metal-tolerant strain, **S. acutiformis** (14). At the other extreme, an LC50 of 0.1 mg Ni^{2+}/L was found for a metal-sensitive strain, **Scenedesmus sp.** (15). The concentration of Ni(II) used in the present study corresponded to 0.29 mg Ni^{2+}/L, a value deemed of significance to the algal range just described. However, fish toxicity studies gave LC50 values for Atlantic silversides (**Menidia menidia**) of 14.6 mg Ni^{2+}/L and, for the tolerant species of the mummichog (**Fundulus heteroclitus**) of 191.3 mg Ni^{2+}/L for a 72 hour and a 96 hour time of exposure respectively (16). This is almost 300 times the concentrations used in this thesis. Bioaccumulation of Nickel by aquatic macrophytes (alga) range from 3.8 mg/Kg in the leaves of the species **N. variegatum** to 6375 mg/Kg in the leaves of **Potamogeton** (17). The nickel concentrations required to simulate toxic conditions towards fish are much too high for the reaction with PAR (i.e absorbancies would no longer follow Beer's Law). A lower concentration was used so as to achieve a good absorbancy range (0.33 units) while obeying Beer`s Law.

B: Complexation of metals by humic substances:

In this study, a Bh horizon Armadale soil was used as a source of fulvic acid (FA). B layers are zones where there is an accumulation of clays and/or humus material and oxides which originated from the surface, or A layer, having had some diagenetic evolution. The HA content retained in a B horizon depends mainly on the amount of drainage (i.e. leaching out). The FA used in this study was not a raw geochemical substance, but the water-soluble fraction of an alkaline extract of the soil mixture after particulate filtration and extensive ion exchange to convert it to the protonated form. It is of interest because of its significant metal and organic complexing characteristics and mobility within the water cycle but is not itself the only complexing fraction of the soil. Others are HA, clays, and oxides, components which were not considered in this study.

Complexation of metal ions in natural water is largely controlled by the colloidal ligands, humic substances, and hydrous oxides (18). This study has been directed to metal-humic interactions using a stoichiometrically defined soil-derived (pedogenic) fulvic acid (FA) as a representative humic. There exists a variety of structural components that are associated with humic substances. Table I lists some of the more important groups found in the Armadale soil extracts (19,20). The major functional groups in most

Table I: Functional groups found in the Armadale soil extracts (19,20) Concentrations are reported in meq/g.

Functional Groups	Type of Extract		
	HA	Humin	FA
Phenolic-OH	3.3	2.2	3.9
Alcoholic-OH	1.9	-	4.0
Ketonic C O	1.2	3.1	1.4
COOH	4.4	3.1	8.1
Quinonoid C O	1.0	2.0	0.6
Methoxyl	0.3	0.4	0.4

humic substances (HS) include carboxylic, phenolic, enolic, quinone, hydroxyquinone, lactone, ether, ester and hydroxyl as well as S- and N- containing groups, although a significant part of the latter are probably in non-complexing functional groups.

Methods used for determining the types of ligands responsible for metal binding to FA are based on the acidic properties of the polymeric ligand. Fulvic acid's irregularity and complexity obscure individual characteristics and render the analysis of the chemical and physical nature of FA rather complicated (21). Schnitzer developed a popular method for titrating the acidic properties which is called Baryta adsorption (22). It involves a reaction with excess barium hydroxide followed by a titration of the unused base:

$$2HA + Ba(OH)_2 \longrightarrow BaA_2 + 2H_2O + \text{unused base}$$

Total acidity (COOH and phenolic-OH) is then calculable.

Schnitzer (22) also developed a Ca-acetate method for the determination of the carboxylate content. The reaction involves:

$$2R\text{-}COOH + (CH_3COO)_2Ca \longrightarrow (R\text{-}COO)_2Ca + 2CH_3COOH$$

where the production of acetic acid is directly related to the total COOH content and can easily be titrated.

The total hydroxyl (OH) content can be determined using the method of methylation with dimethyl sulphate, or acetylation with acetic anhydride (23). From such results, phenolic-OH is calculated by subtraction of the total carboxylic-OH from the total acidity, and alcoholic-OH is calculated by subtraction of phenolic-OH from total OH. Such results must be accepted with discretion, there being shortcomings too numerous to elaborate (24). This sequence of determinations/calculations is the shortest, simplest route, although other procedures have been exploited, such as: methylation procedures (25), reaction with diborane (26), and reaction with lithium aluminum hydride for the determination of total acidity; an iodometric method (27) and quinoline decarboxylation for the determination of carboxylic-OH; and the Ubaldini method for phenolic-OH determination (28). What must be emphasized is that each method has its advantages and disadvantages. Because of a lack of specificity appropriate to the study of complex polyfunctional ligands such as the humic substances, values obtained must be used with discretion.

Many recent studies have investigated FA and HA using the nuclear magnetic resonance (NMR) techniques (29,30,31), but strong disagreements exist among laboratories as to the interpretation of the results (32,33). H-NMR spectra of humic substances (34) are not easily resolved and have been of interest only for overall functional group classifications. The latter approach supplies little information

about subtleties of structural units. Furthermore, HA and FA have limited solubilities in common NMR solvents. Schnitzer and co-workers (35) have studied, by ^{13}C-NMR, a number of humic substances including the Armadale soil extract used in this study. The major present debate concerns the true aromatic content of the various humic substances. Their method utilized the integration of the areas under the peaks of cross polarization, magic-angle spinning (CPMAS) Carbon-13 NMR spectra (36) between 100 and 160 ppm as assignable to aromatic carbons, which supplies aromaticities when normalized to total area less that for carboxyl carbons according to:

$$f_a = f'_a - f_{COOH}$$

where f_a is the normalized aromaticity, f'_a is the total area for aromatic carbons, and f_{COOH} is the carboxyl carbons. These results have shown that the percent aromaticity for Armadale FA is 35%, compared to 92% for an A1 horizon Inceptisol HA from Shizuoke Japan (37). One of the attributes of the Armadale FA is this fact by ^{13}C-NMR techniques agrees well with the binding estimates based on traditional titration methods. This increases confidence in the values reported in Table I.

One disadvantage to NMR methods is that it does not discern discreet OH peaks, although it does isolate COOH peaks which contain the OH moiety. The OH content found by the methods described earlier can be used to calculate

the appropriate fractions of OH and COOH groups.

Schnitzer and Gamble (38,39) have reported values for the Armadale Bh horizon soil fulvic acid of 3.3 mmoles/g FA of phenolic-OH, with a total -COOH content of 7.7 mmoles/g FA (38,40,41). Aliphatic-OH was 3.6 meq/g FA, ketone was 2.5 meq/g FA and quinoid was 0.6 meq/g FA. Permethylation of FA reveals peaks between 50 and 60 ppm for $COOCH_3$, aromatic OCH_3 and aliphatic OCH_3 groups from which the approxiamte abundances are found. For the Armadale FA, the relative abundance of OH groups associated with phenolics versus carboxylic acid (1.00), was 0.40 (42). This carboxyl/phenol ratio of 2.5 compares well with the 2.3 ratio found with titration data discussed above. The carboxylate and phenolic-OH are of major interest with respect to the metal-humic complexing characteristics (43). These two reactions can be represented as:

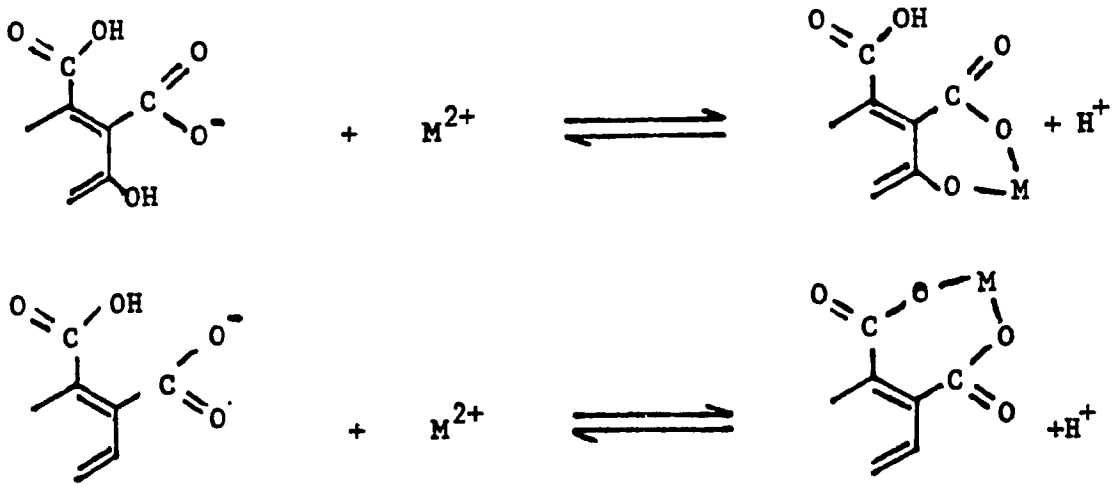

Functional group content can vary significantly depending on the source or type of the humic material. Table I illustrates these differences between the groups analysed for FA and HA from the same soil (44). As an illustration of the wide variety of values for various functional groups that can exist between soils of differing origin, Table II compares estimated values of quinone and ketone content in humus from various substrates (45). Evidence of such widespread disparities makes it obvious that humic material used in any speciation study must be well-characterized in advance. This is indeed the case for the Armadale FA (38-43) and is the major reason for which it was chosen.

The conclusion of this review is that humic substances have many functional groups in common but vary considerably in detail. The sample chosen as a model in the present study is one of the best characterized, and composition determined by either titration methods or by NMR studies are in good agreement. It is also well characterized with respect to stoichiometry of ion exchange and acidity by the detailed titration studies of Gamble (40,41). The results for the first and second end points as reported by Gamble (41) were 3.16 and 7.70 equivalents acid per gram FA respectively.

Table II: Estimated quinone and ketone content for five different soil sources (18).

Source	Quinone (meq/g)	C=O (meq/g) total	Ketone (meq/g)
Woodland soil	1.05	2.92	0.93
Peat	1.26	2.75	0.78
Brown Coal	1.33	2.90	0.78
Weathered brown coal	2.51	3.95	0.72
Weathered bituminious coal	3.27	5.18	0.90

C: Conventional methods of metal species determination:

In a polydisperse system, the total concentration of metal, M_T, for all species (free and complexed) in solution can be algebraically described as:

$$[M_T] = [M^{2+}] + [ML_1] + [ML_2] + \ldots + [ML_n]$$

where $[ML_i]$ is the concentration of the i-th metal-ligand complex, and M^{2+} is the free metal.

Conventional analytical methods commonly applied to water systems are limited by their failure to distinguish number and nature of chemical species in situ, since what is measured is usually total metal and/or free aquo metal (46). For example, the highly sensitive technique of atomic absorption spectrometry (AA) is commonly used to determine the concentration of a separated species, with the seperation accomplished either by ion exchange (47), solvent extraction, or size fractionation (48). Solvent extraction using either chloroform or carbon tetrachloride may permit partial extraction of the metal ions adsorbed on organic colloids and/or inorganic particles (49). Kamp-Neilsen (50) points out that chelation-extraction methods may seriously underestimate organically bound metal species. The use of ligands such as dithizone, diethyl-dithiocarbamate, and ammonium pyrrolidine dithiocarbamate form such strong complexes that the required stability

constant of a natural copper complex would have to be greater than 10^{30} in order to avoid substitution by the diethyldithiocarbamate (49). This not being the case with all metal-humate equilibria, some of the bound species would react and thus be presumed as free metal ions, thus underestimating the true bound species. Even if this were avoided, the method only measures two components, free and bound.

The most sensitive atomic absorption technique, that of graphite furnace atomic absorption (GFAA) has an absolute detection limit of approximately 0.02 ng/mL for most metals using 50 uL samples (51). The optimum concentration range when using conventional flame AA for the detection of Ni^{2+} is 0.3 to 10.0 mg/L with an absolute detection limit of 0.02 mg/l (52,53).

Ion-selective electrodes (54) are metal ion specific but measure only the thermodynamic activity of the ion which is often taken to be equivalent to the "free" metal concentration in solution. As used, two species-types are determinable, the "free" and the bound. The latter is determined by difference from the total known metal concentration, found either by AA or other suitable methods. There does not exist at present any suitable ISE for nickel. CopperISE's are capble of measuring copper ion activity as low as 0.6 ug/l (55), but at these low levels, problems of reproducibility and linear response abound, and the potential readings obtained are ambiguous.

The major problem with ISE's is its relative insensitivity. The lower limit of the copper ISE is 300 times higher than that acheivable using GFAA. Frazer et al. (56) have introduced a method to obtain quantitative analytical data when the EMF outputs are in the Non-Nernstian response region. However, an artificial intelligence computerized method is required to analyse the resultant potential readouts in comparison to stored calibration data, and the lower limit then becomes that level where the ISE noise becomes significant. For example they were able to detect bromide at 6 ppb with a 2 ppb error. This procedure required rigid constant temperature control in order to reduce the error to 0.5 ppb (i.e. it is not a routine procedure). Again, output instability causes the greatest difficulty, and, as mentioned, the complex data analysis scheme required does not lend much appeal to this method.

Conventional ISE is acceptable for determining the free metal ion activity. There is not any direct method for distinguishing between the different species that are bound. Bound species are evaluated by titration methods. Weber et al. (57,58) have used a copper ISE in conjunction with fluorescence quenching measurements. From knowledge of the total and the "free" metal concentrations, the bound total can be thus easily calculated, and fluorescence quenching serves to indicate when maximun ligand complexation has been acheived. A similar approach has been used to determine equilibrium constants for pyrene, phenan-

threne, and anthracene in the presence of FA (59).

Anodic stripping voltammetry (ASV) has the ability to distinguish three categories (60), namely free metal ions, labile species which have stripping potentials cathodic to that of the free species, and those that can be labelled as electroinactive. Total metal can then be determined as well after acid digestion (61) or following UV irradiation in acid-H_2O_2 media (62), the latter being preferred when studying natural organically bound metals. It is a sensitive approach, but is usually limited to only a few elements, namely Cu, Cd, Pb, and Zn (63). Nickel will react with the mercury creating a metal-metal complex.

Cyclic voltammetry, and ASV, study the oxidation (plating step) and reduction (stripping step) steps. A metal ion must physically diffuse to the reaction layer where it must dissociate from its counter ion or ligand before being reduced through electron transfer. The amalgam is formed when the reduced ioon is made available after leaving the diffusion layer (64). The formation of this metal complex:

$$L^{n-} + Me^{m+} \rightleftharpoons MeL^{-(n-m)}$$

must be faster than the oxidation of the amalgam:

$$M(Hg) \rightleftharpoons M^{n+} + ne^{-} + Hg$$

so that there can be recombination of the complex before it has the chance to enter the plating step once again. If

it has not, the two steps are indistinguishable. This can often be the case with fulvic acid which contains many weak binding sites.

One problem that merits consideration when using ASV is the adsorption of a species onto the mercury drop which can cause potential shifting, depressed potential values or the occurence of multiple waves (65). Studies have indicated that humic acid suppresses the reduction currents during the plating step in ASV (66). Suppressions of plating activity is interpreted in terms of the presence of surface-active agents. Surfactants, usually present in natural water, interfere with the quality and reliability of results from ASV.

The "masking" of labile Cu^{2+} by Cl^- arise from shifts in the Hg wave (66,67). These interferences arise from complexation of the analyte and interactions at the droplet interface and Hg phase. Since natural waters contain Cl^-, this interference may occur. Simple interpretations of voltammograms are not satisfactory for speciation studies because of these difficulties.

Another problem encountered in ASV studies occurs when the ratio of the free metal is equal to or higher than that of the ligand-bound metal, a situation arising subsequent to both having been reduced to the amalgam, the ligand diffuses back into the solution and is therefore no longer available to recombine with the fraction of oxidized amalgam originally proportional to it. This obviously

gives rise to erroneously high values for the free metal concentration (68). Thus, alternative methods capable of supporting or verifying ASV analysis are important.

Dialysis has been employed to separate free metal ions and the organically-bound metal species (69,70). Problems associated with the use of dialysis membranes are serious. It is suspected that some humic substances may dissociate at the membrane surface, pass through as smaller units, then reassemble into the aggregate form on the other side. Furthermore, negatively charged complexes diffuse through the wall very slowly (71,72) because the dialysis membranes themselves are negatively charged. Contamination of the membrane by the metal cation is widespread in practice and once they have been decontaminated they tend to adsorb even more strongly than before.

Errors can result if it is assumed that the free metal ion concentration outside the bag, at equilibrium, is equal to the free metal ion concentration inside the bag. The error (73,74) arrises when there is a deficiency of anion passage to the outside. Excess electrolyte can overcome this effect, but supporting electrolyte shifts the equilibrium of weakly bound ligands, favoring an increase in free metal ions according to the ionic strength effect as illustrated with an example using copper and sodium:

$$Cu - L \rightleftharpoons Cu^{2+} + L^{2-} \overset{+Na^{+}}{\rightleftharpoons} Cu^{2+} + LNa_2$$

Ultrafiltration has been used in a similar manner to dialysis. Advantages are similar, disadvantages are similar, but attenuated somewhat. It involves the application of about 3 atmospheres of pressure (usually with nitrogen) to a closed vessel with a filter on the bottom made which is made of a very thin membrane coating (such as polycarbonate) mounted on a porous backing for physical support (75). Buffle and Staub (76,77) have recently used the ultrafiltration method to measure the complexation equilibrium properties (stability constants) of zinc in the presence of both a synthetic ligand and a pedogenic (soil derived) fulvic acid from a natural water. The method works irrespective of the nature of the metal ions involved, and its sensitivity is limited only by the method of detection used to analyse the filtrate. Since the method is applicable to all metals, the method has the advantage of being useful for those metals that are difficult to analyse using other methods. The useful aspect is that the ligand and its complexes are retained by the membrane (78), whereas the free metal ions pass through into the filtrate. However, even the smallest of pore sizes (i.e. molecular weight cut-off of 230) does not completely retain all of the organic ligands found in natural waters where molecular weights average only a few hundred Daltons and dissaociation reassociation can occur (79). By filtering only a small amount of the solution, perturbations of the equilibria can be avoided, and this

also reduces the filtration time.

A high concentration (0.1 M) of noncomplexing electrolyte is an absolute requirement in order to avoid adsorption of the metal ions onto and within the membrane. This is a serious disadvantage since it would certainly perturb the equilibria of the weaker binding sites, which are considered to contribute greatly to the total number of binding sites.

It has even been proposed to regard biological uptake as a measure of speciation. Biological uptake is a physico-chemical process wherein metal uptake is a speciation-sensitive phenomenon. Trace metal uptake invariably invloves passage through a complex multi-cellular membrane (i.e. fish gills). The differences between common measurements (i.e. ISE) and membrane processes include a less well defined diffusion layer thickness and a sometimes saturable adsorption uptake process (81). The common assumption is that uptake measures free ion concentration. Free metal ion concentrations have been measured by bioassays (82) using marine bacteria, where biological activity/response is measure by glucose or amino acid incorporation. Kinetic considerations are of significance and the procedure is quite time consuming. It is non-specific, and the effective concentration range is limited from 1 pM to 1 nM (83).

D: Kinetic Method of Speciation:

In this study species' concentrations and species' rate constants for their reaction with PAR were determined by fitting Equation 1.1 using a kinetic method (84,85). On dissociation of the metal-FA species, a strongly binding reagent produces a common detectable product. A multi-component kinetic treatment identifies the components by their difference in rates of reaction under conditions (i.e. pH, ionic strength) fixed by the reagent solution. The rate expression is:

$$\text{Rate} = \frac{dP}{dt} = k_1[M_1] + k_2[M_2] + \ldots + k_n[M_n] \qquad [\ 1.1\ ]$$

In [1.1] P is the product formed, and k_i 's are the individual dissociation rate constants of the various components. The concentration of reagent is chosen large enough to force pseudo-first-order kinetics. The reagent is 4-(2-Pyridylazo)resorcinol (PAR).

This kinetic method has been apllied previously to iron(III) (86) and aluminum(III) (87). In the latter case, estimates of the rate constants and initial concentrations were obtained from Guggenheim plots (88). Kinetically distinguishable components were recognizable from linear sections of the plots/ The disadvantage of this method is in the uncertainty as to whether the non-linear portions

contain more than one component and that at the most three components were capable of being resolved. A number of other data reduction procedures have been discussed elsewhere (89,90). The lesson is clear. A better method for objective assignment of components is necessary.

The data analysis method adopted for this work identifies the minimal number of components capable of modelling the system and is based on a method introduced by Olson and Shuman (91) in which an approximation of the distribution of the reverse of a Laplace transform as applied to Equation [1.1] was used. The application of this method will be discussed in more detail in Chapter 2.

A kinetic method of speciation has the added advantage of providing an approximation of the kinetic behavior of the various species identifiable in a natural water environment, to the extent that the reagent solution does not produce extreme conditions entirely irrelevant to natural systems.

In the method, the cation is scavanged from the equilibrated Fulvic acid - Nickel(II) complexes (Fa-Ni(II)) by swamping the sample with an excess of the strong complexing reagent, PAR, which has a high stability constant with Ni(II).

The reactions of PAR with the FA-Ni(II) species (and the free Ni^{2+}), can be represented:

$$Ni^{2+} + PAR \xrightarrow{k1} NiPAR$$

$$FA_1\text{-}Ni + PAR \xrightarrow{k2} NiPAR + FA_1$$

$$FA_2\text{-}Ni + PAR \xrightarrow{k3} NiPAR + FA_2$$

$$\vdots \qquad\qquad \vdots$$

$$FA_n\text{-}Ni + PAR \xrightarrow{kn} NiPAR + FA_n$$

where FA_i-Ni is a kinetically distinguishable Ni(II) species. Note that NiPAR is a common product for colorimetric monitoring. With a large excess of PAR (in this case 50 fold) all the above reactions are pseudo-first-order. In this case, the concentration of NiPAR evolves with time according to:

$$C(t) = \sum_{i}^{n} C(0)_i (1 - e^{-k(i)t}) + X \qquad [1.2]$$

where C(t) is the concentration of the NiPAR complex at any time t, $C(0)_i$ is the initial concentration of the i-th species expressed in units of the proportionate quantity of NiPAR produced at t = infinity, and k(i) is the rate constant for the i-th component. Thus, the information on the quantities of various types of ligand sites is given by the $C(0)_i$'s, and qualitative information on lability by the k(i)'s. The X term encompasses time independent

absorbance representing the sum of the "blank" absorbance by PAR, the "blank" absorbance by the FA, plus the blank absorbancies of any products formed by PAR in a time short compared to reagent mixing. Ni^{2+} was chosen because its fastest reaction, that of free $Ni(OH_2)_6^{2+}$ with PAR, may be studied directly at the concentration levels used here. No fast reaction between Ni^{2+} and PAR contributes to X.

E: Characteristics of the PAR reagent:

The acid-base equilibria (92,93,94) of PAR are shown in Figure 2, and the structural forms for the 1:1 and the 2:1 complexes of metals with PAR (95,96) are shown along with the equilibrium constants for Ni(II)-PAR in Figure 3.

Alpha values (α) are used to express the fraction of total ligand that is in a particular protonated state (97). For PAR, the sum of its protonated/deprotonated forms is given by:

$$C = [H_3A^+] + [H_2A] + [HA^-] + [A^{2-}] \qquad [1.3]$$

where C is the total sum of ligands, and A represents PAR. The α_0 fraction for a ligand like PAR, when totally deprotonated, is given by (98):

$$\alpha_0 = \left([H]^3/K_1K_2K_3 + [H]^2/K_2K_3 + [H]/K_3 + 1\right)^{-1} \qquad [1.4]$$

Figure 2: Acid-base dissociation steps for PAR (92).

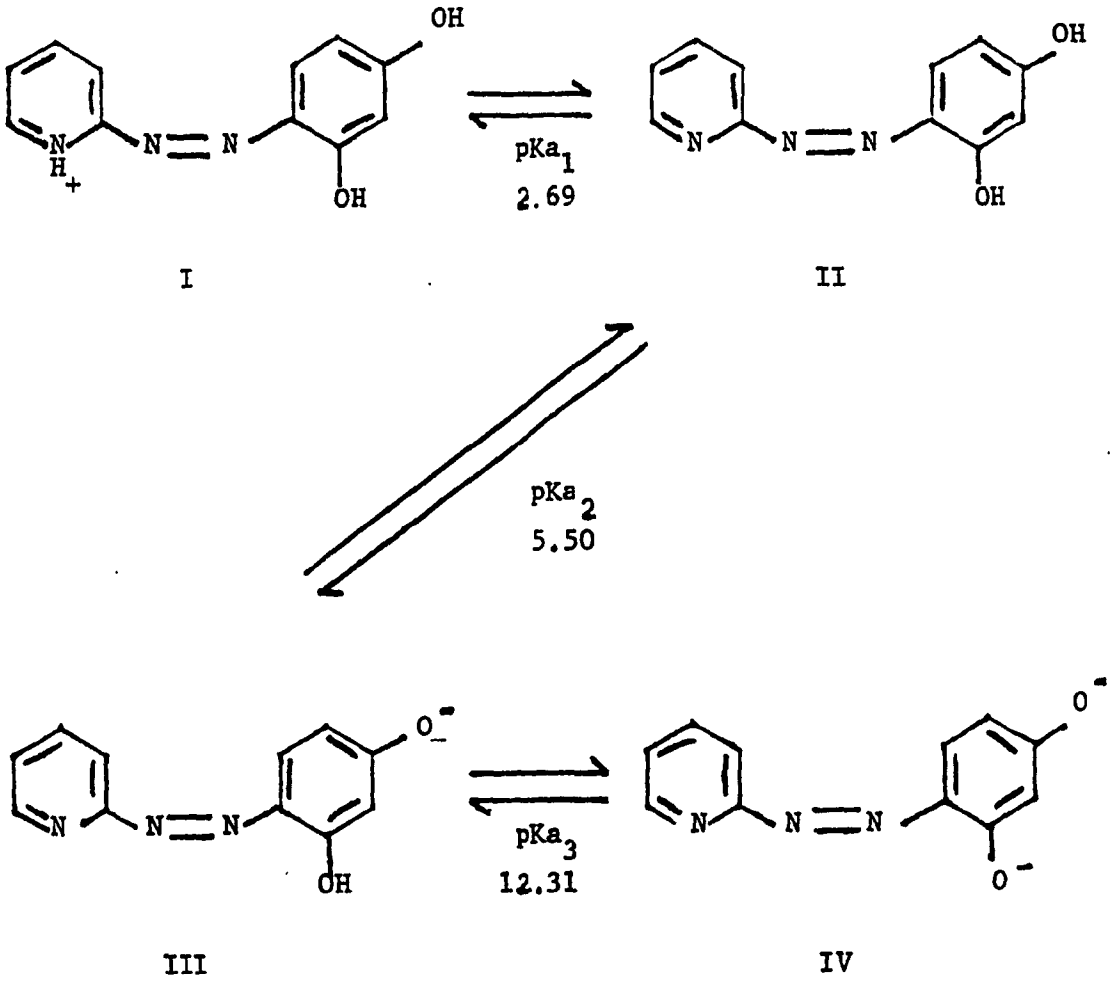

I: Protonated cationic form

II: Electrically neutral form.

III: and IV: Anionic forms

Figure 3: Structures for the 1:1 and 2:1 metal:ligand complexes with PAR, and their equilibrium constants in the case of nickel (95).

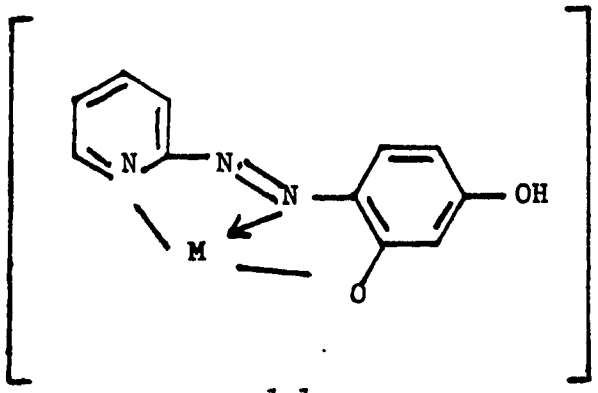

1:1

$$K_1 = \frac{[MHL]}{[M]\,[HL]}$$

$$\log K_1 = 13.2$$

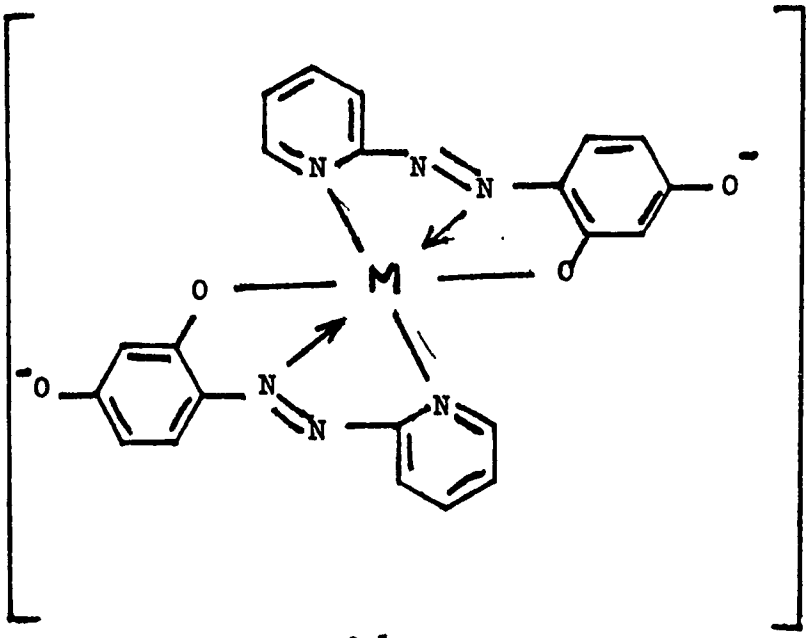

2:1

$$K_2 = \frac{[M(HL)2]}{[MHL]\,[HL]^2}$$

$$\log K_2 = 12.8$$

and where subsequent fractions for monoprotonated, di-protonated and tri-protonated species are given by:

$$\alpha_1 = \alpha_o \frac{[H]}{K_3}, \alpha_2 = \alpha_o \frac{[H]^2}{K_2K_3}, \text{ and } \alpha_3 = \alpha_o \frac{[H]^3}{K_1K_2K_3} \quad [1.5]$$

Using the pK_a's in Figure 2, one obtains, for a pH of 7.8, the following alpha values: 3.07×10^{-5} for $_o$; 0.993 for $_1$; 0.005 for $_2$; and 3.9×10^{-8} for $_3$. Therefore, it is the monoprotonated form III in Figure 2 which is the predominant (99.3%) form for PAR under the kinetic conditions used in this study.

F: Fluorescence quenching of humic substances by metals:

Fluorescence (99) is used in this study as a complement to the kinetic approach. Fluorescence is dependent on the chemical structure and environment of the compound. Few aliphatic compounds fluoresce, but large conjugated systems do, having HOMO pi electrons which are promoted to LUMO antibonding levels when low energy photons are absorbed with minimal skeletal pertubation in the molecule.

Most paramagnetic metal ions quench effectively. Since

in the case of FA, the COO^- groups provide weak field ligand sites for Ni^{2+}, complexes will be paramagnetic in this case and quenching is expected. Previous studies (57,58) used fluorescence quenching in a titration procedure where Cu^{2+} was the titrant. This method was regarded as pertinent to the study of complexation equilibria. The effort to extend the method to Ni-FA revealed problems. There is some reason to suspect that earlier reports were overly optimistic. In our work, good equilibrium models could not be developed from fluorescence data.

CHAPTER 2: REDUCTION OF KINETIC DATA

A: The Laplace Transform:

The success and reliability of kinetic methods of analysis depends critically on the numerical treatment of the experimental multicomponent kinetic data. Any fitted solution automatically involves the mathematical complexity of a 2n-dimensional surface where n is the number of components (one pair of $C(0)_i$ and k_i for each). As is commom in related problem areas such as multiple luminescence decay, non-linear regression (NLR) is used to obtain k_i's and $C(0)_i$'s. This can be readily done for three components present in similar quantities if the k_i's are separated by more than a factor of two. (If quantities are not similar, a factor of 10 may be needed between neighbouring k_i's.) The central problem is the fact that several component non-linear least squares fits are too flexible and some guidance is necessary to choose reasonable component sets and initial parameters.

In the present case, one rate constant can be independently determined, that for reaction of PAR with $Ni(OH_2)_6^{2+}$ (by experiments in the absence of FA). A second can be extracted from the linear part of the $\ln(A_\infty - A_t)$ data at late t by a linear least squares fit. That is, the

last component in Equation 1.2 can be extracted since the reaction is essentially complete with respect to the others. To obtain objective initial values for the remaining components requires a procedure to supplement non-linear regression. In an earlier study (100) the use of a modified Guggenheim plot method was explored. Recently, Shuman and co-workers (91,101) have suggested use of an approximate Laplace transform. Although the derivation used in the analysis has been introduced and described elsewhere (91), a short explanation is given here.

If we multiply a function, f(t), by e^{-st}, where s is equal the complex variable $\sigma + jw$, and perform a one-sided positive integration to infinity, and if the result exists as a function, this is called the Laplace transform of the function f(t) (102), denoted F(s), as in;

$$F(s) = \int_0^\infty e^{-st} f(t)\, dt \qquad [2.1]$$

For equation 1.1, this becomes, when k is considered as a variable of the integration;

$$C(k,t) = \int_0^\infty F(k,t)\, e^{-kt}\, dt \qquad [2.2]$$

The inverse Laplace transform of Equation 2.1 is the function F(k,t). To obtain this function, the inversion can be obtained using the Post-Widder equation (91,103,104) yielding thus;

$$F(k,t) = \lim_{m\to\infty}\left(\frac{(-1)^m}{m!}\right)\left(\frac{m}{k}\right)^{m+1}\frac{\partial^m C(m/k)}{\partial t^m} = \lim_{m\to\infty} F_m(k,t)$$

In the final result, as explained in more detail in Shuman's paper (91) where the mathematical approach was initially developed, the distribution function H(k,t) is obtained as;

$$H(k,t) = \frac{\partial^2 C(k,t)}{\partial(\ln t)^2} - \frac{\partial C(k,t)}{\partial(\ln t)} \qquad [2.4]$$

H(k,t) is a distribution function, from which a spectrum is obtained by plotting H(k,t) vs ln(t) where individual peaks in the curve represent each component. The area under each peak equals that component's initial concentration. Maxima in H(k,t) vs ln(t) are related to k (= 2/t). The difficulty with this procedure is that numerical second-order differentiation can lead to artifactual peaks when the smoothing routine for the original data is susceptible to the production of "ringing". As well, the numerical approximation leads to peak broadening which removes the distinction between well defined species and a continuous distribution of species. Data smoothing procedures, which are essential, ameliorate somewhat the first of these problems and exacerbate the second.

The accuracy of the value obtained for k_i at the maxima in the distribution is determined by the integer m in Equation 2.3. Equation 2.4 was derived with m = 2,

hence in our case $k_i = 2/t$. Higher accuracy was deemed to be unwarranted. However, if one wished to consider extending Equation 2.4, the value of m must be also considered for the expression for $k_i = 2/t$. In this study, the value of m was always restricted to 2.

Our approach uses the Laplace transform to obtain estimates of parameters which are then refined by non-linear regression. The validity of the parameters' objective significance is not demonstrable from numerical analysis alone. The case for parameter validity is finally one of consistency of the rate constants as a function of concentrations and pHs. (This issue is better discussed after the results have been presented in Chapter 5). Trials using artificial data (with noise) showed that whenever erroneous results were obtained with the transform method and the parameters obtained were subsequently used as input for the non-linear regression routine, the algorithm failed to converge. Confidence in parameter validity in a final result is dramatically improved when simulations closely related to the experiments reveals the details of the process of data reduction. Although we acknowledge that this "empirical" approach to validating algorithms is not rigorous, synthetic data were designed to mimic the experimental system to minimize the dangers.

B: Nonlinear regression:

In contrast to the nonlinear regression package that was previously used (105) (a general purpose program from the Computer Center Library), the present program was written exclusively for the purpose of fitting multi-component kinetic parameters (sums of exponentials plus a background signal) to the data, while restraining the results to certain criteria which will presently be further defined.

The mathematical characteristics have been discussed by Mak and Langford (87). The salient features of the program include the capability to compute the exact values of all the partial derivatives that comprise the Hessian matrix **N**. It avoids convergence on negative values by using the coefficients of the fitted polynomial and means to adjust the intermediate parameter values in the course of the regression. The advantage of this feature is obvious. Computational accuracy is improved by eliminating estimates of partial derivatives numerically (as is the case with inputs of arbitrary regression models with the fore-mentionned packages). This in turn assures better fitting in the final solution. This also effectively reduces the probability for the regression to converge onto an erroneous minimum. Otherwise, the NLR algorithm chosen for this work adheres very closely to that described in Bard

(106) and discussed in the kinetic context by Mak and Langford (87).

NLR routines require equal time intervals to work in a minimum time span. For this reason all experimental or simulated data was reconstructed by generating a suitable (C,t) matrix from the original data using the procedure to be described latter in Chapter 4.

The entire noncompiled version of the nonlinear regression as composed by M.K.S. Mak (107) is found in appendix B of this thesis.

A brief description of the algorithm is also provided in this appendix. It is not introduced "point blank" in this Chapter since it is not necessary to understand the subtleties of the software in order to properly use it, and besides the terms used in its description are not appropriate to the basic approach required in this thesis.

CHAPTER 3: EXPERIMENTAL SECTION

A: Materials.

All chemicals were reagent grade unless otherwise noted. The PAR reagent was obtained from Aldrich Chemical Company; $NaNO_3$ and $NaHCO_3$ from Anachemia ; $Ni(OH_2)_6.Cl_2$ from May and Baker ; NaOH pellets and conc. HNO_3 from Allied Chemicals. The water was deionized-distilled with no cations detectable by flame atomic absorption spectroscopy. Chemicals were used without further purification.

Extraction of the soil fulvic acid from a Bh horizon soil obtained from Armadale, Prince Edward Island following procedures of Schnitzer (39), was performed in our Science and Industrial Research Unit (SIRU) laboratories (108). This fulvic acid was chosen because it has been well characterized by Gamble and Schnizter (38,39). A number average molecular weight of 900 a.m.u. (86) was used to calculate "molar" concentrations of the fulvic extract. To appreciate the complexity of the sample, it is worth noting that the weight average molecular weight is near 5000 a.m.u. (109).

The experimental FA was extensively ion exchanged to replace metal ion with H^+. It was not, however, fractionated because most chromatographic, degradative, and mass spectral experiments have indicated a nearly continuous distribution of components and it seems unlikely that

the behaviour of a FA can be readily simulated by the summation of the properties of the pure model organic compounds. One advantage of this study was to use a stoichiometrically well defined natural substance, as is the Armadale FA.

B: Samples:

The mole ratio of fulvic acid to Ni(II) was varied between 1:1 and 9:1 in unit steps. Each solution contained 1.00×10^{-5} M $NiCl_2$, and the appropriate proportion of fulvic acid. Three series were prepared at three pH values; 4.0, 5.0, and 6.4. A pH of 4.0 is just above the pH of the pure FA solutions, and a pH of 6.4 lies beyond the equivalence point in the titration of the carboxylates with NaOH (see Chapter 1). These were obtained by adjustment with extremely small quantities of HNO_3 or NaOH as required. Solutions were then equilibrated for at least 24 hours at room temperature in the dark, and their pH values confirmed.

The PAR reagent was prepared in 50 fold excess to the Ni(II), thus 5.00×10^{-4} M, brought to 0.200 M with $NaNO_3$, and 0.050 M in $NaHCO_3$. After PAR dissolution was assured the pH was adjusted to 7.5 with dilute NaOH.

Sample preparation for the fluorescence quenching experiments are described in part D of this chapter.

C: Kinetics.

To study kinetics, 1.5 ml of one of the sample solutions was mixed with 1.5 ml of the PAR reagent working solution. This dilution gave final concentrations of 5.00 X 10^{-6} M $NiCl_2$, 2.50 X 10^{-4} M PAR, 0.100 M $NaNO_3$, 0.025 M $NaHCO_3$ and pH 7.8. The reagent solution assures constant pH (7.8) and ionic strength for all kinetic runs and an excess of reagent over the metal of 50 fold. This guarantees pseudo-first-order kinetics and rate constants which are consistent throughout. The mixing was done by consecutive injections of aliquots directly into the cuvette such that reactions could be initiated with a maximum t = 0 error of about $\pm$ 0.25 sec. once the reagent solution was introduced as the second injection. The cell block was maintained at 24.5° $\pm$ 0.1°C using a thermostated circulating water bath.

Absorbance values were recorded at 521 nm on a Perkin-Elmer Model 552 spectrophotometer and digitized from chart records at ever increasing time intervals (related somewhat to ln(t) spacings) up to, at most, 9.0 X 10^4 seconds. The molar absorptivity at 521 nm of NiPAR was found to be 6.57 X 10^4 +0.05 X 10^4. PAR does absorb weakly at this wavelength but since it is in 50 fold excess, its contribution to the change of absorbance with time is negligible. FA absorbs slightly at this wavelength as well but its contribution was found to not vary with time under our experimental conditions. Both excess PAR and FA contribute to the X term in equation 1.3. This amount, X, is

constant with time, and varies only with changing FA concentrations. The approach to multi-component analysis is described in Chapter 4.

D: Fluorescence Quenching:

Fluorescence emission was measured at 465 nm following excitation at 365 nm using a Perkin-Elmer Fluorimeter model PE MP44B. Absorbance measurements at both the emission and excitation wavelengths were recorded in order to assess the influence of the absorbancies on the correction factor necessary to recalculate the exact relative fluorescence according to the equation (110):

$$F_{CORR} = \frac{F\, e^{1.151(A\lambda 1 + A\lambda 2)}}{1 + 1.02(A\lambda 1^2 + A\lambda 2^2)\, d^2} \qquad [3.1]$$

where $A\lambda 1$ and $A\lambda 2$ are absorbancies at the excitation and the emission wavelengths respectively, and d is the cell path length.

To a 400 mL solution of FA equilibrated to a pH of 5.0 or 6.4, uL aliquots of a 0.004 M $NiCl_2$ solution (50 to 500 uL) were added, and the pH maintained throughout the titration with dilute NaOH. Fluorescence measurements were recorded after 15 minutes of equilibration on 3mL samples, which were subsequently returned to the vessel before the addition of further titrant.

Three points along the titration curve, equivalent to titration amounts of 1.0, 2.0, and 3.0 mmoles per gram of FA were selected for multi-component kinetic analysis in order to observe the speciation as the titration progressed to an asymptotical maximum quenching. This was done at pH 6.4 only as it was considered the most interesting in the sense that at this pH, the most complexation was observed. These three additions were done on a sample separate to those for the fluorescence quenching titrations and were allowed to equilibrate for 24 hours prior to kinetic analysis.

Multi-component kinetics for all solutions involving fluorescence quenching were performed on a Hewlett-Packard 8452A diode array spectrophotometer at 520 nm and 24.5 ^{o}C. In order to reduce the amount of data obtainable on a continuous kinetic run from 0 to approximately 3,000 seconds, the run was divided into three files such that (i) for 200 to 400 seconds, a reading was recorded at 0.5 second intervals with integration times of 0.1 second each, (ii) subsequently, data at intervals of 30.0 seconds with integration times of 0.7 second were collected until an elapsed t'me of approximately 2500 seconds. These sets were further reduced in size using the algorithm called STANDARD.A, and STANDARD.B as presented in appendix A, programs which cause the data to resemble a logarithmic progression of data acquisition with respect to time.

CHAPTER 4: DATA PROCESSING TECHNIQUES

A. Data simulation:

Data were simulated according to Equation 1.3 by varying both the number of and the values for the various parameters. Noise was introduced by adding or substracting up to 0.6% of the data using a ramdom generator of the noise which was distributed normally. To simulate temporal aspects of the experiment, the values for the time of recordings as obtained in the actual experiments were used. These approximated logarithmically increasing increments. The noise used in the simulations exceeded experimental noise.

Results for a typical simulation are presented in Table III. The NLR-refined results using the generated data sets with 0.6 % noise deviated from the generators between 0 and 12 %. The noise that was introduced was considerably more than that encountered experimentally. Thus, the deviations of the latter are expected to be less. The percent "recovery" of Ni (II) lies within experimental error. The means and standard deviations for each of the four rate constants from successive simulations with randomly varying noise are presented in Table IV. These show reasonable variations, and will be used in discussion of the trends observed for experimental data below.

TableIII: A four component simulation with estimates and NLR refinements as obtained using the adopted approach as described in section C of Chapter 3. [a]

Parameter	Simulation Generators	Laplace Trial Values	NLR Refinement
C1	1.67	1.43	1.77
k1	0.700	0.540	0.606
C2	1.67	1.66	1.78
k2	0.153	0.170	0.157
C3	0.837	0.913	0.830
k3	0.0100	0.0095	0.0102
C4	0.609	0.944	0.617
k4	0.0022	0.0031	0.0023
X	2.13	1.63	2.09
Percent Recovery	100.0%	95.1%	102.4%

[a] Noise level was 0.6%, and t_0 offset was + 0.15 seconds. (Time values used were borrowed from a pH = 6.4 run with a FA to Ni ratio of 4). The terms k1 through k4 are the rate constants. Concentrations in moles per liter X 10^6 are represented by the C terms. Total concentration is 5.0 X 10^{-6} M.

Table IV: Means and standard deviations of the four rate constants recovered from 8 simulations with noise after application of the approach described in section C of Chapter 3. [a]

Parameter:	k1	k2	k3	k4
Mean:	0.6746	0.1375	0.0098	0.0020
Standard Deviation:	0.0624	0.0195	0.0015	0.0006

[a] Rate constants are in units of $sec.^{-1}$.

Table V: Four five component simulations with estimates and NLR refinements as obtained using the adopted approach as described in section C of Chapter 3.[a]

Par.	Gen.	Est.	NLR	Gen.	Est.	NLR
C1	0.500	0.530	0.587	0.120	0.110	0.126
C2	0.070	0.118	0.091	0.035	0.039	0.035
C3	0.020	0.0245	0.020	0.020	0.0205	0.018
C4	0.010	0.0135	0.0051	0.014	0.0084	0.009
C5	0.200	0.197	N/A	0.026	0.0349	N/A
X	0.260	0.260	0.245	0.184	0.187	0.186
C1	0.050	0.042	0.042	0.110	0.096	0.109
C2	0.070	0.075	0.0718	0.050	0.051	0.050
C3	0.050	0.0374	0.0515	0.021	0.019	0.020
C4	0.050	0.0509	0.0383	0.017	0.0123	0.0116
C5	0.150	0.169	N/A	0.039	0.0504	N/A
X	0.250	0.300	0.293	0.184	0.191	0.183

[a] These were not seen in the preliminary experiments from which the procedure was established. The limitation of the NLR to three components excluded its extension to C5. C parameters were in absorbance units, and k parameters were in $sec.^{-1}$, values for which are those obtained from the experimental results.

Table VI: Means and standard deviations of the four rate constants recovered from 4 simulations with noise after application of the approach described in section C of Chapter 3. Rate constants are in $sec.^{-1}$.

Parameter	Rate constant	Mean.	Standard deviation
k1	0.70	0.742	0.0275
k2	0.15	0.159	0.0098
k3	0.022	0.0246	0.0017
k4	0.0026	0.00546	0.00125

Data simulated to correspond to that acquired from the photodiode array spectrophometer (Hewlett Packard model 8452) were made similar to the above simulations and are presented subsequent to the results for the experimental results obtained using the Perkin-Elmer 552 spectrophotometer. Four examples of these simulations are tabulated in Table V. It does not contain the results for the rate constants which were identical for each of the simulations. These are presented in Table VI as the means with their standard deviations. These too were accompanied by randomly generated noise. The 0.6% noise level was used even though experimental noise levels are less with the HP8452.

B. Smoothing:

The natural log of the absorbances as measured manually was plotted against the natural log of time, an example of which is presented in Figure 4. The curves so obtained were reproduced by using the smallest n-th degree polynomial which would faithfully reproduce the curve. The data in Figure 4 were subjected to a seventh degree polynomial. Fitting was done using a least squares polynomial fitting routine in the ASYST software package (111). Choosing the lowest order polynomial in each case reduced the over-reproduction of the data, including digitization errors,

Figure 4: Result of smoothing stripped data of Figure 9 using log-log data and a seventh degree least squares polynomial fit.

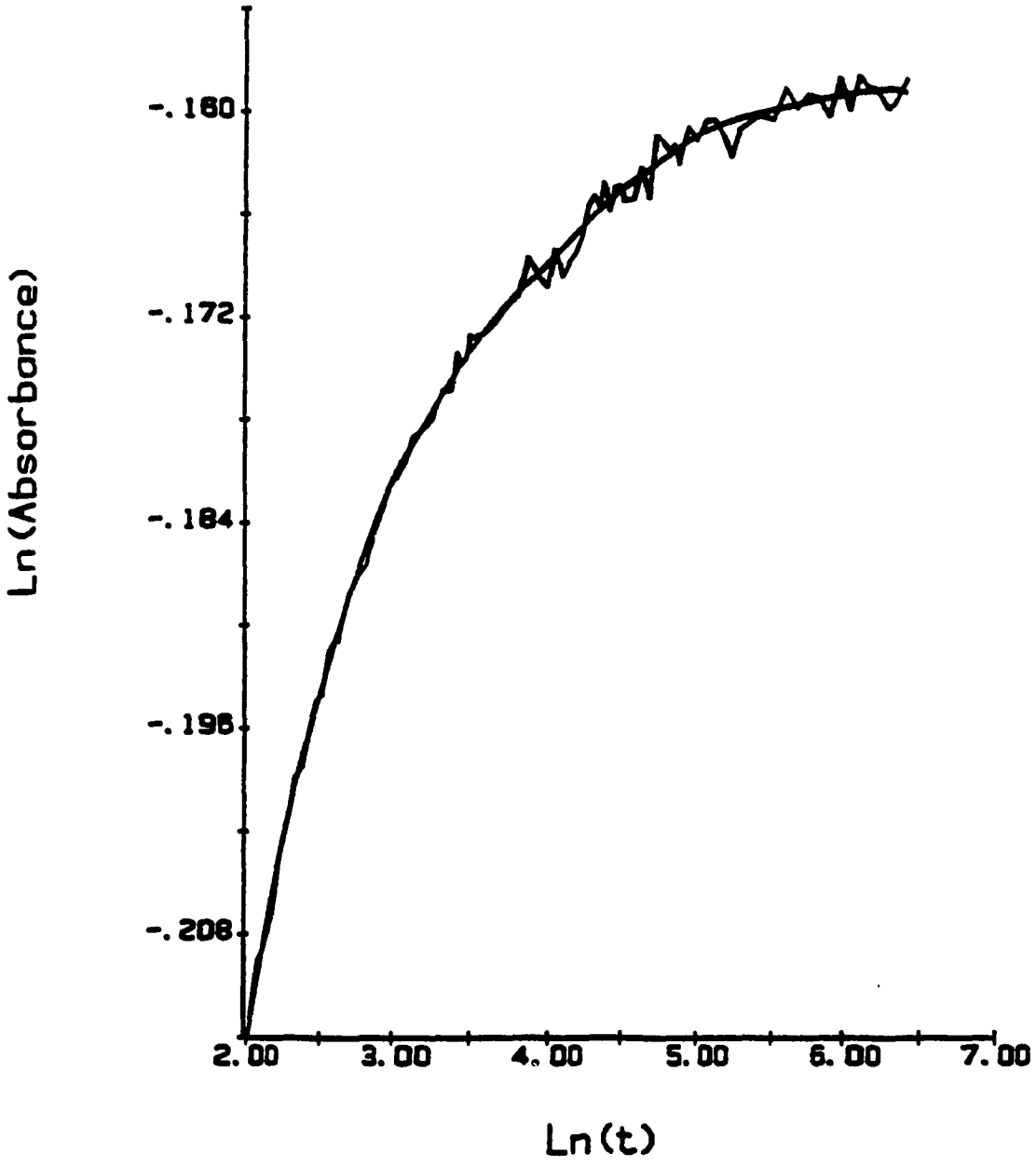

when using a cubic-spline routine. The logarithmic coordinates tend to "optimize" the data for a polynomial fitting. The graphics programs were also built-in features of the ASYST package used for most of the processing on an IBM-PC equipped with an 8087 mathematical co-processor. Graphical printouts were obtained using a Hewlett-Packer HP7470 XY-plotter.

C: Estimating input rate constants:

A Laplace transform profile, which was smoothed using a seventh degree least squares polynomial fit, is shown in Figure 5. It is one of the better cases of five simulations made to mimic the HP8452A output and data reduction scheme, which includes five components, and an X-term, with 0.6% noise. In this example, the first component had been truncated and the fifth component stripped prior to the application of the Laplace routine. In Figure 6, a separate simulation produced less obvious peaks, albeit estimates were accessible.

Following the Laplace transformation of data recorded for reactions which had gone to completion, four distinct components were usually observed in the time-related distributions. However, due to small differences in rate constants (e.g. 0.6 and 0.2 $sec.^{-1}$), peaks overlapped. This

Figure 5: Laplace transform profile (smoothed) for a five component simulation with 0.6% noise added. The first component was truncated and the fifth stripped as explained in this chapter. (generators were: C2 = 0.10, k2 = 0.15 ; C3 = 0.10, k3 = 0.022 ; C4 = 0.10, k4 = 0.0026, where C values are in absorbance units and k's in sec.$^{-1}$.)

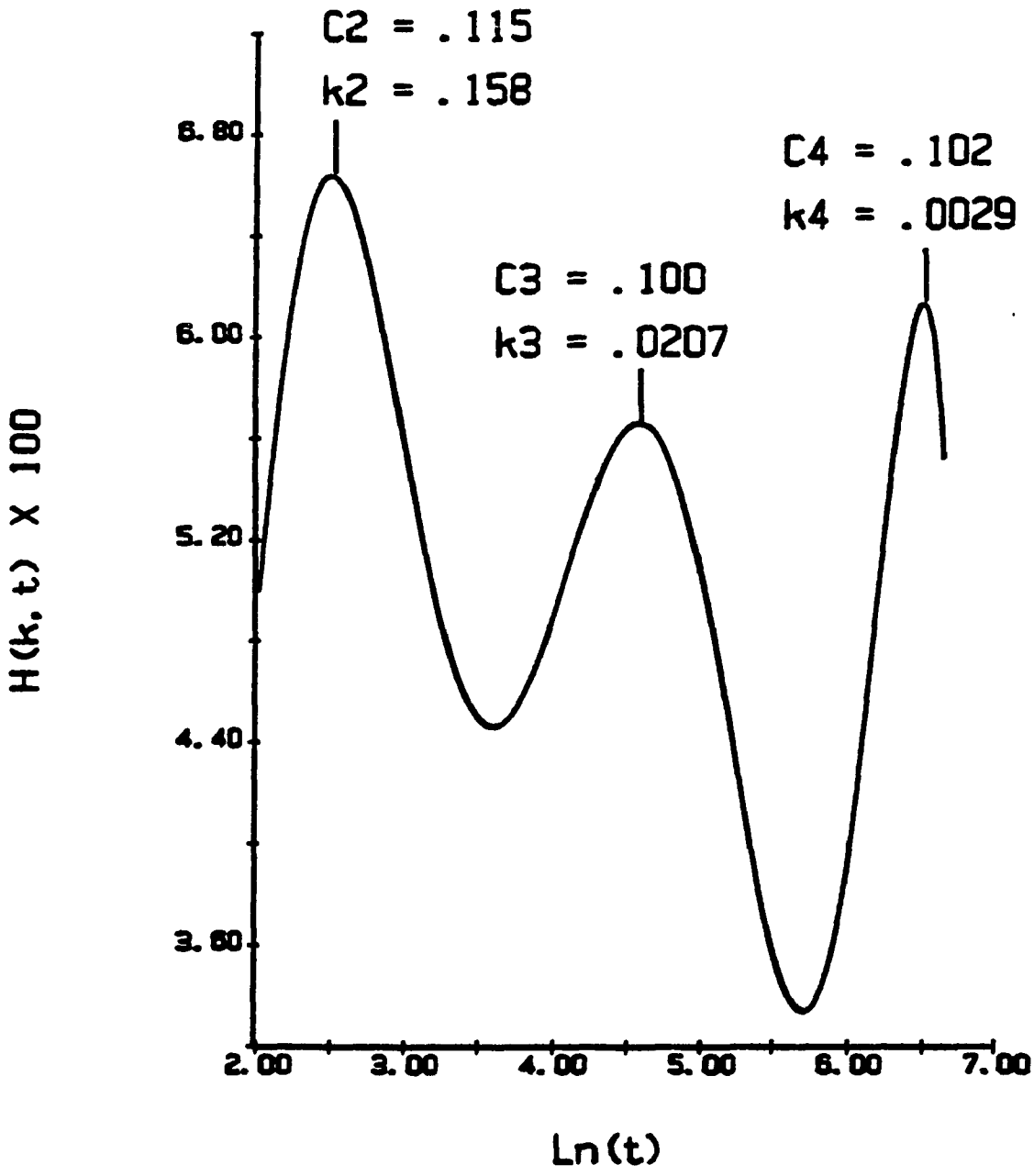

Figure 6: Unsmoothed Laplace transform profile of a five-component poorly resolvable data simulation from which the first component was truncated and the fifth stripped as explained in this chapter. (generators were: C2 = 0.07, k2 = 0.15 ; C3 = 0.02, k3 = 0.022, where Cvalues are in absorbance units and k's in sec.$^{-1}$).

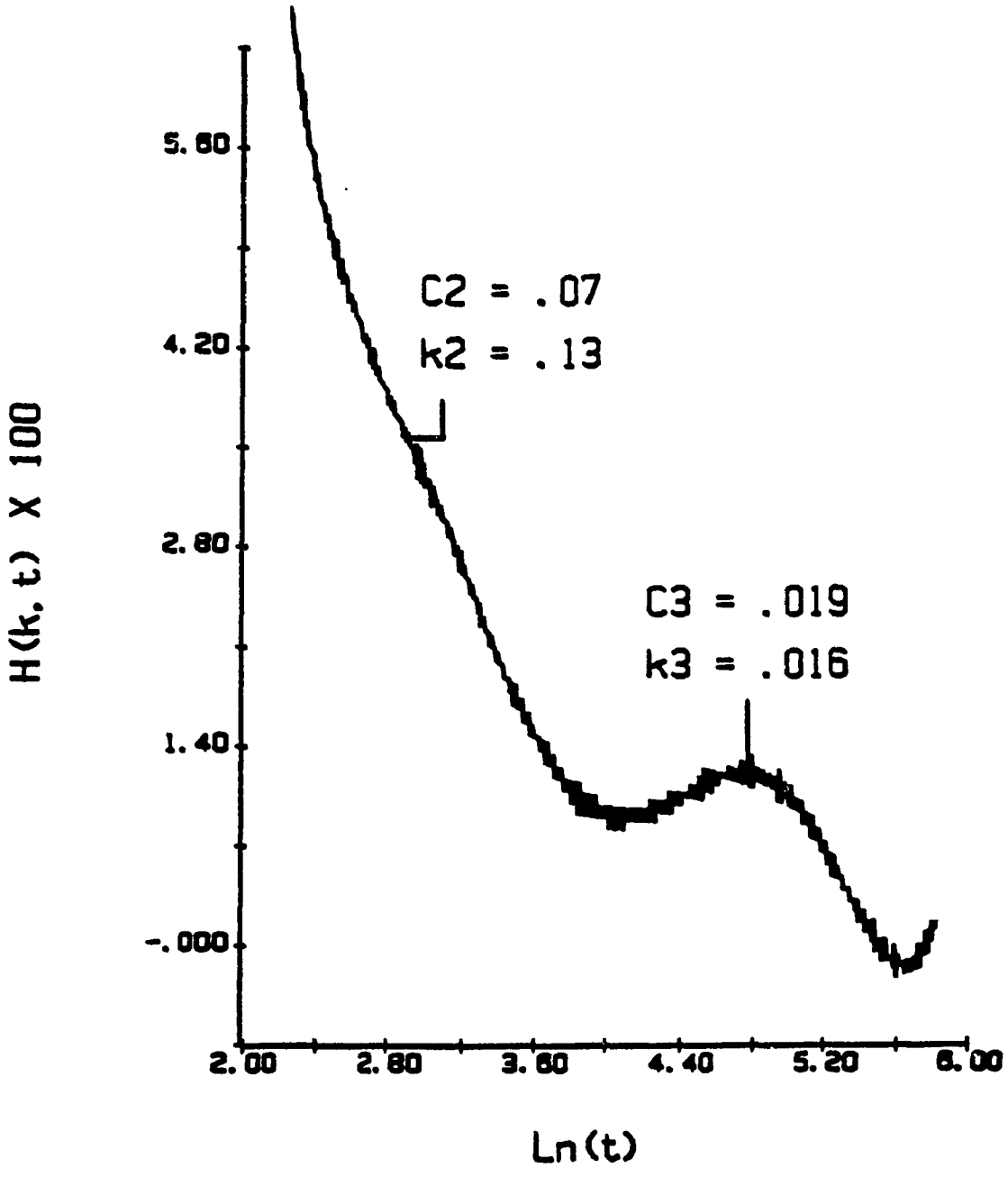

necessitated establishing a standard approach for the evaluation of the minimum number of distinct components required to model the Ni(II)-FA equilibrium. The procedure adopted is the following.

Step (i). The value of t corresponding to a maximum in a curve derived through the Laplace transform method is used to estimate the rate constant of that component as 2/t = k(i). In the case of solutions containing only Ni^{2+} (aq.), the maximum appeared at a time value of 3.2 seconds, or a k_{Ni} of approximately 0.62 sec^{-1}. Therefore, after an elapsed time of only 7 seconds, >98% of the free-Nickel has been accounted for and it is essentially absent from the remaining data. It was found that the time value corresponding to the second peak averaged 14.3 seconds, k2 approximating 0.14 sec^{-1} , and data from 7 seconds onward represents complexed species only when fulvic acid is present. The seven first seconds are analysed separately because of their sensitivity to the t = 0 error of $\pm$ 0.25 sec. and the overlapping of the first two peaks.

There was no ambiguity in assigning the various parameters to the synthetic data when using the approach. However, minor alterations in the usual procedure, such as using a cutoff time of 6.5 seconds rather than 7 for the truncation of the first component, was sometimes required in order to improve on the quality of the resolution of the Laplace spectra, and limit the time required for final

iteration of the NLR results.

Step (ii). Once the first component with its known K1 has been removed the slowest component is estimated from the plot of $\ln(A_\infty - A_t)$ using the linear "tail" section of the plot where only the slowest component contributes. The data are stripped by applying a negative term according to Equation 1.3 using the rate constant obtained from the slope and it's coefficient from the intercept of the line at t = 0. Since any further stripping induces significant accumulating distortion, the remaining components are obtained directly from the Laplace spectrum.

The stripping step usually increased noise levels, in the sense that subsequent estimates become further removed from the correct values. Figure 7 presents, for the same data simulated for Figure 5, the semi-logarithmic plot of Ln $(A_\infty - A_t)$ versus time showing an obvious linear trailing section which was used, as blown-up in Figure 8, to estimate the fifth component. In Figure 9, the effect of stripping the estimated fifth component from the original data is shown. The application of the smoothing routine to the noisy stripped data is illustrated in Figure 4. It suffices to mention here that when doing log-log stripping of kinetic components from absorbances versus time data that if the resulting stripped log-log kinetic curve tends significantly to "descend" after a rise, this indicates that too much of the said component has been stripped and the procedure should be repeated using a smaller section of the

Figure 7: Example of a semi-logarithmic plot of $Ln(A_\infty - A_t)$ vs time for the same data set as in Figure 5. (generated C5 was 0.01 absorbance units , and k5 was 0.00009 $sec.^{-1}$).

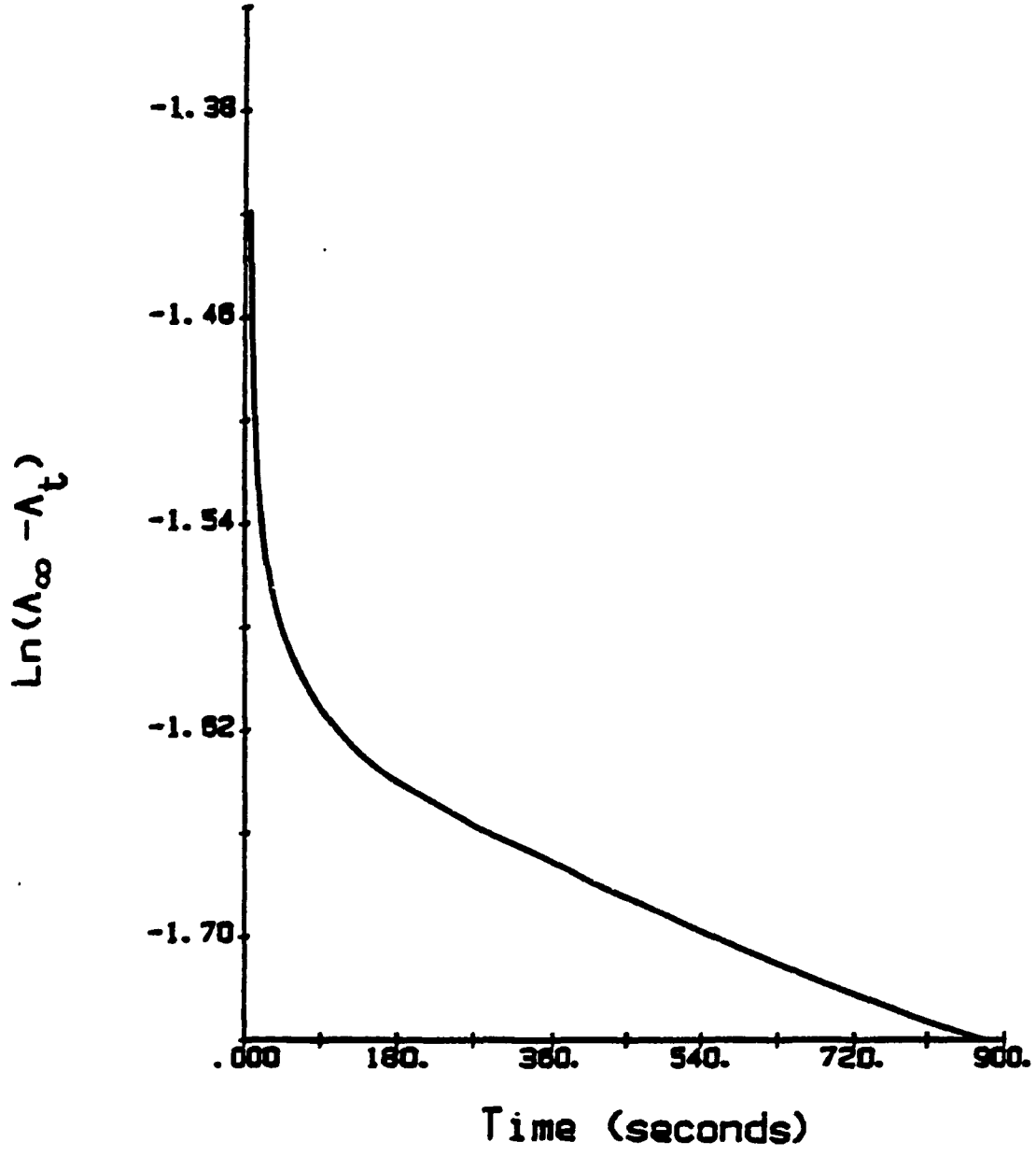

Figure 8: Expanded view of the trailing linear section of the semi-logarithmic plot of Figure 7 used to estimate the fifth component. (generator was C5 = 0.01 absorbance units and, k5 = 0.00009 sec.$^{-1}$).

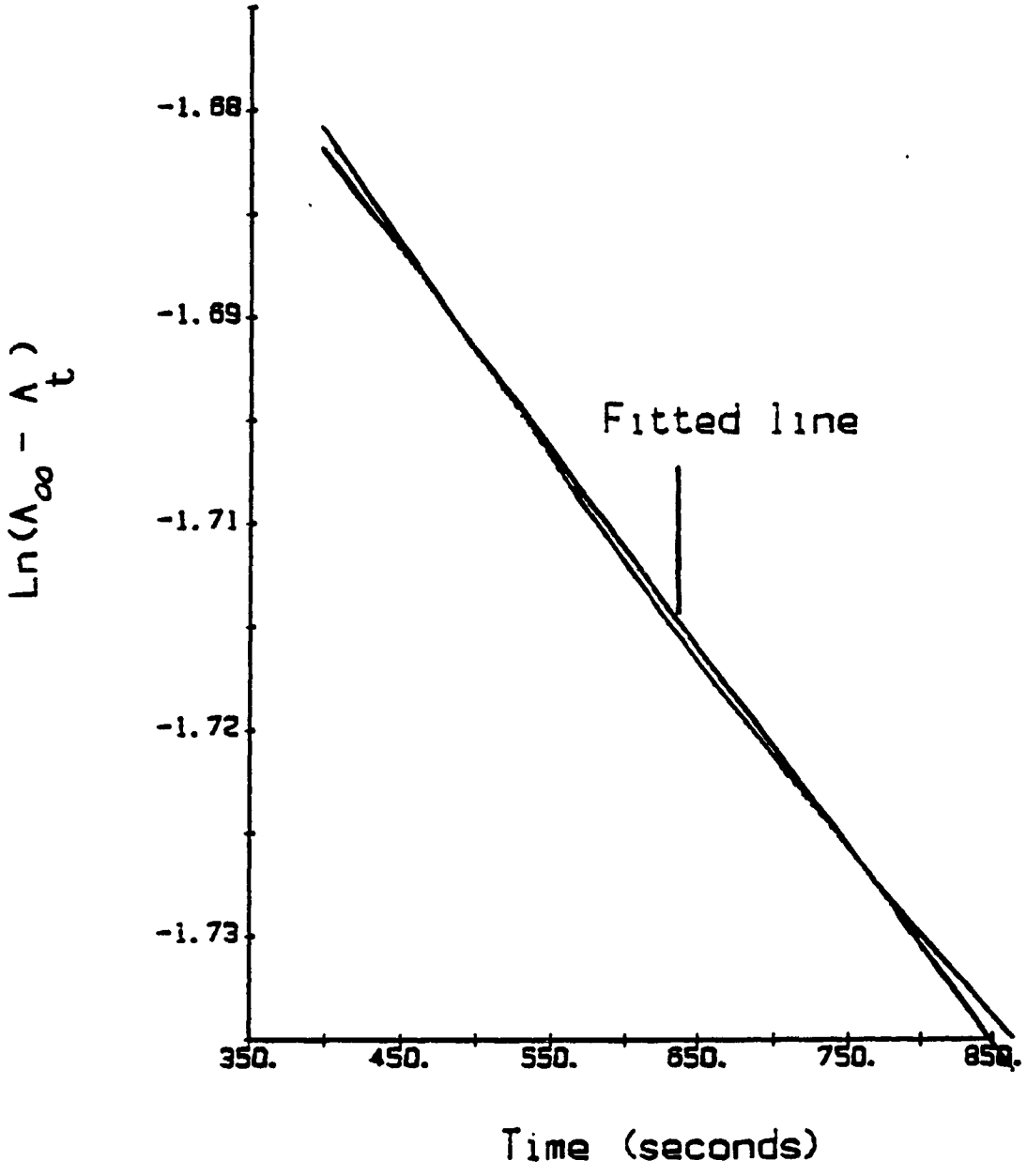

Figure 9: Log-log plot of absorbance vs time of original data as in Figure 5 and of data from which the fifth component was numerically subtracted.

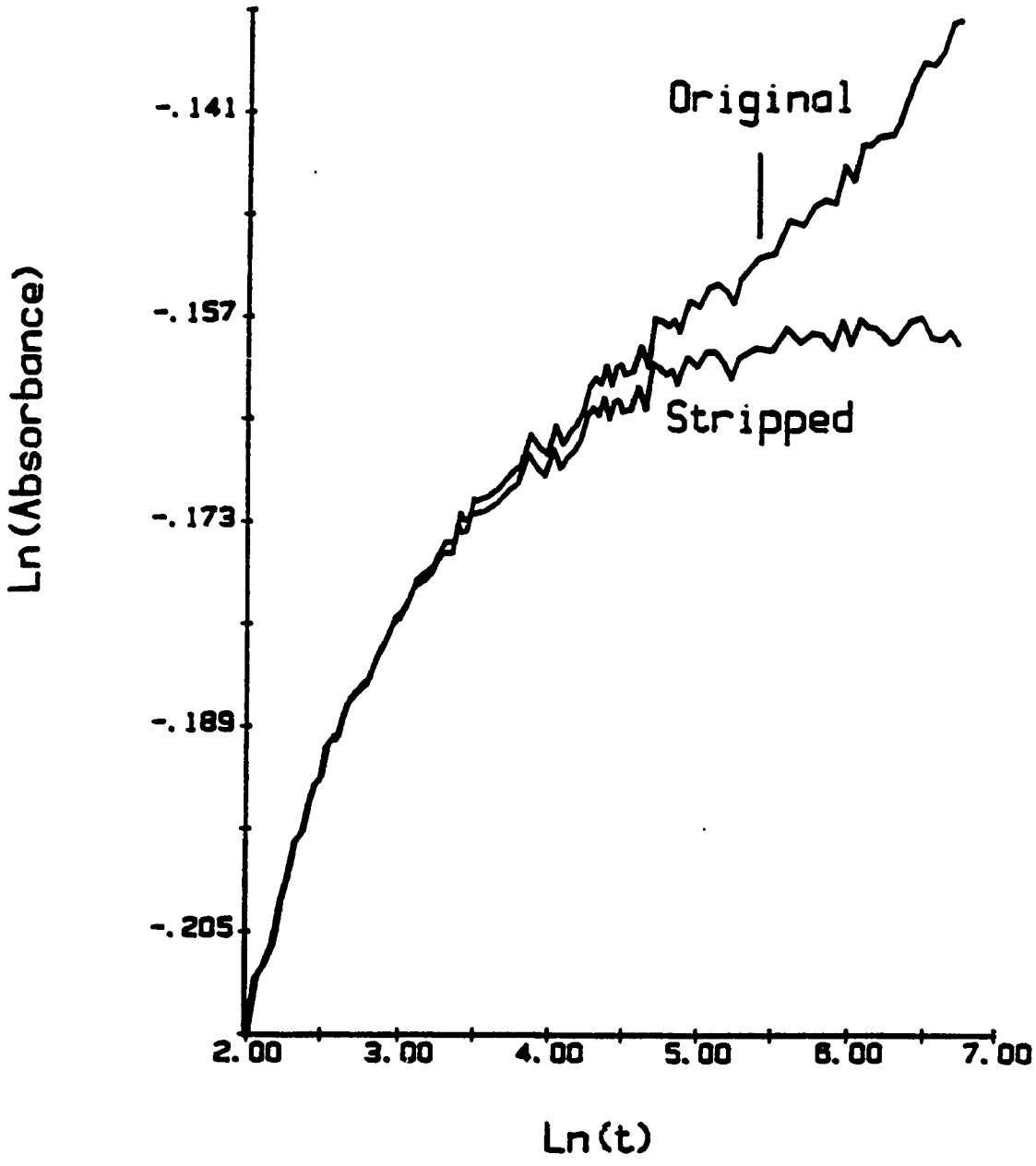

initial trailing end of the semi-logarithmic plot. Conversely if the stripped curve "levels-out", this is a good indication of a reliable estimation, since this signifies that A_t is a constant and the remaining reaction is complete.

Olson and Shuman (91) define the width of a peak at half-height, $H(k,t)_{max/2}$ to have the value $(\ln k)_{1/2} = 1.6973$. We have used this number in the calculation of the area of a triangle used to approximate the area under the curve represented by the peak. Peak height was found to be the best and simplest parameter to use for estimating the initial concentrations of the various components.

On a very few occasions, a fifth component was found. This was stripped out as described for the fourth. It is mentioned but not reported as a component due to ambiguity and irreproducibility of this very small component.

Step (iii). The parameters of the second and third components obtained after step (ii) were used to strip the data and retrieve the C(0) of the free aquo Ni (II) component, and check agreement with the independently determined k1.

The combination of data stripping with the Laplace transform permits resolution of four peaks (components). The analysis described worked extremely well on synthetic data over a reasonable parameter range in the presence of noise.

The X-components (blanks) of equation 1.3 were esti-

mated by extrapolation of a third degree polynomial fitted to the first 6 data points of unaltered untruncated data. These values for the respective X-components were used in all applications of a nonlinear regression to subsequent components.

When acquiring data from the HP 8452A spectrometer, as was the case only for the fluorescence quenching experiments, the two collected files described in the experimental section were reduced to approximate logarithmic spacing similar to chart reading spacings as explained previously. It was often found that in the case of the reduced data from the HP 8452A that all four components were immediately visible from its Laplace transform spectra without prior truncation of the first component. Therefore no semi-logarithmic stripping of the last component was then required for estimation purposes, but it was performed nevertheless. In order to apply the NLR routine, which was limited to three components, the first component was truncated as described previously. In addition, upon application of the semilogarithmic plotting of $Ln(A_\infty - A_t)$ vs time, a fifth component was sometimes seen (in the case of the HP8452A only), which was stripped out as explained earlier to reduce the data to a three component system.

CHAPTER 5: EXPERIMENTAL RESULTS

A: Fulvic acid-nickel speciation results.

We begin with a presentation of the qualitative form of the experimental results.

Figures 10 and 11 show a selection of raw experimental data for single runs of absorbance vs time. The respective X-components of Equation 1.3 were removed since these vary with FA:Ni ratio and would otherwise obscure the comparison of the actual rates under varying conditions. In Figure 11, which shows influence of the pH on the reaction's progress, the differences between a pH of 4 and 5 are slight, whereas at a pH of 6.4 the conversion after 200 seconds is decreased dramatically. This is also seen in the results after the kinetic analysis of the various species observable and will be discussed later. The present direct visual indication increases confidence in the important result to be presented later.

Experimental data were treated in the manner validated on the synthetic data and the results of the mean and standard deviation for each of the four rate constants observed are presented in Table VII. It can be seen that the deviations for experimental data are somewhat greater than those of the synthetic results in Table IV.Since the noise levels are less than is the case in simulations, this

Figure 10: Representative single run experimental data, with "X-components" (see Equation 1.3) removed, of absorbance vs time illustrating the effect of changing the the FA:Ni(II) ratio.

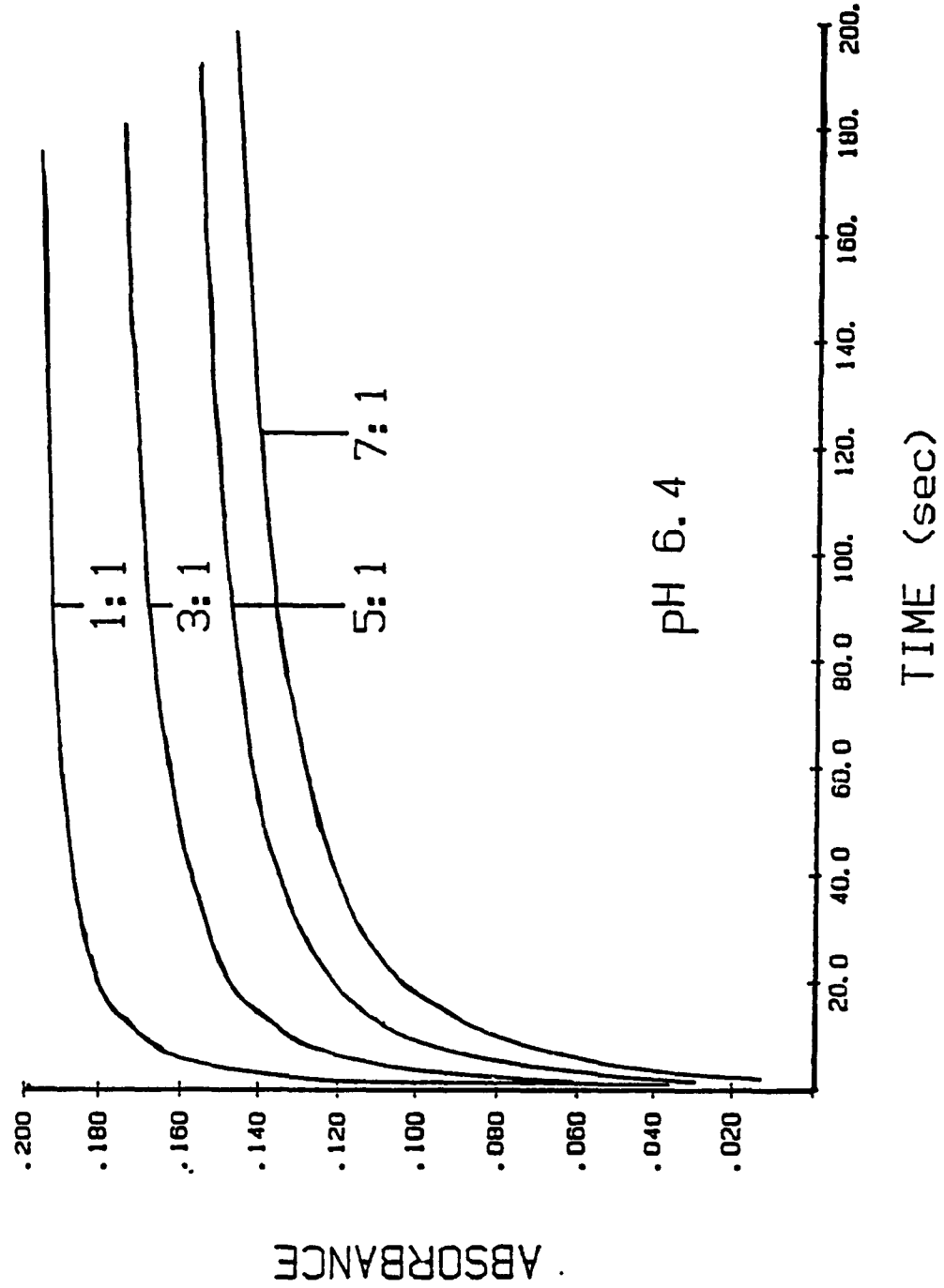

Figure11: Representative single run experimental data, with "X-components" removed, of absorbance vs time illustrating, for a fixed FA:Ni(II) ratio of 5:1, the effect of changing the pH of equilibration. Note especially the reduction of recovery of Ni(II) after 200 seconds at the equilibrium pH of 6.4.

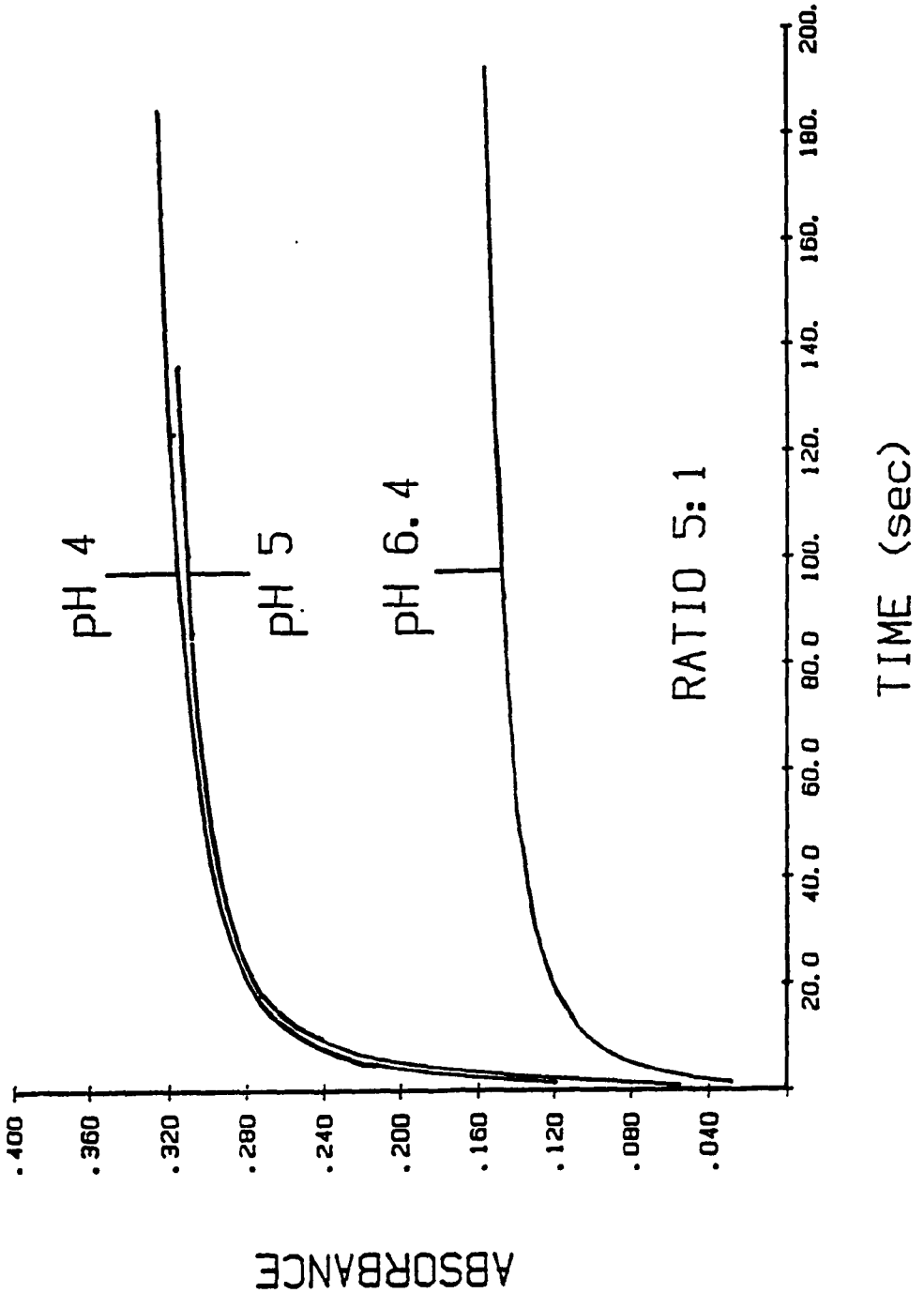

Table VII: Mean and standard deviation for each of the four rate constants encountered with the experimental data sets as a function of pH, and as a pooled, pH-independent, group. [a]

Parameter:		k1	k2	k3	k4
pH 4	m	0.6146	0.1531	0.0208	0.0021
	s.d.	0.1662	0.0364	0.0080	0.0009
pH 5	m	0.6990	0.1386	0.0203	0.0032
	s.d.	0.1332	0.0313	0.0078	0.0015
pH 6.4	m	0.5331	0.1316	0.0197	0.0018
	s.d.	0.0955	0.0258	0.0064	0.0009
POOLED	n	40	39	40	24
	m	0.6693	0.1467	0.0205	0.0026
	s.d.	0.1578	0.0384	0.0082	0.0010

[a] The terms n, m, and s.d. are abbreviations for the number of runs, the mean, and the standard deviation respectively.

may be further indication that the mixture ligand, fulvic acid, does not consist of four discrete components, The k's probalbly represent averages over a distribution of related components. The number of results reported in Table VII for the fourth rate constant, k4, is less than that of the other three. A complete NLR routine rewuires that the three last components be fitted to the original, albeit truncated, data. However this was not always possible. When such was the case, the two middle components (i.e. k2 and k3) were fitted to data stripped of the estimated fourth component. Although such results were not considered final, the rate constants so obtained were reasonable are were used for the statistical reporting in Table VII.

Figure 12 presents an example of a Laplace profile used to assign components and obtain initial estimates. Table VIII lists both the estimates extracted from figure 12 and the resulting NLR refined values for the same run at pH 6.4 and a 1:1 FA to Ni ratio. Note that values presented for concentrations in figure 12 are actually in terms of absorbancies and refer to the kinetic solution conditions (i.e. double those of the kinetic conditions).

The four components are the minimum number of distinct components required to model the FA - Ni(II) equilibrium, and it must be recognized that these components

Figure 12: Laplace spectra of the last three components of experimental data of Table VIIIfor a run at pH 6.4 and a FA:Ni(II) ratio of 1:1 after truncation of the first component. H(k,t), and C, values are expressed in terms of absorbancy changes of the kinetic reaction. Rate constants are in sec.$^{-1}$.

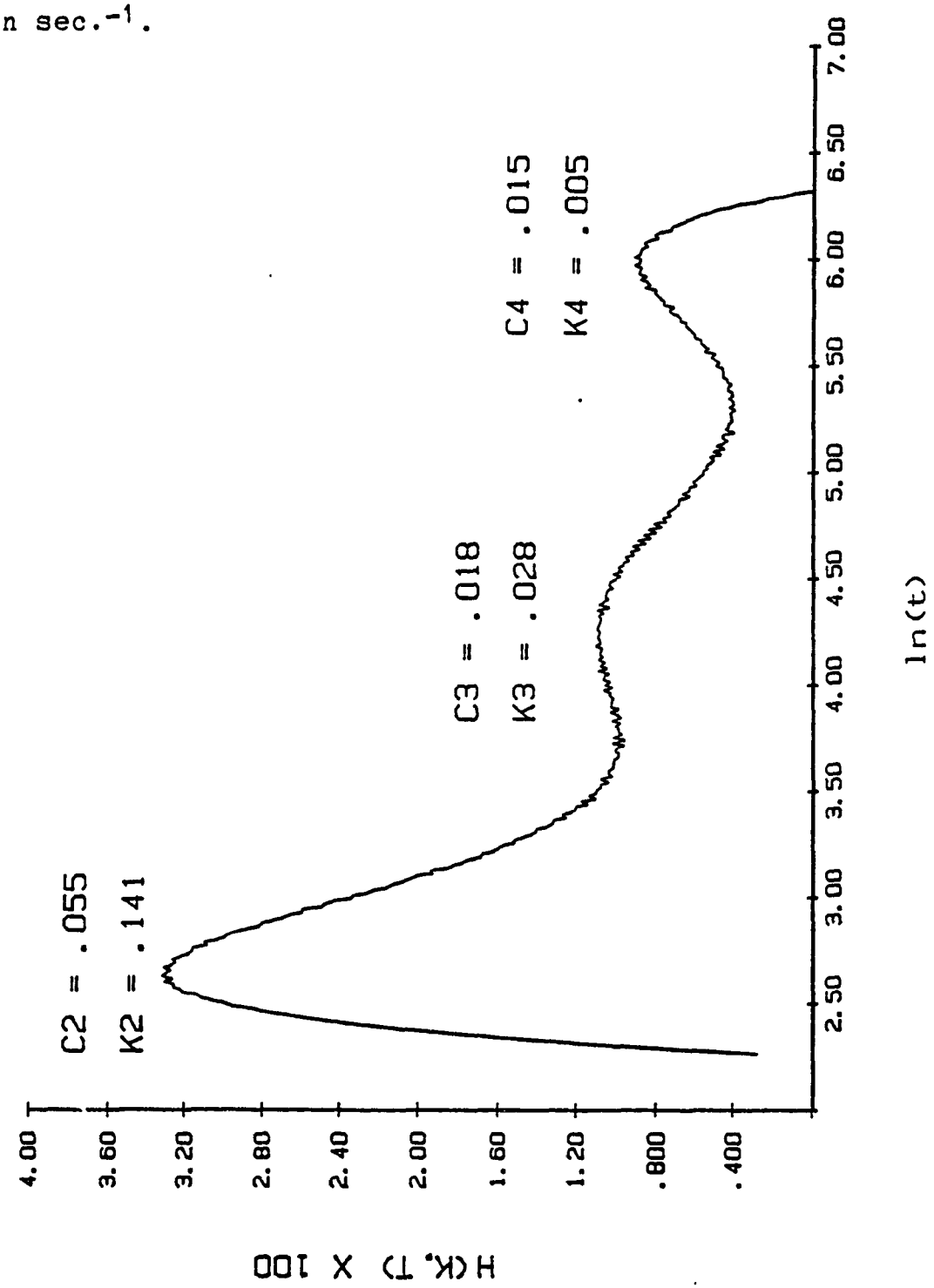

Table VIII: Results for the estimates for the four component model and the NLR calculations of an experimental run at pH 6.4 and an FA:Ni(II) ratio of 1:1.[a]

Parameter	Laplace Trial Values	NLR-refinement
C1	3.64	3.04
k1	0.404	0.512
C2	1.66	1.26
k2	0.140	0.125
C3	0.590	0.490
k3	0.028	0.019
C4	0.456	0.396
k4	0.0019	0.0026

[a] Concentrations (C) are in moles per liter X 10^6 and are for the equilibrium conditions. Rate constants are in $sec.^{-1}$.

(rate constants) could very well be means over three distributions of components since we are dealing with a mixture ligand, fulvic acid. Only the $Ni(OH_2)_6^{2+}$ component is known to be a well defined molecular unit.

The mechanism of the Ni^{2+} reaction is confirmed by some approximate predictive calculations. The anticipated mechanism is:

$$Ni(OH_2)_6^{2+} + PAR \overset{K_E}{\rightleftharpoons} Ni(OH_2)_6^{2+},PAR$$

$$Ni(OH_2)_6^{2+},PAR \overset{k_1}{\rightleftharpoons} Ni(OH_2)_5PAR + H_2O$$

with the latter being the rate determining step. K_E can be predicted to be of the order of 1, whereas k_1 should be aprroximated by the water exchange rate constant divided by either 4 ot 8 if the substitution is dissociative. The water exchange rate constant for Ni^{2+} is about 2×10^4 $sec.^{-1}$ such that k_1 should be about 5×10^3 $sec.^{-1}$. The rate law for dissociation is:

$$rate = K_E k_1 [Ni^{2+}] [PAR] \qquad [5.1]$$

As [PAR] is 2.5×10^{-4} M, pseudo-first-order kinetics will be observed (since Ni^{2+} is 5×10^{-6} M), the rate expression then becomes:

$$\text{rate} = k_{obs} [\ Ni^{2+}\ ] \qquad [5.2]$$

where: $$k_{obs} = K_E k_1 [\ PAR\ ] \qquad [5.3]$$

which calculates 1 $sec.^{-1}$ for k_1. This result, from theory, is quite close to the experimentally observed value of 0.67 $sec.^{-1}$.

Cu^{2+} is the most popular ion in speciation studies. In our case, using conventional kinetics, it is desirable that rate constants be at most 1.5 $sec.^{-1}$ in order to be resolvable. Since Cu^{2+} complexes (d^9) are usually structurally distorted, the ground state has almost attained the dissociative transition state structure, and axial water molecules exchange very rapidly since they are held weakly. The water exchange rate for Cu^{2+} is about 10^8 $sec.^{-1}$ making any ligand exchange rate approximately 10^4 times that obtained for Ni^{2+}, such that Cu^{2+} would have a rate constant with PAR in the order of 6.6×10^3 $sec.^{-1}$, much too fast for conventional kinetics. Stopped-flow has been used elsewhere (100), but the back-diffusion of reactants in a normal set-up would occur on the time scales required for the reaction of any slower components in Equation 1.3, rendering them undeterminable.

Since there is no evidence of change for the four rate constants (or their standard deviations) with a change of pH of equilibration or of FA:Ni ratio, the components of the samples which are identifiable by kinetic analysis (at

a pH of kinetic reaction of 7.8) are necessarily the same regardless of pH of equilibration or FA:Ni ratio. In the work on the Al(III) hydrous oxide - fulvic acid system (87), rate constants were found to be a function of equilibration pH. The present result indicates a simpler pattern of speciaiton for the FA-Ni(II) system, similar to that found for the Fe(III) - FA system (86). In this sense, the four components represent a "physical model" of the speciaiton if it is clear the teh term "physical model" is not intended to deny the heterogeneity of the fulvic acid ligand system. The emphasis is on the word model in the sense that the four components might function well as the terms in a predictive equation for the new conditions (same k values regardless of pH and concentrations).

Figures 13 through 15 show the concentration trends (molar) of the four species, the actual numerical values of which are presented in Tables IX through XI. Notice that the concentration profiles for the species do change with equilibration pH , as expected. The results averaged a 100.0 % recovery for all the pH 4 and pH 5 sets (Figures 13 and 14) but not for the pH 6.4 set (Figure 15) whose results averaged a 60.2 % recovery. This will be further discussed later. As there were again no visible trends to the percent recoveries at any particular pH, use of the averages was taken as a valid normalization procedure in the case of the pH 4 and pH 5 sets. The free aquo species is represented by the first component with a rate constatn of 0.62 $sec.^{-1}$.

Figure 13. Profiles of individual concentrations at equilibrium of the four component model with respect to the FA:Ni(II) ratios at a pH of 4.0. Note, concentrations after dilution with the PAR reagent solution are half these values.

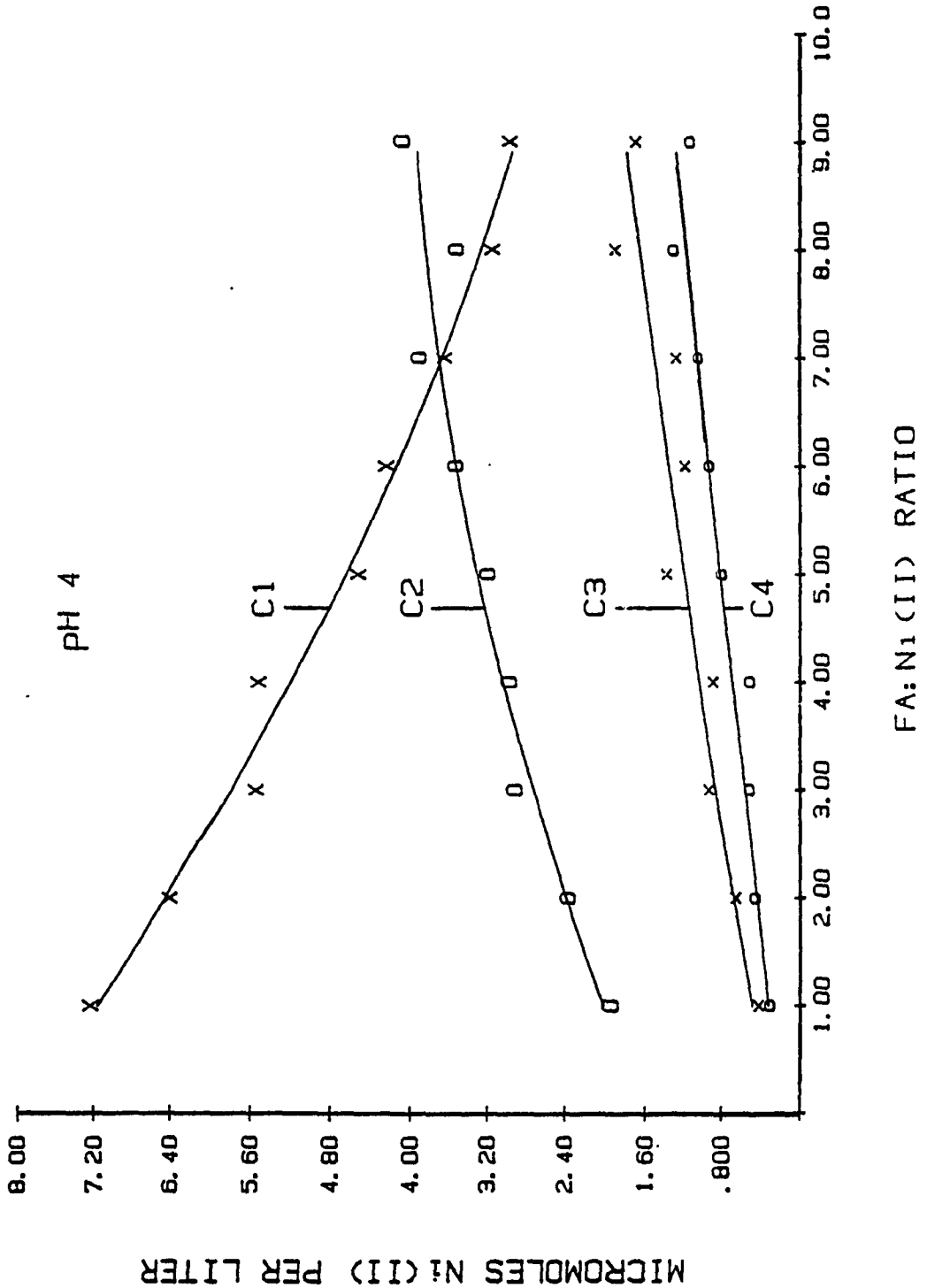

Table IX: Normalized results for the kinetic concentrations of the four species reported for pH 4.[a]

FA:Ni(II)	C1	C2	C3	C4
1:1	3.62	0.970	0.231	0.175
2:1	3.21	1.19	0.346	0.251
3:1	2.78	1.47	0.478	0.279
4:1	2.77	1.50	0.455	0.277
5:1	2.27	1.61	0.704	0.413
6:1	2.13	1.78	0.610	0.478
7:1	1.84	1.97	0.655	0.538
8:1	1.59	1.78	0.958	0.669
9:1	1.50	2.06	0.860	0.584

[a] Concentrations are in moles per liter X 10^6. Rate constants are in $sec.^{-1}$.

Figure 14. Concentration profiles for an equilibration pH of 5.0.

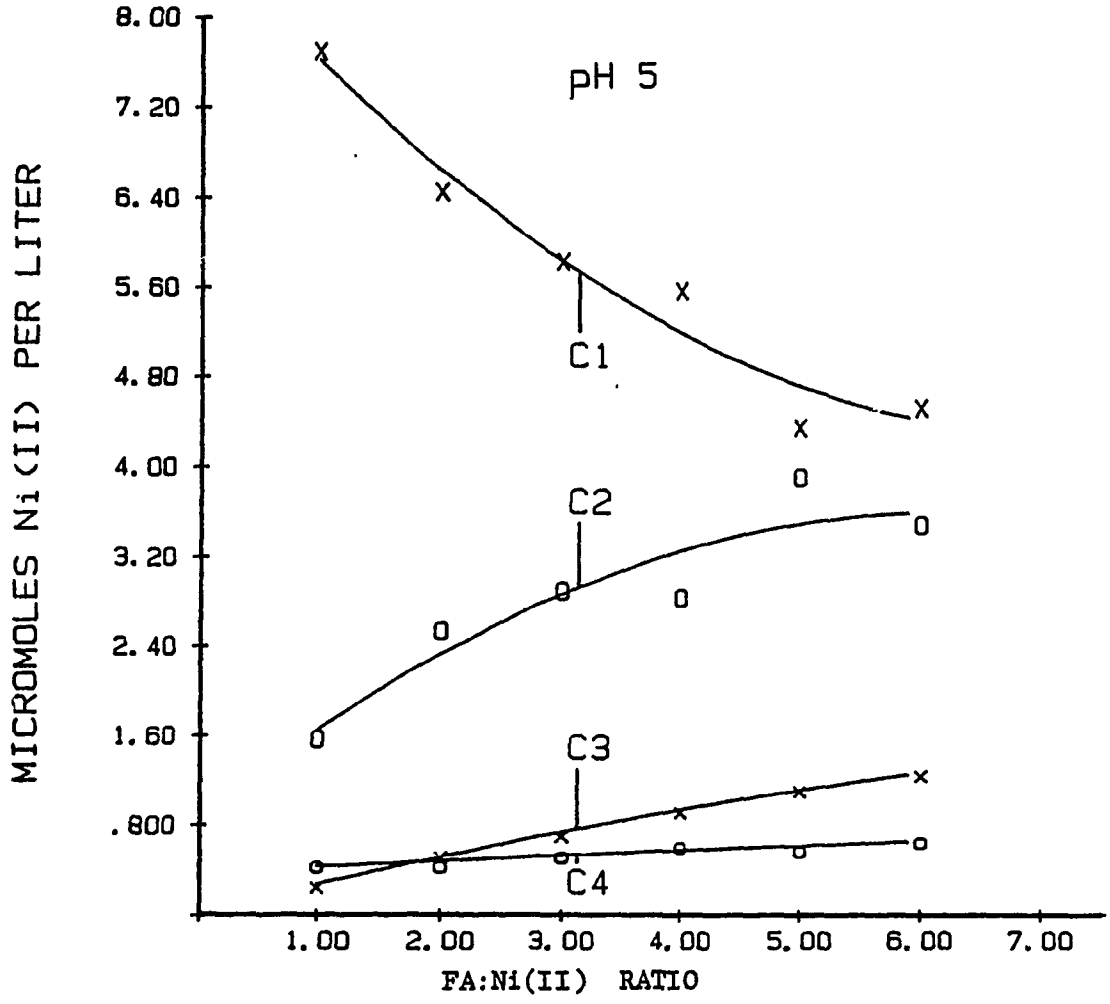

Table X: Normalized results for concentrations under kinetic conditions for the four species reported for pH 5.[a]

FA:Ni(II)	C1	C2	C3	C4
1:1	3.85	0.785	0.227	0.137
2:1	3.23	1.27	0.228	0.272
3:1	2.92	1.45	0.271	0.364
4:1	2.79	1.42	0.315	0.472
5:1	2.18	1.96	0.298	0.568
6:1	2.27	1.75	0.337	0.635

[a] Concentrations are in moles per liter X 10^6.

Figure 15: Concentration profiles for an quelibration pH of 6.4.

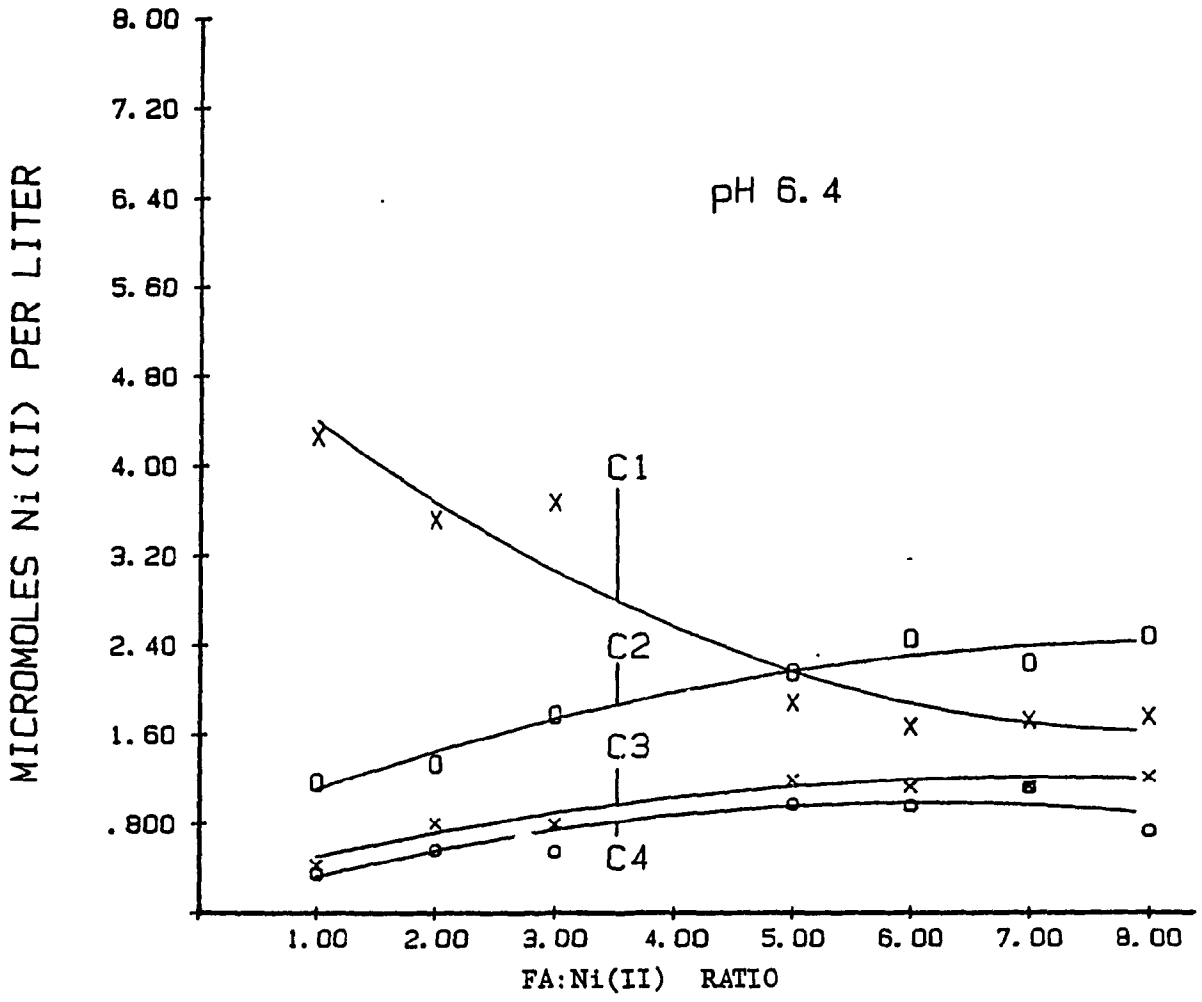

Table XI: Non-normalized results for the concentrations under kinetic conditions for the four species reported for pH 6.4. [a]

FA:Ni(II)	C1	C2	C3	C4
1:1	2.00	0.655	0.227	0.224
2:1	1.76	0.796	0.260	0.292
3:1	1.53	0.996	0.429	0.152
5:1	1.07	0.930	0.405	0.274
6:1	0.828	1.04	0.472	0.393
7:1	0.682	0.965	0.633	0.457
8:1	0.914	1.15	1.07	0.464

[a] Concentrations are in moles per liter X 10^6.

This value was varified using free Ni(II) without any fulvic acid present. The three other components reported model "bound" Ni(II) species, and, as can be expected, the total "bound" concentration increases with a decrease in protonic loading (i.e. an increase in pH where more ligands become available). Percentage recovery after 24 hours was found to be such that for pH's 4 and 5, all the Ni(II) species have reacted with the PAR reagent. At pH 6.4, however, recoveries are about 60 % after 24 hours. 40 % of the Ni(II) at pH 6.4 is shifted to a significantly less labile component, with a corresponding decrease of all the more labile components. The total Ni(II) can, however, be recovered by the PAR after up to 10 days meaning that this is a very slow component with a kinetic rather than a thermodynamic relationship to amss balance considerations.

At pH 4 or pH 5 teh results indicate a $Ni(OH_2)_6^{2+}$ species plus three "bound" species. These three components have reasonably stable and reproducible rate constants and sensible mass action trends as FA:Ni(II) ratios and pH vary. In this sense the results resemble those obtained for Fe(III) (86). They are unlike the Al(III) results (87) where variable rate constants suggested a single continuous distribution of species which cannot be consistently subdivided.

The most interesting result is, perhaps, the one that shows that equilibration of Ni(II) with FA at a pH beyond the titration equivalence point for acid carboxylic

protons leads to a new species which is very much less labile than those formed where proton competition is greater. It is noteworthy that the more labile forms persist but a new relatively non-labile one has been added. The result underlines, once again, the unexpected features that the complex mixture character of humic ligands can confer on their metal complexing.

B: Fluorescence quenching titrations.

Figure 16 presents emission spectra as scanned from 430 nm to 560 nm with an excitation wavelength of 365 nm. In Table XII are the fluorescence intensities for five relevant FA concentrations along with corrections for their absorbancies at the emission and excitation wavelengths of 465 and 365 nm respectively. The resulting calibration curves for both original and corrected fluorescence intensities are presented in Figure 17. The pertinent information which these results furnish towards the experiments performed for this thesis is the measure of the signal to noise increase as the FA concentration is lowered, due to the necessity of increasing the gain of the spectrometer in order to get a full signal.

Initial titrations were performed at the three eqilibrated pH's of 6.4, 5.0, and 4.0 for a fixed FA concen-

Figure 16: Emission spectra of FA scanned from 430 to 530 nm at an excitation wavelength of 365 nm for the five FA concentrations in Table XII.

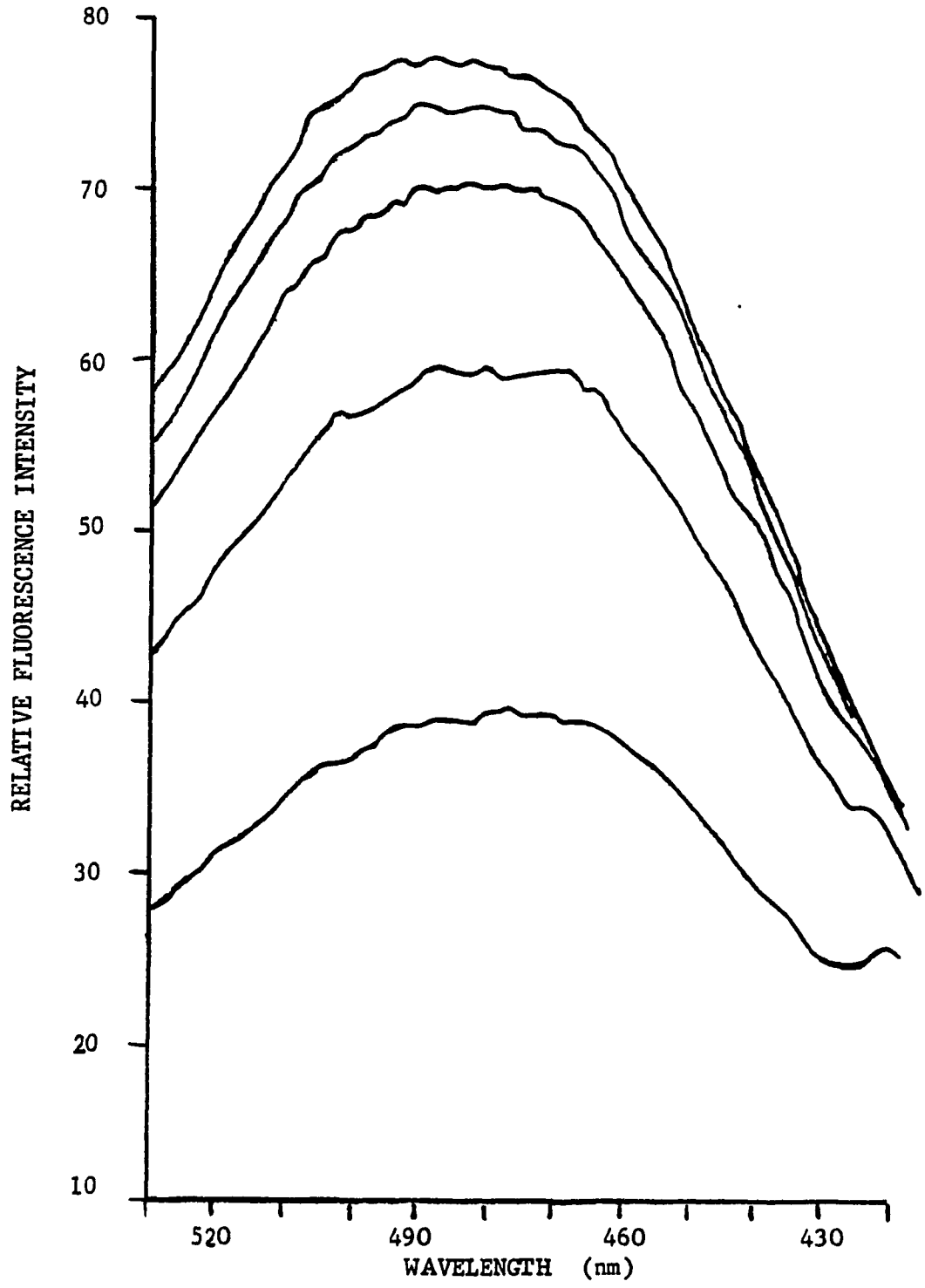

Table XII: Original fluorescence intensities and intensities corrected for absorbancies at the emission and excitation wavelengths.

[FA]^a	Absorbancies		Fluorescence intensity	
	365 nm	465 nm	Original	Corrected
5.0	0.414	0.144	73.0	138.5
4.0	0.330	0.115	71.8	119.7
3.0	0.248	0.087	67.9	99.8
2.0	0.166	0.058	58.1	75.2
1.0	0.083	0.029	38.8	44.3

[a] Concentrations in moles/litre X 10^5.

Figure 17: Original and corrected fluorescence intensities for the 465 nm emission at an excitation wavelength of 365 nm for the five FA concentrations of Table XII.

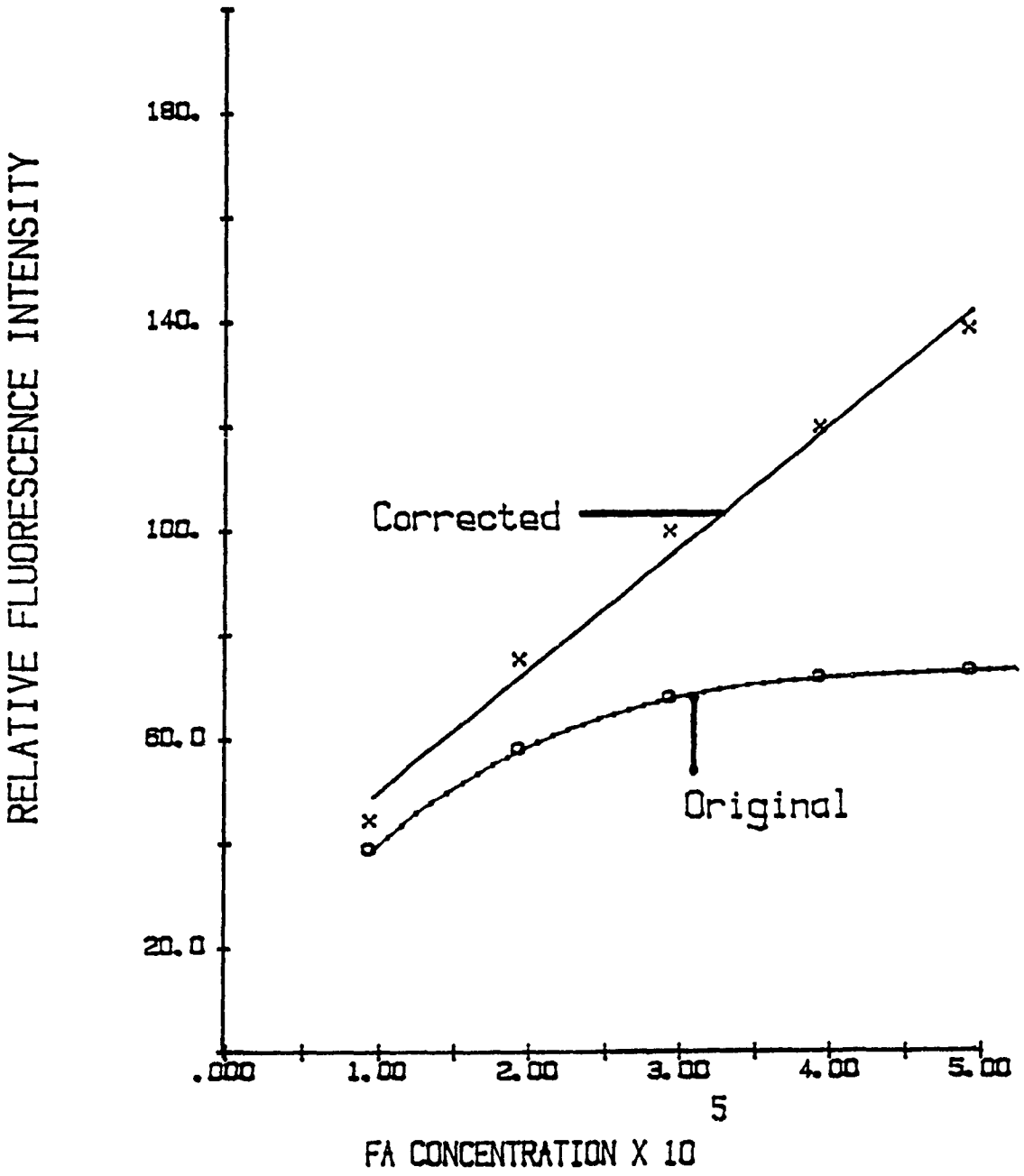

Figure 18: Titration curves for fluorescence quenching by Ni^{2+} of a solution containing 8.0 X 10 $^{-6}$ M FA at the three pH values of 6.4, 5.0, and 4.0.

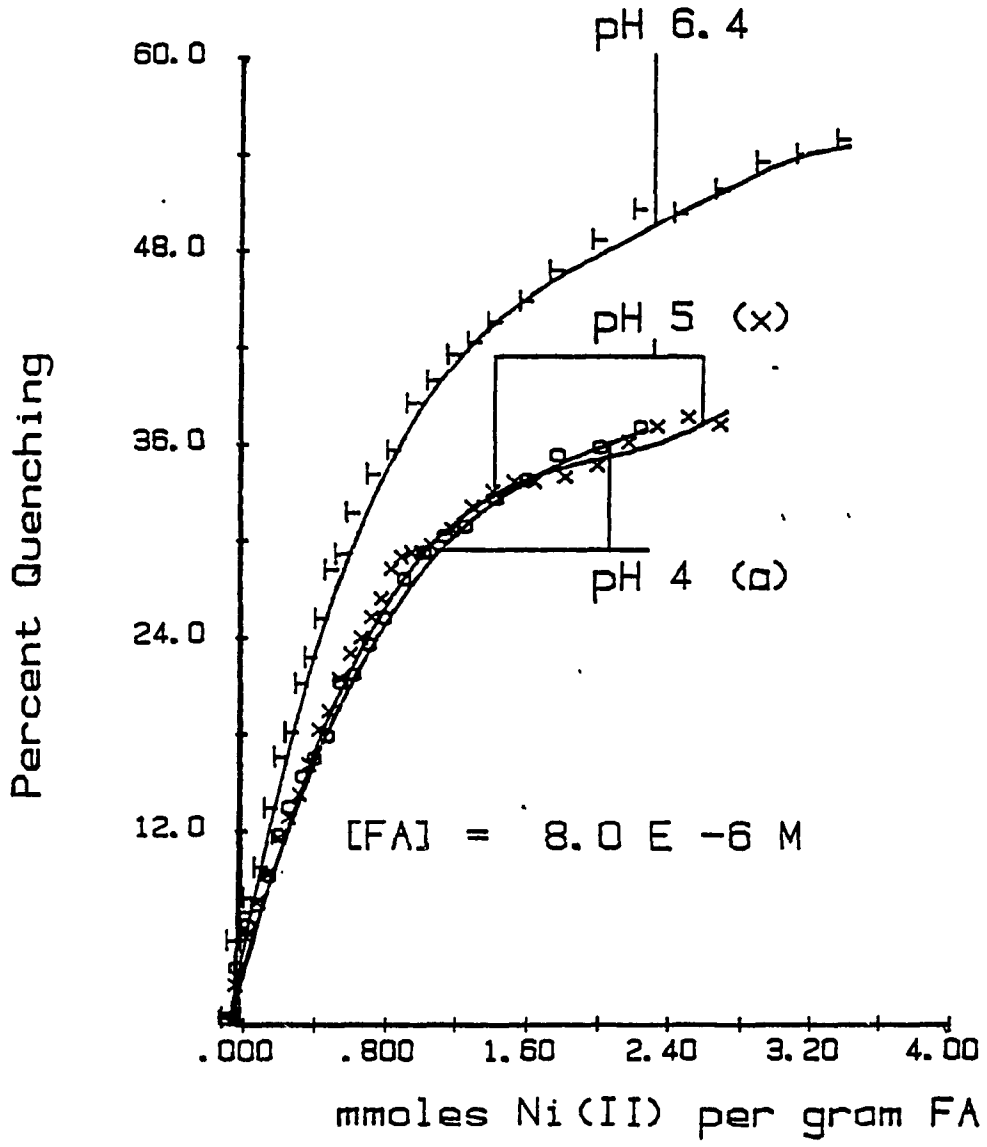

tration of 8.0 X 10^{-6} M. These are presented in Figure 18 and were not analysed by the kinetic technique. It is evident once again that there is not much difference of Ni^{2+} loading at either pH 5.0 or 4.0, as was clearly seen in Figures 10 through 14 in section A of this chapter. This is an important fact which supports part of the results of the multicomponent analyses of section A. Further titrations do not involve the pH 4.0 set as these are evidently nearly redundant to the pH 5.0 cases.

With a FA concentration of 2.0 X 10^{-5} M, the signal to noise ratio was far better. It was initially hoped that the kinetic approach could be applied to the fully complexed solution since at this concentration, result from section A could then be verified. It soon became evident, as was expected, that the required amount of Ni(II) for asymptotic approach to maximum quenching was much too high to be useful for the kinetic analysis. Even though attempted kinetic analyses produced final NLR refinements, the deviation from Beer's Law at these higher concentrations makes it unwise to use these data in a critical discussion. Titration results for pH's of 6.4 and 5.0 are presented in Figure 19, where the point at which the concentration of Ni^{2+} was equal to that in the kinetic experiments of section A is indicated by a vertical line. Far from all the complexing sites of the FA had been titrated during the experiments of section A as shown by the line in Figure 19.

Figure 19: Titration curves for fluorescence quenching by Ni^{2+} of a solution containing 2.0 X 10^{-5} M FA at pH 6.4 and 5.0. Arrow indicates point in the curves at which the experiments analysed in section A performed.

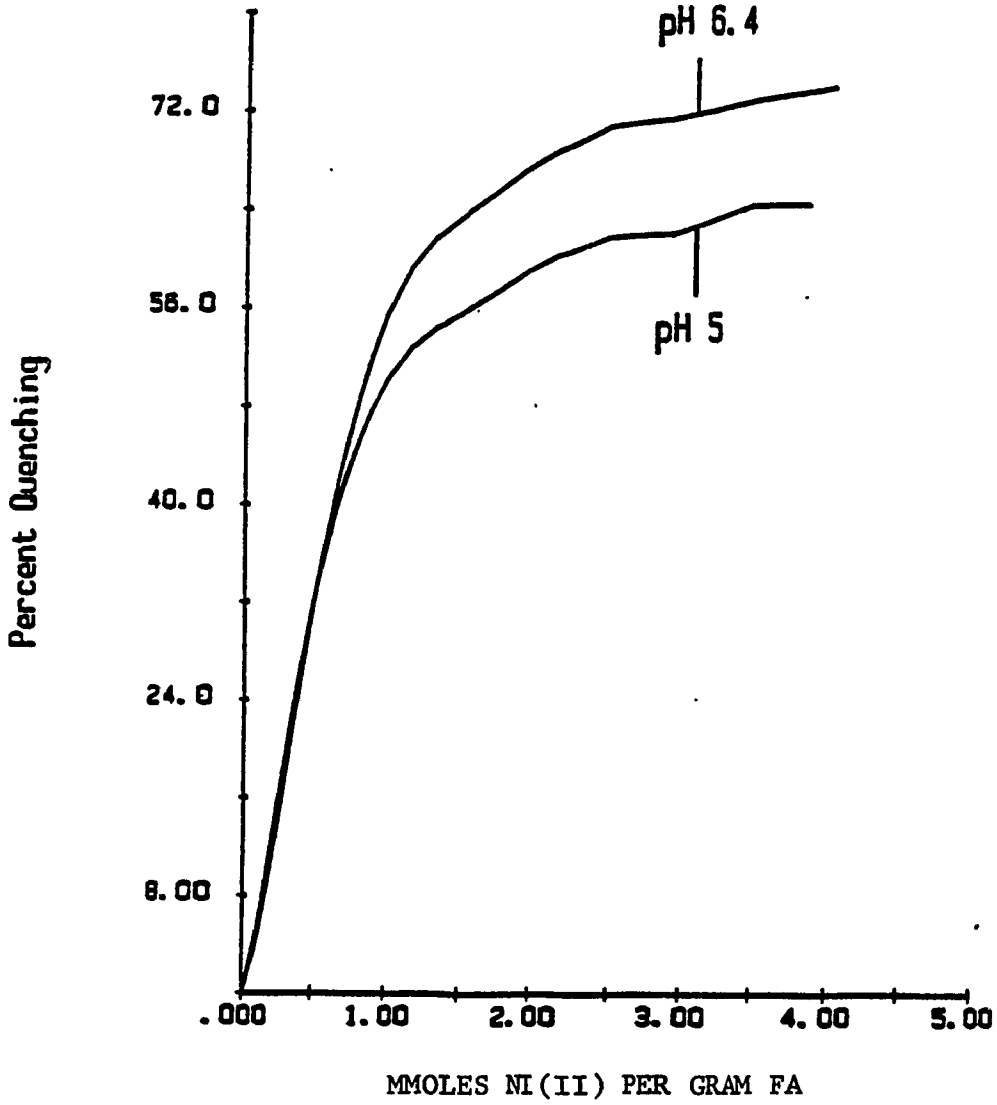

In order to circumvent the problem of having to add excessive amounts of Ni^{2+} in order to approach maximum quenching, the equilibrium FA concentration was reduced by four to 5.0×10^{-6} M. This is half the lowest concentration used in section A. The titration curve is presented in Figure 20.

The decreasing slopes in Figures 19 and 20 are indicative of a decreasing influence of newly-bound Ni(II) on the quenching phenomena, an observation also seen by Underdown (109) in his work with Cu(II). This is due to the titration of successively weaker binding sites.

The assumption as used by Weber (112) and Sposito (113) is that the absolute fluorescence intensity I is related to the sum:

$$I = a_{ML} I^{o}_{ML} + a_{L} I^{o}_{L} \qquad [6.1]$$

where a_{ML} is the molar fraction of metal-complexed FA in total complexing sites of FA, a_L is the molar fraction of metal-free FA to total complexing sites of FA, and where I^{o}_{ML} is the limiting value of I when maximum fluorescence quenching is achieved and I^{o}_{L} is the fluorescence intensity when no metal has been added. It relates the observed intensity to the sum of complexed and non-complexed FA. Weber's Equation 6.1 is a linear function which is based on a one-site model. To be understood correctly, one can

Figure 20: Titration curve for fluorescence quenching by Ni^{2+} of a solution containing 5.0 X 10^{-6} M FA at a pH of 6.4 .

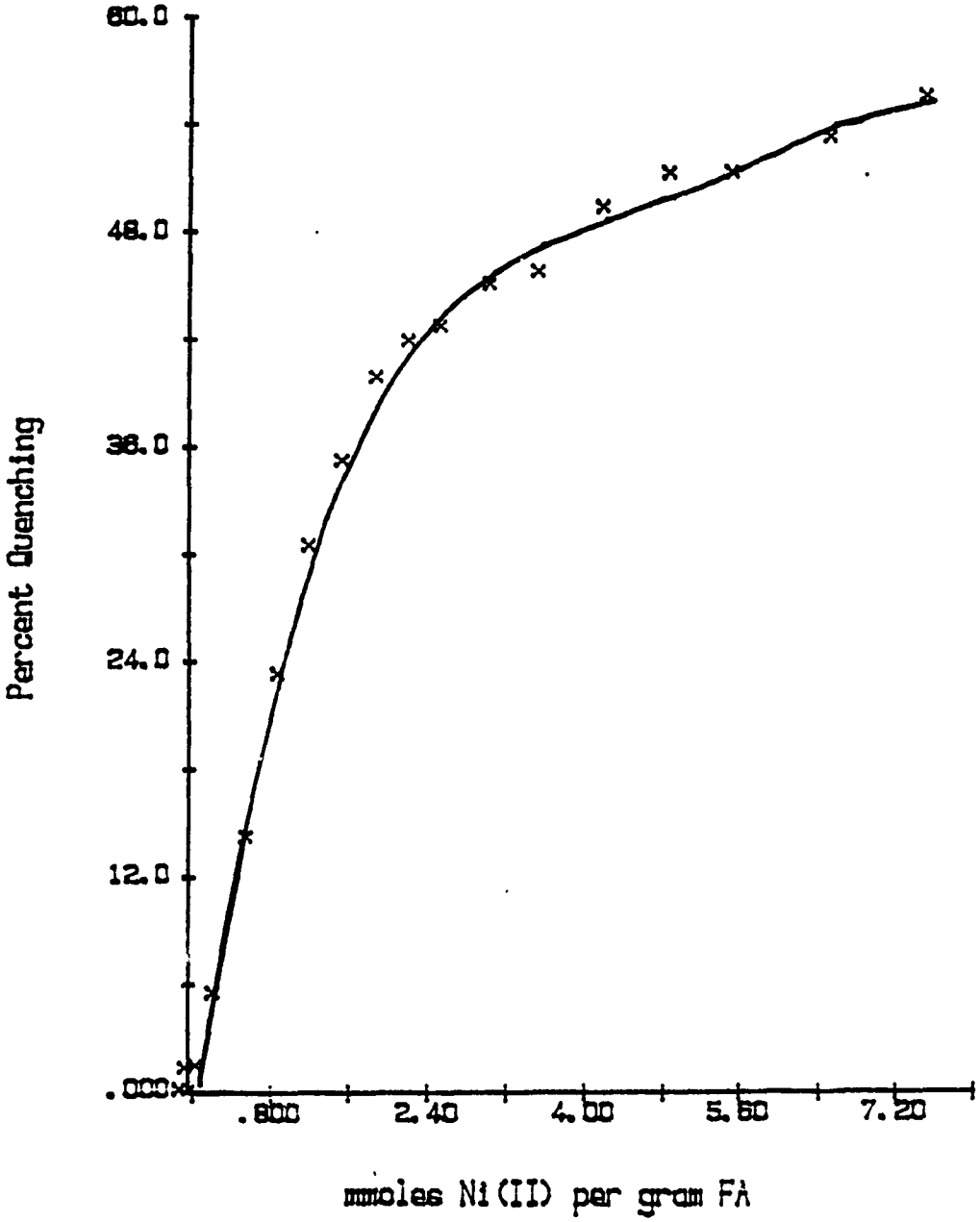

assume that the one-site model is in actual fact related to the total of the complexing sites, taken as a whole.

If the two fluorescence intensity contributions of Equation 6.1 are available experimentally, kinetic multicomponent investigations should permit a check on the validity of the empirical model (Equation 6.1) set forth, as well as a means of fitting the results to a binding capacity for the FA-Ni^{2+} system under similar conditions. However, I^{o}_{ML} is not directly obtainable from experiments because of the huge Ni^{2+} levels required to saturate sites and the complications from aggregation that can ensue. Figure 21 and Table XIII present profiles of absorbancies for the four species C1 through C4 of Ni-PAR at three titration points along the curve in Figure 20, where C1 is the free aquo species, and C2 through C4 are the complexed species. The strongest complexing species, C4, does saturate at low concentrations of nickel, which is expected. C2, the weakest binding site, begins to saturate near the end of the titration, and C1, the free species, increases more rapidly as the binding sites are approaching saturation. These three results represent reasonbale trends for a multicomponent titration with a metal. The species C3 increases almost linearly along the titration curve, and, again, there is about 40% of the reaction which does not appear in calculation, an important feature put forward in section A. As is, these species' concentrations do not give the maximum binding capacity. As mentionned in

Figure 21: Profile of the absorbancies for the four species found by multi-component analyses of the three titration points in figure 20.

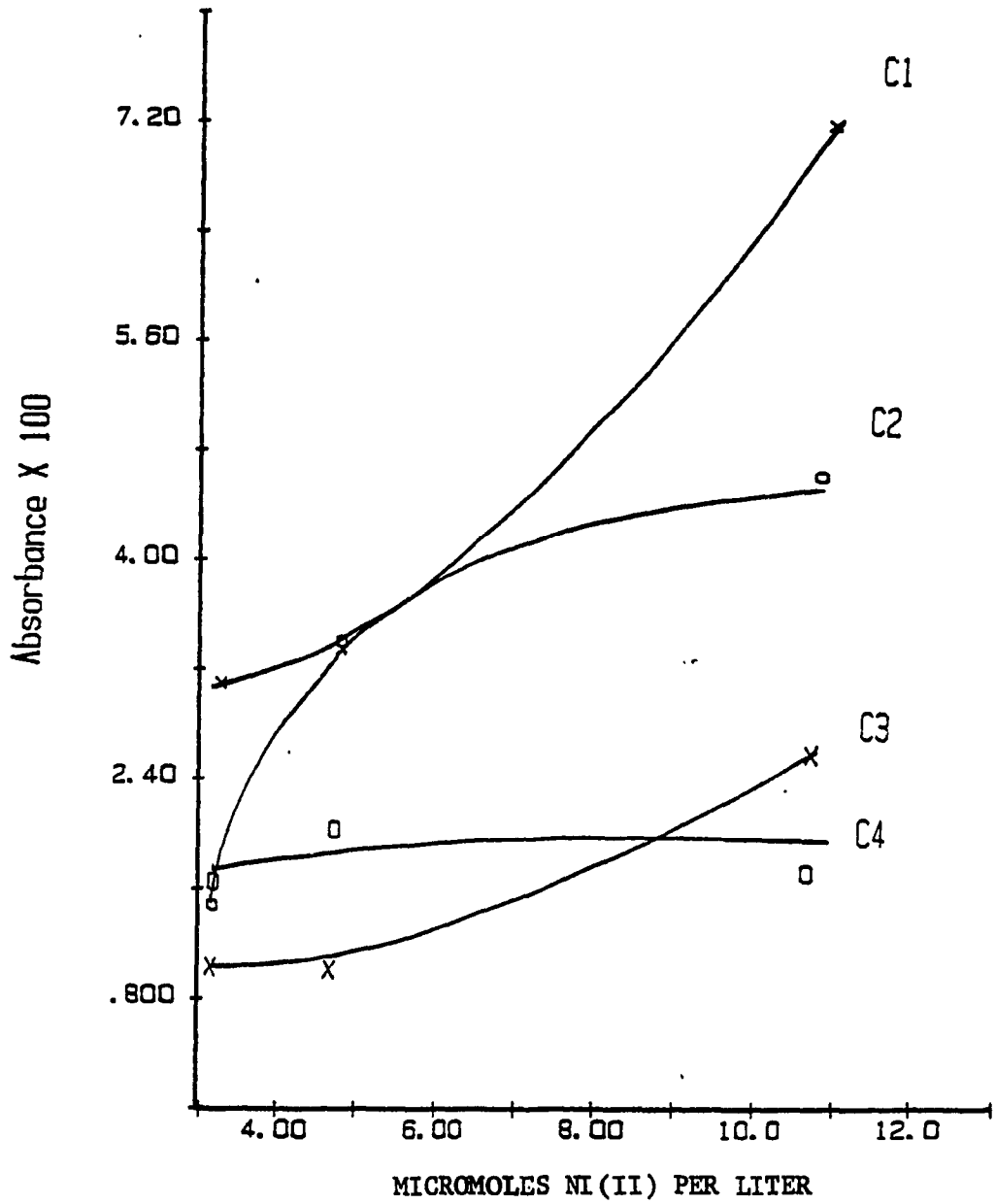

TableXIII: Concentrations for equilibrium conditions of the three titration points of figure 20 as analysed by the multi-component routine.[a]

Parameter	Initial concentrations		
	3.0×10^{-6} M	4.5×10^{-6} M	10.5×10^{-6} M
C1	8.58	9.44	21.40
C2	3.66	9.58	13.60
C3	2.22	2.26	7.36
C4	4.10	5.26	4.74

[a] Concentrations are in moles per liter X 10^7.

earlier arguements, the Ni^{2+} loading required to attain full coverage of all complexing sites is too high. A value for the concentration of complexing sites per gram for the Armadale FA is that reported by Underdown et al. from results obtained using an ion selective electrode to study the Cu^{2+} titration of Armadale FA at pH 6.0 (114). They report a minimum binding capacity of 3.1 meq/g for the FA sample and Cu^{2+} at pH 6.0.

Figure 22 presents the percentage difference between calculated fluorescence intensities using Equation 6.1 and the quenching titration results of Figure 20, as a function of projected values of I^{o}_{ML} when using a binding capacity of 3.1 meq/g. The values for a_{ML} were calculated from speciation results using the multi-kinetic routine of Chapter 4, results of which are tabulated in Table XIII and presented in Figure 21, for which a mass balance was used as in:

$$a_{ML} = (C_T - C_1) / L , \qquad [6.2]$$

where C_1 is the concentration of the free metal species, and C_T is the total metal added. It is used in preference to the sum of the complexed sites since it is the only ascertainable, chemically "known" species, that of the free metal ion. L is the total binding capacity (umoles/L). The term a_L is simply :

Figure 22: Percent errors of calculated fluorescence for a binding capacity of 3.1 mmoles complexing sites per gram FA when the minimum fluorescence intensity I^{o}_{L} is varied from zero to 45.0, in arbitrary units of fluorescence. The three concentrations analysed are shown. Dashed line indicates area of least mutual minimum differences.

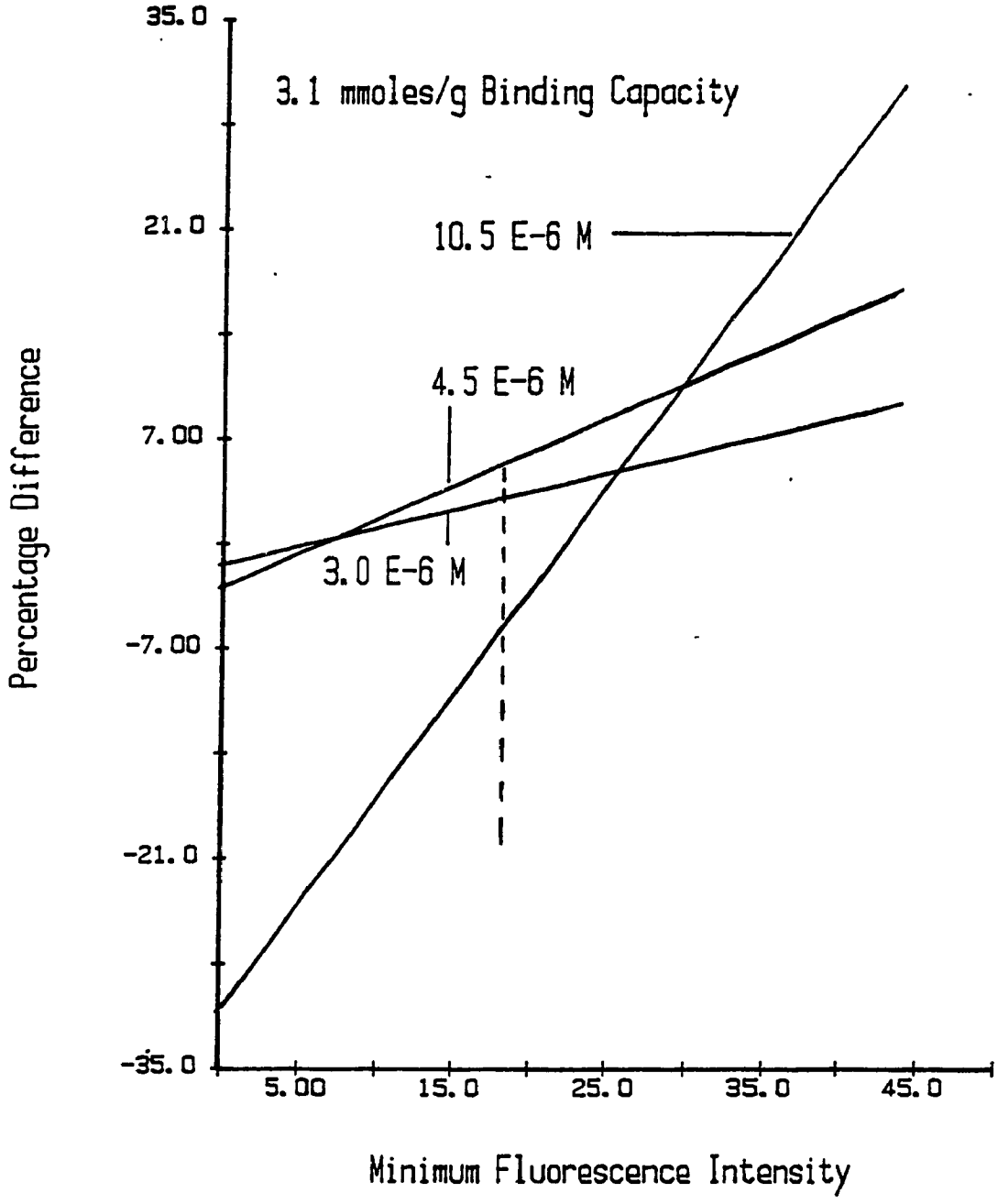

$$a_L = 1 - a_{ML} , \qquad [6.3]$$

by definition. Note that the calculated fluorescence values from Equation 6.1 through 6.3 when using Underdown et al.'s binding capacity of 3.1 mmole per gram have high percentage differences from observed fluorescence results when using, for the value of I^o_{ML}, the final titration point in Figure 20 (which was 33.1 arbritrary units). This does not imply, however, that the value of their reported binding capacity is wrong, but rather that the value used for I^o_{ML} is too high. The value of I^o_{ML} which includes all three titration situations within a minimum range of percentage differences (F_{obs} vs F_{calc}) is in the vicinity of 18. It is not expected thatI^o_{ML}will attain a null value because of inefficient quenching by metal complexes, enhancement of fluorescence by metal complexation, and the existence of fluorophores that do not complex metals. This value of 18 for I^o_{ML} is a plausible projection of the asymptote of Figure 20.

The definition of binding capacity usually implies a constant. However, FA behaves differently, i.e. as in the formation of aggregates at higher concentrations, and therefore any "effective" complexing capacity reported here is restricted to concentrations in the vicinity of 5.0 X 10^{-6} M FA. Weber postulated that at the lower concentrations that the FA has an expanded conformation, thus allowing for a higher complexing capacity. The results of section A have gradually decreasing Ni^{2+} loadings as the

concentration of the FA is increased. The highest loadings were 0.67 mmoles/g at a pH of 6.4 and an FA:Ni ratio of 1:1, all other subsequent solutions having progressively lower loadings.

Lee et al. reported a value of 3.3 mequ/g or less for an FA concentration of 10 mg/L (115). In the fluorescence titrations herein, the FA concentration is 4.5 mg/g. If, in contrast to experimental results of Lee, we adopted Weber's idea, mentioned earlier, a slightly higher binding capacity would be implied. The projections of I^{o}_{ML} for a arbitrary binding capacity of 4.0 mmoles/g are presented in Figure 23. This case tends towards a null in the minimum fluorescence intensitiy much more quickly than the 3.1 mmoles/g case, and the later is better suited to our sample. Considering that our results show that for a binding capacity of 3.1 mmoles/g that I^{o}_{ML} reduces to a plausible 18 units and that independent laboratory studies support the value, this is the best value for fitting the present experiments and with it we can successfully fit fluorescence titrations to the 2-component model of Equation 6.1.

An attempt was made to project values of I^{o}_{ML} and the binding capacity to a situation where the C2 species do not contribute to fluorescence such that Equation 6.2 becomes;

$$a_{ML} = [\, C_T - (C1 + C2) \,] / L \qquad [6.4]$$

This resulted in a shift of the diagrams for the projec-

Figure 23: Percent errors of calculated fluorescence for a binding capacity of 4.0 mmoles complexing sites per gram FA when the minimum fluorescence intensity I^{o}_{L} is varied from zero to 45, in arbitrary units of fluorescence. The three concentrations nalysed are shown. Dashed line indicates area of least mutual differences.

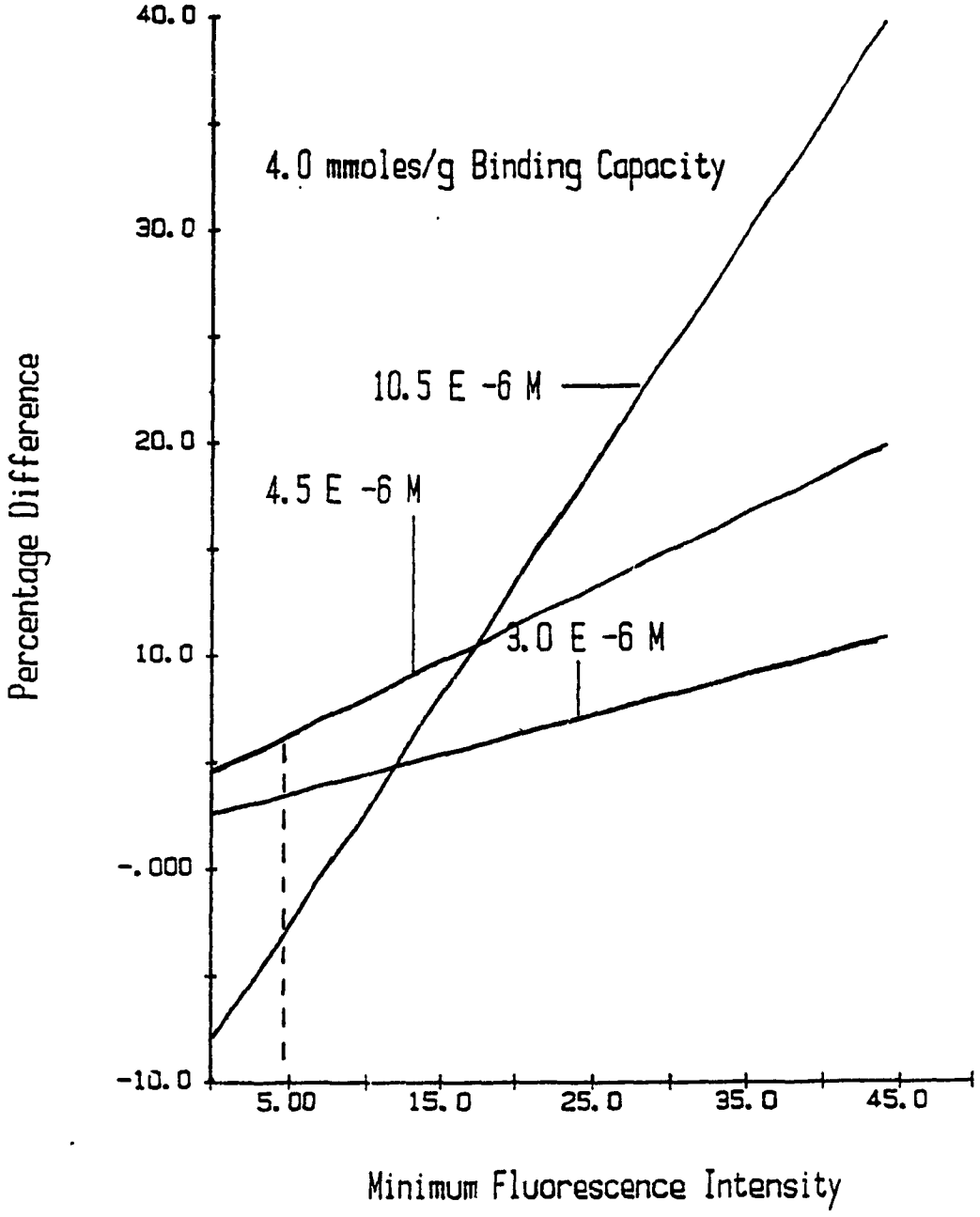

tions at various binding capacities towards significantly lower and implausible values of I^{o}_{ML}. It can thus be presumed that all species that complex with the FA are responsible for the quenching phenomenum, albeit some may contribute more than others.

The result of this effort to evaluate fluorescent titration methods reveals that a single species model (Equation 6.1) is adequate but that it leaves large enough error to accomodate the multi-component model. Our initial hope that the success of single species model for fluorescence would allow correlation between fluorescence and one of the components was frustrated. Apparently, all species which were identified in kinetic analysis make significant contributions to fluorescence.

CONCLUSIONS

Most previous attempts to define or classify the metal binding sites of humic subtances involved thermodynamic studies of the metal cation , or H^+, binding and assignment of stability constants. Log K values were observed as a function of total metal added. Due to the nature of humic substances and of the experimental function, these methods usually supplied a continuous distribution of log K values or at most a fitting by two or three discrete distributions by a nonlinear regression routine. The present study proposed to distinguish, by a multi-component kinetic approach, the minimal number of components capable of representing the experimental data of reactions between metal-humate species and a colorimetric reagent. Equilibrated solutions of Ni^{2+} and an Armadale soil derived fulvic acid where treated with excess (over Ni^{2+} by 50 fold) of PAR. The different rate constants for release of nickel to PAR for the various species was then derived.

To assign the number of components, a Laplace transform technique derived from ideas of Olsan and Shuman was used. The parameter estimates were refined by a customized non-linear multi-exponental least squares regression routine. The latter was a definite requirement since the Laplace routine on its own was ambiguous due to the overlapping and interference of adjacent components.

This novel approach proved reproducable and reliable

when applied to reasonable simulations of up to five components (plus background) even with noise. When applied to experimental data, the rate constants obtained for the free Ni^{2+} was 0.67 sec. $^{-1}$ when nickel was studied independently of the FA and between 0.53 and 0.69 sec.$^{-1}$ when in equilibrium with a FA solution, regardless of the FA concentration and of the pH of equilibration.

The study included 9 different FA concentrations between 1.0 and 9.0 X 10^{-5} M with a Ni^{2+} concentration of 1.0 X 10^{-5} M for three different pH's of 4.0, 5.0, and 6.4. Consistent results were obtained for rate constants of three other "bound" components regardless of FA concentration and pH value. This proved that the approach was robust under all conditions used in this study. It also indicates that the method is providing significant insight with respect to the binding characteristics of the FA used. No attempt was made at elucidating the conventional chemical structure of these components, but they are no doubt related to the carboxylate functional groups which are titrated across this pH range.

The results for pH 4.0 and 5.0 were similar and exhibited trends in concentration for the four components that followed tendencies predicted by mass balance action considerations as concentrations of FA were increased. All of the Ni^{2+} added was recoverable in these two cases. At pH 6.4, however, convergence of the NLR routine and the estimates always resulted in a mass balance which leaft about

40 % of the Ni^{2+} added was not accounted for. This remaining Ni^{2+} could be recovered by long reaction times with PAR. Complete recovery takes less than ten days. The additional component not seen at either pH 4.0 or 5.0 is termed "kinetically inert". This is the first observation of this sort and is probably of significance in terms of time of uptake and absorption by organisms (as well as by PAR).

For the first time, following this study, it is clear that a reliable method for fitting a kinetic model to a metal-humate sample is available. The method shows stability in rate constants suggesting the successful classification of types of binding sites. The approach provides the first insights into the dynamic dimension of the problem of bioavailability of metal cations.

An attempt to establish the binding capacity of Ni^{2+} to the FA at pH 6.4 was done by studying the fluorescence quenching of the FA by Ni^{2+}. Using a model similar to that used recently by Weber and Sposito, we were capable of supporting, although not directly establishing, that Gamble et al.'s value of 3.1 mmoles bidentate binding sites per gram of the Armadale FA as a plausible result. An attempt at fitting the fluorescence data to a four component binding model was met with frustration. Cabaniss and Shuman (private communication) have recently encountered similar difficulty in the attempt to extent fluorescence methods. It seems unlikely that fluorescence samples binding sites homogeneously.

REFERENCES

(1) Jensen, A.; Jorgensen, S.E.; Analytical Chemistry Applied to Metal Ions in the Environment, in Metal Ions in Biological Systems, vol. 18, Circulation of metal ions in the environment. Edited by Helmut Sigel; Marcel Dekker, Inc., N.Y., 1984, pp. 5-60.

(2) Florence, T. M.; Batley, G.E., Chemical Speciation in Natural Waters. CRC Reviews in Analytical Chemistry. 1980 vol. 9, no. 3, pp. 229-237.

(3) Guy, R.D.; Chakrabarti, C.L.; Analytical Techniques for Speciation of Trace Metals. in; Proceedings of the International Conference on Heavy Metals in the Environment, vol. 1; Hutchison, T., Ed., University of Toronto, Ontario, 1975, pp. 275-294.

(4) Buffle, J.; Trends Anal. Chem., 1981, 1, (4), pp. 90-95.

(5) "Heavy Metals in the Environment." International Conference. Heidelberg, Fed. Rep. of Germany, vol. 1, 1983, CEP Consultants, U.K., p. 1-8.

(6) ref. 1), p. 10.

(7) Bryan, G.W., Proc. Roy. Soc., London B, 1971, 177, p. 389.

(8) Campbell, P.G.C.; Stokes, P.M.; Galloway, J.N., "Effects of Atmospheric Deposition on the Geochemical Cycling and Biological Availability of Metals." vol. 2, 1983, pp. 760-763.

(9) Frey, C.M.; Stuehr, J.; "Kinetics of Metal Ion Interactions with Nucleotides and Base Free Phosphates.", in "Metal Ions in Biological Systems", 1974, Sigel, H., Ed., Marcal Dekker, vol. 1, p. 69.

(10) ref. 3), p. 270

(11) Sclater, F.R.; Boyle, E.; Edmond, J.M., Earth Planet. Sci., 1976, 31, p. 119.

(12) "Effects of Nickel in the Canadian Environment." National Research Council of Canada. Publication no. NRCC 18568 of the Environmental Secretariat, 352 pp. 1981, p. 87.

(13) ref. 12), p. 57.

(14) Stokes, P.M., Adaptation of green algae to high levels of copper and nickel in aquatic environments., in "Proceedings of the International Conference on Heavy Metals in the Environment", 1975, Toronto, Ontario, Hutchinson, T.C., ed., 2, pp. 137-154.

(15) Hutchinson, T.C., Water Pollut. Res. Can., 1973, 8, pp. 68-90.

(16) Nickel: ambient water quality criteria, EPA, 1978, U.S. Environmental Protection Agency, Washington, D.C., Document No. PB 296 800, US NTIS.

(17) ref. 12), p. 93.

(18) Choulhry, G.G., Humic Substances: Structural, Photophysical, Photochemical, and Free Radical Aspects and Interactions with Environmental Chemicals; Current Topics in Environmental and Toxicological Chemistry, vol. 7, YEAR, Gordon and Breach Science Publishers, N.Y., p. 7.

(19) Roach, K.B., M.Sc. theis, 1983, Concordia University, Montreal, Quebec, p. 8.

(20) Gamble, D.S.; Schnitzer, M., in "Trace Metal and Metal Organic Interactions in Natural Waters.", 1973, Singer, P.S., ed., Ann Arbor Sciences, Ann Arbor, MI, p. 265.

(21) Gamble, D.S.; Underdown, A.W.; Langford, C.H.; Anal. Chem.; 1980, 52, pp. 1901-1908.

(22) Schnitzer, M.; "Chemical, Spectroscopic, and Thermal Methods for the Classification and Characterization of Humic Substances.", Proc. Intern. Meetings on Humic Substances, 1972, Pudoc, Wageningen, pp. 293-310.

(23) Stevenson, F.J., "Humus Chemistry", 1982, Wiley and Sons Inc., p. 227.

(24) ref. 23), pp. 234-239.

(25). Farmer, V.C.; Morrison, R.I.; Sci. Proc. Roy. Dublin Soc., Sec. A., **1960**, 1, p. 85.

(26) Dubach, P.; Mehta, N.C.; Jakab, T.; Martin, F.; Boulet, N.; Geochim Cosmochim. Acta, **1964**, 28, p.1567.

(27) Wright, J.R.; Schnitzer, M.; Trans. 7th Intern. Congr. Soil Sci., **1960**, 2, p. 120.

(28) ref. 23), p. 229.

(29) Wilson, M.A., J. Soil Sci., **1981**, 32, pp. 167-186.

(30) Wilson, M.A.; Jones, A.J.; Williamson, B., Nature, vol. 276 nov. 30, **1978**, pp. 487-489.

(31) Wilson, M.A.; Barron, P.F.; Gillam, A.H., Geochimica et Cosmochimica Acta, **1981**, 45, pp. 1743-1750.

(32) Wilson, M.A.; Goh, K.M., Critical Comment, Geochimica et Cosmochimica Acta, **1981**, 45, pp. 489-490.

(33) Puggiero, P.; Interesse, F.S.; Sciacovelli, O., Author's Reply, Geochimica et Cosmochimica Acta, **1981**, 45, pp. 491-492.

(34) Schnitzer, M., "Charaterization of Humic Constituents by Spectroscopy," in McLaren, A.D. and Skujins, J., Eds., Soil Biochemistry, Marcel Dekker, N.Y., **1971**, vol. 2, pp. 60-95.

(35) Hatcher, P.G.; Schnitzer, M.; Dennis, L.W.; Maciel, G.E., Soil Sci. Soc. Am. J., **1981**, 45, pp. 1089-1094.

(36) Lyerla, J.R.; Yannoni, C.S., IBM J. Res. Develop., july, **1983**, 27 (4), pp. 302-306.

(37) Matsuda, K.; Schnitzer, M., Soil Sci., **1972**, 114, pp. 185-193.

(38) ref. 20), chapter 9.

(39) Schnitzer, M.; Khan, S.U.; "Humic Substances in the Environment.", **1972**, Marcel Dekker, N.Y.

(40) Gamble, D.S.; Can. J. Chem., **1970**, 48, p. 2662.

(41) Gamble, D.S.; Can. J. Chem., **1972**, 50, p. 2680.

(42) Hatcher, P.G.; Breger, I.A.; Dennis, L.W.; Maciel, G.E., Solid-State ^{13}C-NMR of Sedimentary Humic Substances: New Revelations on Their Chemical Composition." chapter 3 in; "Aquatic and Terrestrial Humic Material.", Christman, R.F. and Gjessing, E.T., eds., **1983**, Ann Arbor Science, Ann Arbor, MICH, p. 37-82.

(43) Gamble, D.S.; Schnitzer, M.; Hoffman, I.; Can. J. Chem., **1970**, 48, p. 3197.

(44) Senesi, N.; Schnitzer, M.; Soil Sci., **1977**, 123, p. 224.

(45) Maximov, O.B.; Glebko, L.I.; Geoderma, **1974**, 11, p. 17.

(46) Benes, P.; Steinnes, E.; Migration Forms of Trace Elements in Natural Fresh Waters and the Effect of Water Storage. Water Research, **1975**, 9, pp. 741-749.

(47) Fernandez, F.J., At. Absorpt. Newsl., 16, **1977**, p. 33.

(48) Burrell, D.C.; Atomic Spectrometric Analysis of Heavy Metal Pollutants in Water. **1974**, Ann Arbor Science, Ann Arbor.

(49) Stowey, J.F.; Jeffrey, L.M.; Hood, D.W.; Nature, **1967**, 214, p. 377.

(50) Kamp-Nielsen, L.; Deep Sea Res., **1972**, 19, p.899.

(51) Guy, R.D.; Chakrabarti, C.L.; Analytical Techniques for Speciation of Heavy Metal Ions in the Aquatic Environment. Chem. in Can., **1976**, vol. 2, no. 10, pp. 26-29.

(52) Jensen, A.; Jorgensen, S.E.; Analytical Chemistry Applied to Metal Ions in the Environment, chjapter 2 in; Metal Ions in Biological Systems, vol. 18, Sigel, H, Ed., Marcel Dekker Inc., N.Y., **1984**, p. 38.

(53) McBeath, W.H.; Preston, D.B.; Canham, R.A.; Eds., Standard Methods for the Examination of Water and Wastewater, **1981**, American Public Health Association,

Washington, D.C., p. 194.

(54) Ion-Selective Electrode Reviews; Applications, Theory and Development. Thomas, J.D.R., edt., 1982, vol.4, no. 1, 141 pages.

(55) Blaedel, W.F.; Dinwiddie, D.E.; Anal.Chem., 1974, 46, p. 873.

(56) Frazer, J.W.; Baladan, D.J.; Brand, H.R.; Robinson, G.A.; Lanning, S.M.; Determination with Ion-Selective Electrodes in the Low-Level Non-Nernstian Response Region. Anal. Chem., 1983, 55, pp. 855-861.

(57) Ryan, D.K.; Weber, J.H.; Anal. Chem., 1982, 54, p.986.

(58) Saar, R.A.; Weber, J.H.; Anal. Chem., 1980, 52, pp. 2095-2100.

(59) Gauthier, T.D.; Shane, E.C.; Guerin, W.F.; Seitz, W.R.; Grant, C.L.; Environ. Sci. Technol., 1986, 20, pp. 1162-1166.

(60) Ref. 3), pp. 276-280.

(61) Florence, T.M.; Batley, G.E.; Talanta, 1977, 24, p.151.

(62) Batley, G.E.; Farrar, Y.J.; Anal. Chim. Acta, 1978, 99, p. 283.

(63) Saar, R.A.; Weber, J.H., Environ. Sci. Technol., 1982, 16, (9), p. 510A-517A.

(64) Ref. 3), p. 279.

(65) Schmid, R.W.; Reilley, C.N.; J. Am. Chem. Soc., 1958, 80, pp. 2087-2094.

(66) Alzand, I.K.; Langford, C.H., Can. J. Chem., 1985, 63, pp. 643-650.

(67) Florence, T.M.; Batley, G.E., J. Electroanal. Chem., 1977, 75, p. 791.

(68) Ref. 3), p. 288.

(69) Benes, P.; Steinnes, E.; Water Res., 1974, 8 , pp. 947-953.

(70) ref. 2), p. 233.

(71) ref. 2), p. 234.

(72) ref. 3), p.p. 289-290.

(73) ref. 3), p. 289.

(74) Kotyk, A.; Janacek, K.; Cell Membrane Transport, 1975, Plenum, N.Y.

(75) Amicon, 1972 Publication No. 426A. Lexington, Mass.: Amicon Corp.

(76) Buffle, J.; Staub, C.; Anal. Chem., **1984**, 56, pp. 2837-2842.

(77) Staub, C.; Buffle, J.; Haerdi, W.; Anal. Chem., **1984**, 56, pp. 2843-2849.

(78) Tuschall, J.R.; Brezonik, P.L.; Anal. Chim. Acta, **1983**, 149, pp. 45-58.

(79) Buffle, J.; in "Circulation of Metals in the Environment."; Sigel, H., Ed., **1984**, vol. 18, chapter 6, Marcel Dekker, Inc, N.Y., pp. 165-221.

(80) ref. 12), p. 284.

(81) Turner, D.R., in "Metal Ions in Biological Systems", vol. 18, Chpt. 5, Sigel, h., ed., **1984**, Marcel Dekker Inc., N.Y., pp. 137-164.

(82) Sunda, W.G.; Ferguson, R.L., in "Trace Metals in Seawater", Wong, C.S., et al., eds., **1983**, Plenum, N.Y., 871 pp.

(83) ref. 81), p.153.

(84) Langford, C.H.; Mak, M.K.S.; Comments Inorg. Chem., **1983**, 2, no. 3-4, pp. 127-143.

(85) Langford, C.H.; Mak, M.K.S.; Inorg. Chim. Acta, **1983** 70, pp. 237-246.

(86) Langford, C.H.; Wong, S.M.; Underdown, A.W.; Can. J. Chem., **1981**, 59, no. 2, pp. 181-186.

(87) Langford, C.H.; Mak, M.K.S.; can. J. Chem., **1982**, 60, no. 15, pp. 2023-2028.

(88) Guggenheim, E.A.; Phil. Mag., **1926**, 2, p. 538.

(89) Mak, M.K.S.; Langford, C.H.; Khan, T.R.; J. Indian Chem. Soc., LIV, **1977**, Jan., Feb., Mar., 51.

(90) Wilkins, R.G., "The Study of Kinetics and Mechanism of Reactions of Transition Metal Complexes.", **1974**, Allyn and Bacon, Inc., Boston, 403 pp.

(91) Olson, D.L.; Shuman, M.S.; Anal. Chem. **1983**, 55, pp. 1103-1107.

(92) Flaschka, H.A.; Barnard, A.J.; "Chelates in Chemistry.", **1972**, Marcel Dekker, Inc., N.Y., p. 118.

(93) Geary, W.J.; Nickless, G.; Pollard, F.H.; Anal. Chem., **1962**, 26, p. 575.

(94) Geary, W.J.; Nickless, G.; Pollard, F.H.; Anal. Chem., **1962**, 27, p. 71.

(95) ref. 92), p. 128.

(96) Corsini, A.; Yik, I.M.L.; Fernando, Q.; Freiser, H.; Anal. Chem., **1962**, 34, p.1090.

(97) Guenther, W.B., "Chemical Equilibrium", 1975, Plenum Press, NY, 248 pp.

(98) ref. 97), p. 60.

(99) Wehry, E,L.;Structural and Environmental Factors in Fluorescence, chpt. 2, in, "Fluorescence: Theory, Instrumentation and Practice.", Guilbault, G.G., ed., Marcel Dekker, Inc., N.Y., 1967

(100) Mak, M.K.S.; Ph.D. thesis; "Kinetic Analysis of Aluminum in Environmentally and Geochemically Relevant Problems.", 1980, Carleton University, Ottawa, Ontario, 187 pages.

(101) ref. 42), chapter 17, pp. 349-370.

(102) Kreysig, E., chapter 5 in; "Advanced Engineering Mathematics." 5-th edt., 1983, Wiley, N.Y., 988 pp.

(103) Widder, D.V.; "The Laplace Transform", Princeton University Press, Princeton, N.J., 1946

(104) Bellman, R.; Kalaba, R.E.; Lockett, J., "Numerical Inversion of the Laplace Transform.", American Elsevier, N.Y., 1966

(105) IMSL, User's Manual, (International Mathematical and Statistical Libraries, Inc.) IMSL LIB1-0006, Revised, July, 1977.
Product: IMSL S/370-360, Edition 6, 1977.

(FORTRAN IV) IBM S/370-360, Xerox-Sigma S/6-7-9-11-560.

(106) Bard, Y., "Nonlinear Parameter Estimation.", Academic, N.Y., 1974

(107) Mak, M.K.S., Concordia University, Montreal, Quebec, Personal communication.

(108) Aysola, P., Science Industrial Research Unit, Concordia University, Montreal, Quebec. Personal communication.

(109) Underdown, A.W.; Ph.D. thesis, "Light Scattering and Spectroscopic Studies of Aggregation Processes in a Well Chatracterized Fulvic Acid." 1982, Carleton University, Ottawa, Ontario, 204 pp.

(110) Ref. 109), Appendix B, pp. 193-197.

(111) Adaptable Laboratory Software: ASYST: A Scientific System., Mac Millan Software Co., N.Y., 1985

(112) Ryan, D.K.; Weber, J.H., Environ. Sci. & Technol., 1982, 16, pp. 866-872.

(113) Blaser, P.; Sposito, G., Soil Sci. Soc. Am. J., 1987, 51, pp. 612-619.

(114) Gamble, D.S.; Langford, C.H.; Underdown, A.W., The Interrelationship of Aggregation and Cation Binding of Fulvic Acid, in "Complexation of Trace Metals in Natural Waters.", 1984, Martinus Nijhoff/Dr. W. Jung Publishers,

The Hague, Netherlands, pp. 349-356.

(115) ref. 42), chapter 11, pp. 219-230.

APPENDIX A: THE ASYST PROGRAMS FOR ESTIMATIONS

The programs allready compiled under "KINETIC.2" are presented here in the sequence that they should be used to successfully estimate all the parameters required for the non-linear regression routine of Appendix B. Alterations can be made to suit the user if required.

The dimensions of array and scalar definitions are as follows;

>Under file DIM.ASY ;<

```
REAL DIM[ 2000 ] ARRAY Y
REAL DIM[ 2000 ] ARRAY X
>These arrays serve as the basic receiver/holders of the
raw data as aquired from DOS.<

REAL DIM[ 2000 ] ARRAY NEWY
REAL DIM[ 2000 ] ARRAY NEWX
>These arrays are for the smoothed/interpolated values for
all newly generated x,y fits.<

REAL DIM[ 2000 ] ARRAY DIFF1
REAL DIM[ 2000 ] ARRAY DIFF2
REAL DIM[ 2000 ] ARRAY NEWSET
>These arrays are used in the calculation of the Laplace
profile<

REAL DIM[ 2000 ] ARRAY LOGS
REAL DIM[ 2000 ] ARRAY SY
REAL DIM[ 2000 ] ARRAY SX
REAL DIM[ 2000 ] ARRAY BUFFER
>These arrays serve to make calculations without altering
x,y, and newy<

REAL DIM[ 15 ] ARRAY COEFF
REAL DIM[ 10 ] ARRAY RATE
REAL DIM[ 10 ] ARRAY CONC
>These arrays are for saving coefficients of polynomial
fits, and for generating new data<
```

```
>The following scalars are mostly self-explanatory and can
be better understood by studying the actual applications in
the algorithms.<
INTEGER SCALAR NEXT
INTEGER SCALAR N.O.P
INTEGER SCALAR NUMBER
INTEGER SCALAR INT
INTEGER SCALAR SECT
INTEGER SCALAR COUNT
INTEGER SCALAR RATES
INTEGER SCALAR DEGREE
REAL SCALAR U
REAL SCALAR U1
REAL SCALAR U2
REAL SCALAR U3
REAL SCALAR U4
REAL SCALAR U5

>The foolowing "WORDS" are used to perform the functions
they define and reduce thereby the amount of typing
required to do such things as clearing the screen, etc...<
: G GRAPHICS.DISPLAY ;
: N NORMAL.DISPLAY ;
: C SCREEN.CLEAR ;
: ZZ STACK.CLEAR ;
: S STACK.DISPLAY ;
: A.P XY.AUTO.PLOT ;
: D.P XY.DATA.PLOT ;

>Under file "ODDS&.END" :<

>To set up the readout of the array positions on the
screen;<
: A.R
array.readout
normal.coords
.6 .9 readout>position
world.coords
;

>To display the original or active x,y array<
:  RESET
X SUB[ 1 , N.O.P ]
Y SUB[ 1 , N.O.P ]
A.P
;

>To truncate the data set, use the word TRUNK:<

: TRUNK
CR ." FROM WHICH INDEX ONWARD? :" #INPUT NEXT :=
X SUB[ NEXT , N.O.P NEXT - ] X SUB[ 1 , N.O.P NEXT - ] :=
Y SUB[ NEXT , N.O.P NEXT - ] Y SUB[ 1 , N.O.P NEXT - ] :=
N.O.P NEXT - N.O.P := ;
```

>To get a rate constant for a particular peak, it is found using the word A.R, and the following; Note that the numbers must be entered before using the words (individually)<

```
: KK EXP 2. SWAP / . ;
: CC LABEL.SCALE.Y * 1.6973 * . ;
```

>Under file READ.ASY ;<

>To enter data from DOS: The number of pairs must be supplied. The order of entry is first a Y, then on the next entry its corresponding x-value, etc... Use the following;<

```
: READ.BAS
CR ." Enter the filename "
"INPUT DEFER> BASIC.OPEN
CR ." Enter the expected number of data pairs;"
#INPUT N.O.P :=
N.O.P 1 + 1 DO
BASIC.READ DROP
Y [ I ] :=
BASIC.READ DROP
X [ I ] :=
LOOP
BASIC.CLOSE
;
```

>Under file STAND.5 ;<

>Once the raw data has been entered, it must be reduced in size. The first step is optional and simply reduces the size of x,y by half by omitting every second pair.<

```
:STANDARD.5
X SUB[ 1 , N.O.P 2 / , 2 ] X SUB[ 1 , N.O.P 2 / ] :=
Y SUB[ 1 , N.O.P 2 / , 2 ] Y SUB[ 1 , N.O.P 2 / ] :=
N.O.P 2 / 1 - N.O.P := ;
```

>File FIND.LN ;,

>This program is used to find the X-component. It requires an estimate of it to be entered. It is a simple iterative search and find routine. The tolerance should not be so small such that it is impossible to obtain, nor increment so large as to pass the tolerance quickly. It will only change the x-values to accomodate the X-component if the user so wishes at the end of the iterations, when the program tells the user of the adjustment it would make, and request permission to do so or continue as is. It is suggested that a third degree fit be used, but if this be too drastic, a 2 cd degree fit may work faster. THIS PROGRAM SHOULD BE USED BEFORE STANDARD.A<

```
: FIND.X
N
CR ." DEGREE ? " CR
#INPUT DEGREE :=
CR ." X-estimate ? " CR
#INPJT U1 :=
CR ." Tolerance ? " CR
#INPUT U2 :=
CR ." Increment ? " CR
#INPUT U3 :=
O NEXT :=
400 1 DO
NEXT 1 + .
O INC :=
3 1 DO
INC 1 + INC :=
1 SECT :=
INC 2 / 1 = IF -1 SECT := THEN
U3 NEXT * SECT * DUP U5 :=
X SUB[ 3 , 6 ] +
Y SUB[ 3 , 6 ]
DEGREE LEASTSQ.POLY.FIT
O.O SWAP POLY[X]
U4 :=
U4 U1 - ABS U2 < IF LEAVE THEN
U4 . U5 .
LOOP
NEXT 1 + NEXT :=
U4 U1 - ABS U2 < IF LEAVE THEN
CR LOOP
CR ." Tolerance criteria met, added factor is = " U5 .
CR ." Save new x ? (YES = 1, NO = 0)  >> " #INPUT
1 = IF X U5 + X := THEN ;
```

>File STAND>ARD ;<

>To reduce the size and spacing of pairs to better apply a log-log polynomial fitting procedure, one must use at least the first of these two. The second is used after a second READ.BAS is performed, where the original is automatically put aside, then the second is reduced, and spliced onto the first. This second read in of data is used when files are too large and must be sized down as explained in the experimental section of this thesis.<

```
: STANDARD.A
X SUB[ 30 , 20 , 2 ] X SUB[ 30 , 20 ] :=
Y SUB[ 30 , 20 , 2 ] Y SUB[ 30 , 20 ] :=
X SUB[ 69 , 20 , 6 ] X SUB[ 50 , 20 ] :=
Y SUB[ 69 , 20 , 6 ] Y SUB[ 50 , 20 ] :=
X SUB[ 188 , 10 , 10 ] X SUB[ 70 , 10 ] :=
Y SUB[ 188 , 10 , 10 ] Y SUB[ 70 , 10 ] :=
X SUB[ 287 , 6 , 20 ] X SUB[ 80 , 6 ] :=
Y SUB[ 287 , 6 , 20 ] Y SUB[ 80 , 6 ] :=
```

```
X SUB[ 406 , 15 , 50 ] X SUB[ 86 , 15 ] :=
Y SUB[ 406 , 15 , 50 ] Y SUB[ 86 , 15 ] :=
X SUB[ 1155 , 8 , 100 ] X SUB[ 101 , 8 ] :=
Y SUB[ 1155 , 8 , 100 ] Y SUB[ 101 , 8 ] :=
300 1 DO
X [ I 1 + ] X [ I ] - X [ I 1 + ] X [ I ] - ABS / -1. =
IF I N.O.P := LEAVE THEN
LOOP
N.O.P OLD.N :=
X SUB[ 1 , N.O.P ] SX SUB[ 1 , N.O.P ] :=
Y SUB[ 1 , N.O.P ] SY SUB[ 1 , N.O.P ] :=
;
```

>And when a second file is fed into the system;<

```
: STANDARD.B
X SUB[ 10 , 5 , 2 ] X SUB[ 10 , 5 ] :=
Y SUB[ 10 , 5 , 2 ] Y SUB[ 10 , 5 ] :=
X SUB[ 20 , 5 , 3 ] X SUB[ 15 , 5 ] :=
Y SUB[ 20 , 5 , 3 ] Y SUB[ 15 , 5 ] :=
X SUB[ 36 , 5 , 4 ] X SUB[ 20 , 5 ] :=
Y SUB[ 36 , 5 , 4 ] Y SUB[ 20 , 5 ] :=
X SUB[ 58 , 50 , 5 ] X SUB[ 25 , 50 ] :=
Y SUB[ 58 , 50 , 5 ] Y SUB[ 25 , 50 ] :=
210 1 DO
X [ I 1 + ] X [ I ] - DUP ABS / -1. =
IF I N.O.P := LEAVE THEN
LOOP
X SUB[ 1 , N.O.P ] SX SUB[ OLD.N 1 + , N.O.P ] :=
Y SUB[ 1 , N.O.P ] SY SUB[ OLD.N 1 + , N.O.P ] :=
OLD.N N.O.P + N.O.P :=
SX X :=
SY Y :=
;
```

>File FIX.ASY ;<

>The use of this file is unfortunately limited by the ASYST system. The limitations require that the size of the data to be fitted times the degree of fitting be less than 1000. This program fits a polynomial to the log-log data, and interpolates by logarithmic spacings according to the number of new points and degree desired by the user. It is suggested that for a full data set that a tenth degree fit be attempted first, and that for a single component set that a fifth degree fit be done. The size of the raw array may have to be reduced further by using STANDARD.A, and the number of points can be found (after reduction) by typeing **"N.O.P ."**.<

```
: FIX.XY
ZZ
CR ." # new pairs ? " #INPUT NUMBER :=
X SUB[ 1 , N.O.P ] LN
Y SUB[ 1 , N.O.P ] LN
```

```
A.P
CR ." Degree ? " #INPUT DEGREE :=
X [ N.O.P ] LN X [ 1 ] LN - NUMBER 1 - / U :=
NUMBER 1 + 1 DO
I 1 - U * X [ 1 ] LN + EXP NEWX [ I ] :=
LOOP
X SUB[ 1 , N.O.P ] LN
Y SUB[ 1 , N.O.P ] LN
DEGREE LEASTSQ.POLY.FIT
DUP COEFF SUB[ 1 , DEGREE 1 + ] :=
NEWX SUB[ 1 , NUMBER ] LN SWAP POLY[X]
NEWY SUB[ 1 , NUMBER ] :=
NEWX SUB[ 1 , NUMBER ] LN
NEWY SUB[ 1 , NUMBER ] DUP
EXP NEWY SUB[ 1 , NUMBER ] := LN D.P
;
```

>File LAP.ASY ;<

```
>This is the program that applies the Laplace transform
mathematics to the newly interpolated data. No information
need be entered. At the end of the plotting, type A.R to
get cursor/arrays in order to get values for maxima.<
: LAPLACE
NEWX SUB[ 1 , NUMBER ] LN NEWX SUB[ 1 , NUMBER ] :=
NUMBER 1 DO
NEWY [ I 1 + ] NEWY [ I ] - U / DIFF1 [ I ] :=
NEWX [ I 1 + ] NEWX [ I ] + 2. / NEWSET [ I ] :=
I NEXT :=
LOOP
NUMBER 1 - 1 DO
DIFF1 [ I 1 + ] DIFF1 [ I ] - U / DIFF2 [ I ] :=
NEWSET [ I 1 + ] NEWSET [ I ] + 2. / NEWSET [ I ] :=
LOOP
NUMBER 2 - 1 DO
DIFF1 [ I 1 + ] DIFF [ I ] + 2. / -1. *
DIFF2 [ I ] + -1. * DIFF2 [ I ] :=
LOOP
NEWSET SUB[ 1 , NUMBER 3 - ]
DIFF2 SUB[ 1 , NUMBER 3 - ]
NEWX SUB[ 1 , NUMBER ] EXP NEWX SUB[ 1 , NUMBER ] :=
A.P
;
```

>File SMOOTH.ASY ;<

```
>This program will smooth the Laplace profile if required.
It is not very often necessary, but if NUMBER exceeds 600,
it occasionally is.<
: SMOOTHER
NEWSET SUB[ 1 , NUMBER 3 - 4 / , 4 ]
DIFF2 SUB[ 1 , NUMBER 3 - 4 / , 4 ]
```

```
CR ." DEGREE ? " CR
#INPUT LEASTSQ.POLY.FIT
NEWSET SUB[ 1 , NUMBER ]
SWAP POLY[X]
NEWSET SUB[ 1 , NUMBER ] SWAP D.P ;
```

>File LOG.ASY ;<

>The following program is used to estimate the last component if it was not found using LAPLACE. If there were three known component after LAPLACE, the new data should be transfered to DOS using the program words NEW.XY and TRANSFER which are to be explained later. The value of A-infinity must be supplied, and the linear trailing section is looked at closer by using the word CUT.IT<

```
: LOG.IT
CR ." A-Inf> ? " CR
#INPUT U1 :=
NUMBER 1 DO
U1 NEWY [ I ] - LN LOGS [ I ] :=
LOOP
NEWX SUB[ 1 , NUMBER 1 - ]
LOGS SUB[ 1 , NUMBER 1 - ]
A.P
;

: CUT.IT
CR ." N.O.P = " NUMBER 1 - .
CR ." First index ? "
CR #INPUT COUNT :=
CR ." Last ? " CR
#INPUT NEXT :=
NEWX SUB[ COUNT , NEXT COUNT - ]
LOGS SUB[ COUNT , NEXT COUNT - ]
A.P
NEWX SUB[ COUNT , NEXT COUNT - ]
LOGS SUB[ COUNT , NEXT COUNT - ]
1 LEASTSQ.POLY.FIT
DUP COEFF SUB[ 1 , 2 ] :=
NEWX SUB[ COUNT , NEXT COUNT - ]
SWAP POLY[X]
NEWX SUB[ COUNT , NEXT COUNT - ]
SWAP D.P
CR ." Rate constant=" CR
COEFF [ 1 ] -1. * .
CR ." Abs-value =" CR
COEFF [ 2 ] EXP .
;
```

>File STRIP.ASY ;<

```
>This program strips rate constant COEFF [ 1 ] and Abs.-
value COEFF [ 2 ] LN from the original (active) x,y array.
It is not a dedicated function, and after the plots of
original vs stripped are found acceptable, this new x,y set
must be saved by typing ORIG.SAVE;<
: STRIP.ORIG
N.O.P 1 + 1 DO
Y [ I ] COEFF [ 1 ] X [ I ] * EXP 1. SWAP -
COEFF [ 2 ] EXP * - BUFFER [ I ] :=
LOOP
X SUB[ 1 , N.O.P ] LN
Y SUB[ 1 , N.O.P ] LN
A.P
X SUB[ 1 , N.O.P ] LN
BUFFER SUB[ 1 , N.O.P ] LN D.P
;
: ORIG.SAVE
BUFFER SUB[ 1 , N.O.P ] Y SUB[ 1 , N.O.P ] :=
;
```

>File TRANS.FER ;<

```
>This program interpolates log-log data with a polynomial
fit with a user's choice degree value according to spacings
based on equal time intervals in order to be compatible
with the nonlinear regression routine. It is a bit fussier
that FIX.XY for a good fit. If it skips too much of the
initial data, the x,y data set must be reduced in size
(change N.O.P) or the number of new pairs must be
increased.<
: NEW.XY
N CR ." number of "
CR ." new pairs? " cr
#INPUT NUMBER :=
X SUB[ 1 , N.O.P ] LN
Y SUB[ 1 , N.O.P ] LN
CR ." DEGREE ? " #INPUT DEGREE :=
DEGREE LEASTSQ.POLY.FIT
COEFF SUB[ 1 , DEGREE 1 + ] :=
X [ N.O.P ] X [ 1 ] - NUMBER 1 - / U1 :=
NUMBER 1 + 1 DO
I 1 - U1 * X [ 1 ] + NEWSET [ I ] :=
LOOP
NEWSET SUB[ 1 , NUMBER ]
LN
COEFF SUB[ 1 , DEGREE 1 + ] POLY[X]
LOGS SUB[ 1 , NUMBER ] :=
X SUB[ 1 , N.O.P ] LN
Y SUB[ 1 , N.O.P ] LN A.P
NEWSET SUB[ 1 , NUMBER ] LN
LOGS SUB[ 1 , NUMBER ] D.P ;
```

```
>This program transfers the new data to a file compatible
with the nonlinear regression routine. If the trailing end
of the fit dips below the original data, the size of NUMBER
must be reduced to eliminate this problem. It is important
not to touch the keyboard during transfer as this will jam
the system.<
: TRANSFER
1 NEXT :=
CR ." Filename ? "
cr "INPUT DEFER OUT>FILE
NUMBER 1 + 1 DO
LOGS [ I ] EXP .
CR
NEWSET [ I ] .
CR
LOOP
OUT>FILE.CLOSE
;
```

APPENDIX B:NONLINEAR REGRESSION

This is a listing, in Turbo-Pascal language , of the program called EXPFIT.PAS and ran by typing EXPFIT once it has been appropriately compiled. The data file which is to be fed into the program must be in the form:

```
[1]*.2343    (This is usually in units of absorbtion)
[2]*1        (Time values)
etc...
```

where the alternating numbers are for y, then x. No other information can be in that file. The program will cease reading the file after 250 pairs have been entered, but this can be altered in line 4 of the program listing below. The number of parameters should not exceed 7, which include, in the following entry order: [1] = C1, [2] = k1, and so forth, with the final parameter being the X-component. It is highly recommended that the final question asked be always answered by "N" unless the program has failed to converge in which case "Y", but be warry of these latter results for they have restricted eigenvalues. The program will converge when the sum of least squares is less than 10^{-8}. An alternate criteria is incorporated, but the use of its regression results is discouraged.

The NLR algorithm chosen for this work adheres closely to that described by Bard (106) and discussed in the kinetic context by Mak and Langford (87). The following is a description of the NLR algorithm. It is not necessary for the reader to understand it in order to effectively use the routine.

Briefly, to determine the step direction for each new iteration, the inverse scaled decomposition of the Hessian matrix **N** is computed. The eigenvalue decomposition of the scaled Hessian matrix **C** was accomplished by the following sequence; (i) initial application of the Givens-Householder algorithm to reduce **C** to the tridiagonal form, (ii) diagonalization of the tridiagonal matrix by the QR algoritm with origin shifts, and (iii) successive orthogonal transformations of the unit matrix to obtain the eigenvectors. After the step direction is established, the step length is determined by an interpolation-extrapolation algorithm. Computations were terminated when a series of further iterations failed to reduce the value of the objective function which is the absolute difference between the regression model value in a previous iteration and the regression model value of the current iteration.

```
          EXPFIT.PAS                              derv1
 1      const
 2           matmax = 10 ;
 3           word = 16 ;
 4           maxnop = 250 ;
 5      type
 6           matdim = 1..matmax ;
 7           xary = array [matdim,matdim] of real ;
 8           yary = array [matdim] of real ;
 9           datadim = 1..maxnop ;

10           zary = array [datadim] of real ;
11      var
12           i,j,size,k,m : matdim ;
13           a,v,g1,z,ninv : xary ;
14           b,w,u,p,q,r,q2,v1,b1,a1,a11,ab,ac,az : yary ;
```

```
15              y,y1,aa,delta1 : zary ;
16               e,e1,e2,s,x,c,d,f,h,g,c1,p1,x1,r1,d1,q1,s1,bs,
17              dphi,sum,delta,deltat,z1,z2,rho,ratio :  real ;
18              iter : integer ;
19              nop,i1 : datadim ;
20              choice : char ;
21              test,check : boolean ;
22              datain : string[15] ;
23              datafile : text ;
24          (*the following is a series of functions calcu-
25           lating the partial derivatives of the regression
             model with respect to each variable*)
26  1           function derv1 : real ;
27  1           begin
28  1           derv1 := 1-exp(-a1[2]*aa[i1])
29               end ;
30  1           function derv2 : real ;
31  1           begin
32  1           derv2 := a1[1]*aa[i1]*exp(-a1[2]*aa[i1])
33               end ;
34  1           function derv3 : real ;
35  1           begin
36  1           derv3 := 1-exp(-a1[4]*aa[i1])
37               end ;
38  1           function derv4 : real ;
39  1           begin
40  1           derv4 := a1[3]*aa[i1]*exp(-a1[4]*aa[i1])
41               end ;
42  1           function derv5 : real ;
43  1           begin
44  1           derv5 := 1-exp(-a1[6]*aa[i1])
45               end ;
46  1           function derv6 : real ;
47  1           begin
48  1           derv6 := a1[5]*aa[i1]*exp(-a1[6]*aa[i1])
49               end ;
50  1           function derv7 : real ;
51  1           begin
52  1           derv7 := 1.0
53               end  ;
54          (*the following is a series of procedures to calcu-
              late the sum of squares
55           psi; and the respective gradient vector,
              Hessian matrix etc.*)
56  1       Procedure soss (var delta : real) ;
57  1        (*soss calculates the sum of squares*)
58  1           begin
59  1                delta := 0.0;
60  1                for i1 := 1 to nop do
61  2                begin
62  3                case size of
63  3                3 : y1[i1] := a1[1]*(1-exp(-a1[2]
                      *aa[i1]))+a1[3];
64  3                5 : y1[i1] := a1[1]*(1-exp(-a1[2]
```

```
 65  3            *aa[i1]))+a1[3]*(1-exp(-a1[4]*aa[i1]))
                    +a1[5];
 66  3          7: y1[i1] := a1[1]*(1-exp(-a1[2]
 67  3           *aa[i1]))+a1[3]*(1-exp(-a1[4]*aa[i1]))+
                    a1[5]*(1-exp(-a1[6]*aa[i1]))+a1[7];
 68  2            end;
 69  2            delta1[i1] := y[i1]-y1[i1] ;
 70  2            delta := delta+sqr(delta1[i1]);
 71  1            end;
 72          end;
 73  1    Procedure gragient (var q2 : yary ) ;
 74  1    (*computation of the initial gradient vector*)
 75  1          begin
 76  2          case size begin of
 77  3          3 : begin
 78  3                for i := 1 to size do
 79  4                begin
 80  4                q2[i] := 0.0;
 81  4                for i1 := 1 to nop do
 82  5                case i of
 83  5                1 : q2[i] := q2[i]-2*delta1[i1]*derv1 ;
 84  5                2 : q2[i] := q2[i]-2*delta1[i1]*derv2 ;
 85  5                3 : q2[i] := q2[i]-2*delta1[i1]*derv7
 86  4                end;
 87  3                end;
 88  2               end;
 89  3          5 : begin
 90  3                for i := 1 to size do
 91  4                begin
 92  4                q2[i] := 0.0;
 93  4                for i1 := 1 to nop do
 94  5                case i of
 95  5                1 : q2[i] := q2[i]-2*dealt1[i1]*derv1;
 96  5                2 : q2[i] := q2[i]-2*delta1[i1]*derv2;
 97  5                3 : q2[i] := q2[i]-2*delta1[i1]*derv3;
 98  5                4 : q2[i] := q2[i]-2*delta1[i1]*derv4;
 99  5                5 : q2[i] := q2[i]-2*delta1[i1]*derv7
100  4                end;
101  3                end;
102  2               end;
103  3           7 : begin
104  3                for i := 1 to size do
105  4                begin
106  4                q2[i] := 0.0;
107  4                for i1 := 1 to nop do
108  5                case i of
109  5                1 : q2[i] := q2[i]-2*delta1[i1]*derv1;
110  5                2 : q2[i] := q2[i]-2*delta1[i1]*derv2;
111  5                3 : q2[i] := q2[i]-2*delta1[i1]*derv3;
112  5                4 : q2[i] := q2[i]-2*delta1[i1]*derv4;
113  5                5 : q2[i] := q2[i]-2*delta1[i1]*derv5;
114  5                6 : q2[i] := q2[i]-2*delta1[i1]*derv6;
115  5                7 : q2[i] := q2[i]-2*delta1[i1]*derv7
116  4                end;
```

```
117  3            end;
118  2            end;
119  1          end;
120        end;
121  1   Procedure Hessian (var b1 : yary; var a : xary);
122  1   (*computation of the initial Hessian matrix
          elements*)
123  1       begin
124  1            for i := 1 to size do
125  1            for j := 1 to size do
126  1            a[i,j] := 0.0;
127  1            for i1 := 1 to nop do
128  2            begin
129  3            case size of
130  4            3 : begin
131  4                 for k := 1 to size do
132  5                 begin
133  5                 z1 := 0.0;
134  6                 case k of
135  6                 1 : z1 := derv1;
136  6                 2 : z1 := derv2;
137  6                 3 : z1 := derv7
138  5                 end;
139  5                 for m := 1 to size do
140  6                 begin
141  6                 if (m<k) then
142  6                 z2 := 0.0
143  6                 else
144  7                 begin
145  7                 z2 := 0.0;
146  8                 case m of
147  8                 1 : z2 := derv1;
148  8                 2 : z2 := derv2;
149  8                 3 : z2 := derv7
150  7                 end;
151  7                 a[k,m] := a[k,m]+2*(z1*z2);
152  7                 a[m,k] := a[k,m];
153  6                 end;
154  5                 end;
155  4                 end;
156  3               end;
157  4            5 : begin
158  4                for k := 1 to size do
159  5                begin
160  5                z1 := 0.0;
161  6                case k of
162  6                1 : z1 := derv1;
163  6                2 : z1 := derv2;
164  6                3 : z1 := derv3;
165  6                4 : z1 := derv4;
166  6                5 : z1 := derv7
167  5                end;
168  5                for m := 1 to size do
169  6                begin
```

```
170  6                  if (m<k) then
171  6                  z2 := 0.0
172  6                  else
173  7                  begin
174  7                  z2 := 0.0;
175  8                  case m of
176  8                  1 : z2 = derv1;
177  8                  2 : z2 := derv2;
178  8                  3 : z2 := derv3;
179  8                  4 : z2 := derv4;
180  8                  5 : z2 := derv7
181  7                  end;
182  7                  a[k,m] := a[k,m]+(z1*z2);
183  7                  a[m,k] := a[k,m];
184  6                  end;
185  5                  end;
186  4                  end;
187  3                end;
188  4          '7 : begin
189  4                 for k := 1 to size do
190  5                 begin
191  5                 z1 := 0.0;
192  6                 case k of
193  6                 1 : z1 := derv1;
194  6                 2 : z1 := derv2;
195  6                 3 : z1 := derv3;
196  6                 4 : z1 := derv4;
197  6                 5 : z1 := derv5;
198  6                 6 : z1 := derv6;
199  6                 7 : z1 := derv7
200  5                 end;
201  5                 for m := 1 to size do
202  6                 begin
203  6                 if (m<k) then
204  6                 z2 := 0.0
205  6                 else
206  7                 begin
207  7                 z2 := 0.0;
208  8                  case m of
209  8                 1 : z2 := derv1;
210  8                 2 : z2 := derv2;
211  8                 3 : z2 := derv3;
212  8                 4 : z2 := derv4;
213  8                 5 : z2 := derv5;
214  8                 6 : z2 := derv6;
215  8                 7 : z2 := derv7
216  7                 end;
217  7                 a[k,m] := a[k,m]+2*(z1*z2);
218  7                 a[m,k] := a[k,m];
219  6                 end;
220  5                 end;
221  4                 end;
222  3                 end;
223  2                 end;
```

```
224  1              end;
225  1              writeln;
226  1              writeln;
227  1             writeln ('the Hessian matrix elements
                     row x row are : ');
228  1              for i := 1 to size do
229  2              begin
230  2              writeln;
231  2              for j := 1 to size do
232  2              write ('  ',a[i,j] : 9);
233  1              end;
234  1              (*scaling of the matrix*)
235  1              for i := 1 to size do
236  2              begin
237  2                   if (a[i,i]+0) then
238  2                   b1[i] := 1.0
239  2                   else
240  2                   b1[i] := sqrt(abs(a[i,i]));
241  1              end;
242  1              for i := 1 to size do
243  1              for j := 1 to size do
244  2              begin
245  2                   if (i=j) then
246  2                   a[i,j] := a[i,j]
247  2                   else
248  2            a[i,j] :=  a[i,j]/sqrt(abs(a[i,i]*
                          a[j,j]));
249  1              end;
250  1              for i := 1 to size do
251  1              a[i,i] := 0.0;
252            end;
253  1     Procedure matinv (var dphi : real ; var v1,a11 :
            yary);
254  1     (*matrix inversion begins via Givens-Householder
            and QR methods*)
255  1     var
256  1          max,min : real ;
257  1     begin (*computation of e*)
258  1          e := 1.0;
259  1          for k := 1 to word do
260  1          e := e*2.0;
261  1          e := 1.0/e;
262  2     begin (*computation os s,e1,and e2*)
263  2          s := 0.0;
264  2          for i := 1 to size do
265  2          for j := 1 to size do
266  2          s := s+a[i,j]*a[i,j];
267  2          e1 := e*sqrt(2.0*s);
268  2          e2 := e1/(size*size);
269  2          writeln;
270  2          writeln;
271  2          writeln ('the values of e1 and e2 are : ');
272  2          writeln (e1,'    ',e2);
273  1     end  ;
```

```
274  2     begin (*generate an identity matrix of SIZE*)
275  2          for i := 1 to size do
276  2          for j := 1 to size do
277  2          if i<>j then v[i,j] := 0.0
278  2          else v[i,j] := 1.0;
279  1     end;
280  2     begin
281  2          for i := 1 to (size - 2) do
282  3               begin
283  3                    if a[(i+1),i] >= 0.0 then x := 1.0
284  3                    else x := -1.0;
285  3                    c := 0.0;
286  3                    for j := (i+1) to size do
287  3                    c := c+a[j,i]*a[j,i]
288  3          d := x*sqrt(c);
289  3          b[i] := -d;
290  3          f := 1.0/(c+abs(a[(i+1),i]*d));
291  3          w[i+1] := a[(i+1),i]+d;
292  3          for j := (i+2) to size do
293  3          w[j] := a[j,i];
294  3          for j := (i+1) to size do
295  3          u[j] := f*w[j];
296  3          for k := 1 to size do
297  4               begin
298  4               p[k] := 0.0;
299  4               for j := (i+1) to size do
300  4               p[k] := p[k]+v[k,j]*w[j];
301  3               end;
302  3          for k := 1 to size do
303  3          for j := (i+1) to size do
304  3          v[k,j] := v[k,j]-p[k]*u[j];
305  3          for k := (i+1) to size do
306  4               begin
307  4               q[k] := 0.0;
308  4               for j := (i+1) to size do
309  4               q[k] := q[k]+a[k,j]*u[j];
310  3               end;
311  3          h := 0.0;
312  3          for k := (i+1) to size do
313  3          h := h+q[k]*u[k];
314  3          h := h/2.0;
315  3          for k := (i+1) to size do
316  3          q[k] := q[k]-h*wu[k]
317  3          for j := (i+1) to size do
318  3          for k := (i+1) to size do
319  3          a[j,k] := a[j,k]-q[j]*w[k]-w[j]*q[k];
320  2          end;
321  2          writeln;
322  2          writeln;
323  2          writeln ('the numerical elements of the
                 final tridiagonal matrix are ; ');
324  2          writeln;
325  3          for i := 1 to size do
326  3          begin
```

```
327  3          writeln;
328  3          for j := 1 to size do
329  3          write ('  ',a[i,j] : 9) ;
330  2          end;
331  2          (*QR decomposition*)
332  2          b[size-1] := a[(size-1),size];
333  2          for i := 1 to size do
334  2          r[i] := a[i,i];
335  2          m := size
336  2          g := 0.0;
337  3          repeat
338  3          test := true;
339  3          c1 := 1.0;
340  3          f := r[m];
341  3          p1 := r[1];
342  3          for i := 1 to (m-1) do
343  4               begin
344  4               if abs(b[i]) <= e2
345  5               then begin
346  5               b[i] := 0.0;
347  5               d := 0.0;
348  5               c := p1 ;
349  4               end;
350  5               else begin
351  5                    x1 := sqrt (p1*p1+b[i]*b[i]);
352  5                    d := b[i]/x1;
353  5                    c := p1/x1;
354  5                    for j := 1 to size do
355  6                         begin
356  6                         h := c*v[j,(i+1)]-d*v[j,i];
357  6                         v[j,i] := d*v[j,(i+1)]+c
                               *v[j,i];
358  6                         v[j,(i+1)] := h;
359  5                         end;
360  5                    end;
361  4               r1 := c*p1+d*b[i];
362  4               d1 := c*c1;
363  4               q1 := d1*b[i]+d*r[i+1];
364  4               r[i] := d1*r1+d*q1;
365  4               if i > 1 then
366  4               b[i-1] := s1*r1;
367  4               s1 := d;
368  4               p1 := c*r[i+1]-s1*c1*b[i];
369  4               c1 := c;
370  3               end;
371  3          b[m-1] := s1*p1;
372  3          r[m] := c1*p1;
373  3          bs := 0.0;
374  3          for k := 1 to (m-1) do
375  3          bs := bs+abs(b[k]);
376  3          if (bs <= e1) and (test=true)
377  4          then begin
378  4               for k := 1 to m do
379  4               r[k] := r[k]+g;
```

```
380  4              test := false;
381  3              end ;
382  3         while (abs(b[m-1]) <= e2) and (test=true) do
383  4              begin
384  4              if m >= 2 then
385  5              begin
386  5              r[m] := r[m]+g;
387  5              m := m-1;
388  4              end
389  4              else
390  5                   begin
391  5                   if (abs(abs(r[m]/f)-1) > 0.5) and
                          (test=true) then
392  5                   test := true
393  5                   else
394  6                   begin
395  6                   g := g+r[m];
396  6                   for k := 1 to m do
397  6                   r[k] := r[k]-r[m];
398  5                   end
399  4                   end;
400  4              if m >= 2 then
401  4              test := true
402  4              else
403  4              test := false ;
404  3              end;
405  2              until test := false ;
406  2              (*Eigenvalue adjustments if necessary
                     begins*)
407  2              for i := 1 to size do
408  2              r[i] := abs(r[i]);
409  2              if choice='y' then
410  3              begin
411  3              max := r[i] ;
412  3              min := r[i] ;
413  3              for i := 2 to size do
414  4              begin
415  4              if r[i]>max then
416  4              max := r[i] ;
417  4              if r[i]<min then
418  4              min := r[i] ;
419  3              end ;
420  3              if (min/max)<0.000005 then
421  4              begin
422  4              writeln ;
423  4              writeln ;
424  4              writeln ('the Hessian matrix or the
                      initial estimates are ill-conditioned') ;
425  4              writeln ;
426  4              writeln ('the value of max/min is :',
                      max/min) ;
427  4              for i := 1 to size do
428  4              r[i] := 0.000005*max+r[i] ;
429  3              end ;
```

```
430  2          end ;
431  2          writeln ;
432  2          writeln ;
433  2          writeln ('the eigenvalues are:');
434  2          for k := 1 to size do
435  2          write (' ',r[k] : 9);
436  2          writeln;
437  2          writeln;
438  2          writeln ('the eigenvectors are:');
439  2          for i := 1 to size do
440  3          begin
441  3          writeln ;
442  3          for j := 1 to size do
443  3          write ('  ',v[j,i] : 9) ;
444  2          end
445  1     end;
446  1     for i := 1 to size do
447  1     for j := 1 to size do
448  1     g1[i,j] := 1/b1[i]*v[i,j];
449  1     for i := 1 to size do
450  1     for j := 1 to size do
451  1     z[i,j] := g1[i,j]*1/r[j];
452  1     for i := 1 to size do
453  2     begin
454  2          sum := 0.0;
455  2          for k := 1 to size do
456  3          begin
457  3          sum := 0.0;
458  3          for j := 1 to size do
459  3          sum := sum+z[i,j]*g1[k,j];
460  3          ninv[i,k] := sum;
461  2          end;
462  1     end;
463  1     writeln;
464  1     writeln;
465  1     writeln ('the values of ninv [i,k] are : ');
466  1     for i := 1 to size do
467  2     begin
468  2     writeln ;
469  2     for j := 1 to size do
470  2     write ('  ',ninv[i,j] : 9);
471  1     end ;
472  1     for i := to size do
473  2     begin
474  2          v1[i] := 0.0;
475  2          for j := 1 to size do
476  2          v1[i] := v1[i]+ninv[i,j]*(-q2[j]);
477  1     end;
478  1     writeln;
479  1     writeln;
480  1     writeln ('the values of v1[i] are : ');
481  1     for k := 1 to size do
482  1     writeln ('v1[',k,'] = ',v1[k] : 9);
483  1     dphi := 0.0;
```

```
484  1     for i := 1 to size do
485  1     dphi := dphi+v1[i]*q2[i];
486  1     writeln;
487  1     writeln;
488  1     writeln ('the value of "dphi" is : ');
489  1     write (dphi : 9);
490  1     for i := 1 to size do
491  1     a11[i] := a1[i] ;
492  1     end;
493  1     procedure stepsiz (var a1 : yary ; var check :
           boolean );
494  1     label 99
495  1     var
496  1          ab : yary ;
497  1          max0,max,dummy,max1,delta1,min : real ;
498  1          count,index : integer ;
499  1          size1 : matdim ;
500  1          (*the following function NRHO is to compute
501  1          the stepsize proportionality factor*)
502  2          function nrho : real ;
503  2          begin
504  2          nrho := dphi*sqr(rho)/(2*(dphi*rho+deltat-
                delta))
505  1          end;
506  2          procedure doss )var delta :real);
507  2          var
508  2               i1 : datadim;
509  2          begin
510  2               delta := 0.0;
511  2               for i1 := 1 to nop do
512  3                    begin
513  4                    case size of
514  4                    3 : y1[i1] := a1[1]*(1-exp(-a1[2]
                          *aa[i1]))+a1[3];
515  4                    5 : y1[i1] := a1[i]*(1-exp(-a1[2]*
516  4                    aa[i1]))+a1[3]*(1-exp(-a1[4]*
                          aa[i1]))+a1[5];
517  4                    7 : y1[i1] := a1[1]*(1-exp(-a1[1]*
518  4                    aa[i1]))+a1[5]*(1-exp(-a1[6]*
                          aa[i1]))+a1[7];
519  3                    end;
520  3                    delta1[i1] := y[i1]-y1[i1];
521  3                    delta := delta+sqr(delta1[i1]);
522  2                    end;
523  1          end;
524  1          (*the main procedure stepsiz begins below*)
525  1          begin
526  1               check := trua ;
527  1               count := 0 ;
528  1               max1 := 1.0 ;
529  2               repeat
530  2               count := count+2 ;
531  2               if (abs(v1[count])>max1 then
523  2               max1 := abs(v1[count]) ;
```

```
533  1              until count := size-1 ;
534  1              dummy := 1.0 ;
535  1              max0 := 0.5 ;
536  1              if max1>0.5 then
537  2              repeat
538  2              dummy := dummy*0.5 ;
539  2              max0 := max1*dummy ;
540  1              until max0<=0.5 ;
541  1              writeln ;
542  1              writeln;
543  1              writeln;
544  1             writeln ('the initial adjusted a1[i]
                     values are : ') ;
545  1              writeln ;
546  1              for i := 1 to size do
547  2              begin
548  2              v1[i] := v1[i]*dummy ;
549  2              a1[i] := a11[i]+v1[i] ;
550  2              writeln ('a1[i',i,'] = ',a1[i] : 9);
551  1              end;
552  1              deltat := delta ;
553  1              doss(delta ;
554  1              min := 0.0 ;
555  1              for i := 1 to size do
556  1              if a1[i]<min then
557  1              min := a1[i] ;
558  1              if (delta<deltat) and (min>0.0) then
559  2              begin
560  2              writeln ;
561  2              writeln ('the initially adjusted
                     a1[i] values are used directly') ;
562  2        writeln('for extrapolation/
                     interpolation.') ;
563  1              end
564  1              (*Greenstadt Type adjustments begins*)
565  1              else
566  2              begin
567  2              for i := 1 to size do
568  2              ab[i] := a1[i] ;
569  2              delta1 := deltat ;
570  2              index := 0 ;
571  2              count := 0 ;
572  3              repeat
573  3              count := count+2 ;
574  3              if ab[count]<0.0 then
575  4              begin
576  4              a1[count] := abs(ab[count]*0.15) ;
577  4              index := index+1 ;
578  3              end ;
579  3              if ab[count-1]<0.0 then
580  4              begin
581  4              a1[count-1] := abs(ab[count-1]*0.75) ;
582  4              index := index+1 ;
583  3              end ;
```

```
584  2              until count = size-1 ;
585  2              if ab[size]<0.0 then
586  3              begin
587  3              a1[size] := abs(ab[size]*0.5) ;
588  3              index := index+1 ;
589  2              end ;
590  2              for i := 1 to size do
591  3              begin
592  3              if ab[i]>0.0 then
593  3              a1[i] := a1[i]-a1[i]*(index*0.15) ;
594  2              end ;
595  2              doss(delta) ;
596  2              if delta<delta1 then
597  3              begin
598  3              writeln ;
599  3              writeln ('the "scaled" values of a1[i]
                     are : ') ;
600  3              for i := 1 to size do
601  3              writeln ('scaled a1[i] = ',a1[i] : 9) ;
602  2              end
603  2              else
604  3              begin
605  3              count := 0 ;
606  4              repeat
607  4              delta1 := delta ;
608  4              count := count+1 ;
609  5              case size of
610  5              3 : size1 := 1;
611  5              5 : size1 := 2;
612  5              7 : size1 := 3
613  4              end;
614  4              for i := 1 to size1 do
615  5              begin
616  5              if ab[i*2]<0.0 then
617  5              a1[i*2] := a1[i*2]+abs(ab[i*2]*0.1) ;
618  4              end ;
619  4              doss(delta) ;
620  3              until (delta<delta1) or (count=8) ;
621  3              if delta1<=delta then
622  4              begin
623  5              case size of
624  5              3 : size1 := 2;
625  5              5 : size1 := 3;
626  5              7 : size1 := 4
627  4              end;
628  4              for i := 1 to size1 do
629  5              begin
630  5              if ab[2*i-1]<0.0 then
631  5              a1[2*i-1] := a1[2*i-1]*1.2 ;
632  4              end ;
633  3              end ;
634  3              delta1 := delta ;
635  3              doss(delta) ;
636  3              if delta1<delta then
```

```
637  4              begin
638  4              for i := 1 to size1 do
639  5              begin
640  5              if ab[2*i-1]<0.0 then
641  5              a1[2*i-1] := a1[2*i-1]*(2/3) ;
642  4              end ;
643  3              end ;
644  3              delta1 := delta ;
645  3              doss(delta) ;
646  3              if delta1<delta then
647  4              begin
648  5              case size of
649  5              3 : size1 := 1;
650  5              5 : size1 := 2;
651  5              7 : size1 := 3
652  4              end;
653  4              for i := 1 to size1 do
654  5              begin
655  5              if ab[2*i-1]<0.0 then
656  5              a1[2*i-1] := abs(ab[2*i-1]*0.5) ;
657  5              if ab[2*i]<0.0 then
658  5              a1[2*i] := abs(ab[2*i]*0.15) ;
659  4              end ;
660  4              if ab[size]<0.0 then
661  4              a1[size] := abs(ab[size]*0.5) ;
662  3              end ;
663  3              writeln;
664  3              writeln ('the "scaled" values of a1[i]
                     are : ') ;
665  3              for i := 1 to size do
666  3              writeln ('scaled a1[i] = ', a1[i] : 9) ;
667  2              end ;
668  1              end ;
669  1              for i := 1 to size do
670  1              az[i] := 0.0001*(a1[i]+0.001) ;
671  1              ratio := az[i]/abs(v1[1]) ;
672  1              for i := 2 to size do
673  2              begin
674  2              if (az[i]/abs(v1[i]))<ratio then
675  2              ratio := az[i]/abs(v1[i]) ;
676  1              end ;
677  1              if abs(deltat-delta)<1.0e-08 then
678  2              begin
679  2              check := false ;
680  2              goto 99 ;
681  1              end
682  1              else
683  2              begin
684  2              writeln;
685  2             writeln ('the boolean value of delta
                     and deltat are:') ;
686  1              end;
687  1              rho := 1.0 ;
688  1              writeln;
```

```
689  1          writeln ('the new values of delta and
                 deltat are :') ;
690  1          writeln (delta : 9,'     ',deltat : 9) ;
691  1          if delta<deltat then
692  2          begin
693  2          if nrho<0 then
694  2          dummy := 2*rho
695  2          else
696  2          dummy := nrho ;
697  2          writeln;
698  2          writeln ('the value of dummy is :') n;
699  2          writeln (dummy : 9) ;
700  2          if abs(dummy-rho)<(0.1*rho) then
701  2          dummy := rho
702  2          else
703  2          dummy := dummy ;
704  2          for i := 1 to size do
705  2          a1[i] := abs(a11[i]+dummy*v1[i]) ;
706  2          doss(delta);
707  2          if delta>deltat then
708  2          dummy := rho
709  2          else
710  2          dummy := dummy ;
711  2          for i := 1 to size do
712  3          begin
713  3          a1[i] := abs(a11[i]+dummy*v1[i]) ;
714  3          a11[i] := a1[i] ;
715  2          end ;
716  2          writeln ;
7172           writeln ('the a1[i] values by
                 extrapolation are : ') ;
718  2          for i := 1 to size do
719  2          writeln ('EXT a1[',i,'] = '.a1[i] : 9) ;
720  1          end
721  1          else
722  1          writeln ;
723  1          writeln ;
724 1          writeln ('interpolation begins at this
                 point :') ;
725  2          begin
726  2          count := 0 ;
727  3          repeat
728  3          count := count+1 ;
729  3          writeln ;
730  3          writeln ('the value of rho and nrho
                 respectively are :') ;
7313           writeln ('rho = ',rho,'     ','nrho =
                 ',nrho) ;
732  3          if nrho<(0.75*rho) then
733  3          dummy := nrho
734  3          else
735  3          dummy := 0.75*rho ;
736  3          if dummy<(0.25*rho) then
737  3          dummy := 0.25*rho
```

```
738  3              else
739  3              dummy := dummy ;
740  3              for i := 1 to size do
741  3              a1[i] := abs(a11[i]+dummy*v1[i]) ;
742  3              doss(delta) ;
743  3              rho := dummy ;
744  3              writeln ;
745  3              writeln ('the current interpolation
                     cycle is : ',count) ;
7463                writeln ('the values of a1[i] by
                     intrepolation are : ') ;
747  3              for i := 1 to size do
748  3              writeln ('INT a1[',i,'] = ',a1[i] :9) ;
749  2              until (delta<deltat) or (count=15) ;
750  2              if ratio>abs(nrho) then
751  3              begin
752  3              check := false ;
753  3              writeln ;
754  3              writeln ;
755  3              writeln ('iterations terminated by
                     way of alternative criterion') ;
756  2              end ;
757  1              end ;
758                 99 : end ;
759                 begin
760                 (*main programme begins*)
761                 writeln ;
762                 writeln ('what is the name of your
                     data file ? ') ;
763                 read (datain) ;
764                 writeln ;
765                 writeln ;
766                writeln ('input the number of
                     parameters to be fitted or SIZE :') ;
767                 read (size);
768                 writeln ;
769                 writeln ;
770                 writeln ('input initial estimates of
                     parameters; i.e.,a[1]...a[size]') ;
771                 for i := to 1 to size do
772  1              begin
773  1              writeln ('Enter a1[',i,'] : ') ;
774  1              readln (a1[i]);
775
776                 writeln ;
777                writeln ('do you wishto restrict
                     eigenvalues? - answer "y" or "n"') ;
778                 read (choice) ;
779                 writeln ;
780                 writeln ;
781                writeln ('the valuesofthe initial
                     estimates are : ');
782                 for i := 1 to size do
783  1              begin
```

```
784  1              ac[i] := a1[i] ;
785  1              writeln ('a1[',i,'] = ',ac[i] : 9);
786                 end ;
787                 assign (datafile,datain);
788  1              begin
789  1              reset (datafile);
790  1              nop := 0;
791  1              while not eof(datafile) and
                     (nop<maxnop) do
792  2              begin
793  2              while not eoln(datafile) and
                     (nop<maxnop) do
794  3              begin
795  3              nop := nop+1 ;
796  3              read(datafile,y[nop],aa[nop])
797  2              end;
798  2              readln(datafile);
799  1              end;
800  1              close (datafile);
801                 end;
802                 writeln;
803                 writeln;
804                 writeln ('the value of nop is : ');
805                 write (nop);
806                 writeln;
807                 writeln;
808                  writeln ('the values of y[i1]s, and
                     aa[i]s are : ');
809                 for i := 1 to nop do
810                 writeln (y[i],'    ',aa[i]);
811                 iter := 0 ;
812  1              repeat
813  1              iter := iter+1 ;
814  1              check := true ;
815  1              soss(delta;
816  1              writeln;
817  1              writeln;
818 1               writeln ('the value of delta/sum of
                     squares is : ');
820  1              gradient(q2);
821  1              writeln;
822  1              writeln;
8231                writeln ('the gradient vector of
                     dimension size is : ');
824  1              for i := 1 to size do
825  1              writeln ('q2[',i,'] = ',q2[i] :9);
826  1              hessian(b1,a);
827  1              writeln;
828  1              writeln;
829  1              writeln ('the diagonal elements of
                     matrix B1 is : ');
830  1              for i := 1 to size do
831  1              writeln ('b1[',i,'] = ',b1[i] : 9);
832  1              writeln;
```

```
833  1              writeln;
834  1              writeln ('the elements of matrix A is :
                     ');
835  1              for i := 1 to size do
836  2              begin
837  2              writeln ;
838  2              for j := 1 to size do
839  2              write ('  '.a[i,j] : 9) ;
840  1              end ;
841  1              matinv (dphi,v1,a11);
842  1              stepsiz (a1,check);
843                 until check := false ;
844                 writeln;
845                 writeln;
846                 writeln ('iterations terminated/boolean
                     check is : ', check) ;
847                 writeln ('the final values of the
                     regression parameters are :');
848                 for i := 1 to size do
849                 writeln ('a1[',i,'] = ',a1[i] : 9) ;
850                 writeln ;
851                 writeln ;
852                 writeln ('the original parameter
                     estimates were : ') ;
853                 for i := 1 to size do
854                 writeln ('a1[',i,'] = ',a1[i] : 9) ;
855                 writeln ;
856                 writeln ('number of iterations thus
                     far :') ;
857                 writeln (iter)
858                 end .
```